



UNIVERSITEIT VAN PRETORIA
UNIVERSITY OF PRETORIA
YUNIBESITHI YA PRETORIA

Investigating phenotypic differences of *Plasmodium falciparum* parasites following
exposure to classical antimalarial drugs

By

Alicia Joshua

11046024

Submitted in partial fulfilment of the degree

Magister Scientiae

Biochemistry

Faculty of Natural and Agricultural Sciences, University of Pretoria

September 2018

Submission declaration

University of Pretoria

I, Alicia Joshua, declare that the dissertation, which I hereby submit for the degree *Magister Scientiae* in the Department of Biochemistry, at the University of Pretoria, is my own work and has not previously been submitted by me for a degree at this or any other tertiary institution.

Signature:..........

Date:....28th...of...September...2018...


Declaration of originality University of Pretoria

Full name:Alicia....Joshua.....

Student number:.....11046024.....

Title:.....Investigating phenotypic differences of *Plasmodium falciparum* parasites following exposure to classical antimalarial drugs.....

1. I understand what plagiarism is and am aware of the University's policy in this regard.
2. I declare that this dissertation (eg essay, report, project, assignment, dissertation, thesis, etc) is my own original work. Where other people's work has been used (either from a printed source, Internet or any other source), this has been properly acknowledged and referenced in accordance with departmental requirements.
3. I have not used work previously produced by another student or any other person to hand in as my own.
4. I have not allowed, and will not allow, anyone to copy my work with the intention of passing it off as his or her own work.

Signature:..........

Date:...28th...of...September...2018...

Acknowledgements

First and foremost, I would like to thank God for blessing me with the opportunities and strength to pursue my dreams and complete my dissertation.

I would like to express my sincere gratitude to the following exceptional persons, with whom I have been privileged to share this journey with:

My supervisor, Dr. Jandeli Niemand and co-supervisor, Prof. Lyn-Marie Birkholtz for your guidance and support.

The staff from the University of Pretoria, specifically, Saronda Fillis and Sandra van Wyngaardt. Thank you for all your kindness and support.

My parents, Elizabeth and Quinton Stuart Joshua and brother, Quinton Ignatius Joshua for all your support, endless prayers and always being a pillar of strength and support for me.

Thank you to my friends, and students in the Malaria Parasite Molecular Laboratory (M²PL) research group, especially, Jessica, Mariska, Janie, Dikeledi and Tasneem for all your support and encouragement.

My friend, Newt Fourie, for all your encouragement and support throughout this journey.

I would like to thank the National Research Foundation of South Africa for the financial support provided throughout this study.

Finally, I dedicate this dissertation to my grandfather who passed away on the 25th of July 2018, although you are not with me in person, I know that you are with me in spirit.

Summary

Malaria remains a leading health problem with an estimated 445 000 deaths occurring in 2016 of which the majority of deaths occurred in Africa. Currently, the World Health Organization recommends artemisinin-based combination therapies for the treatment of uncomplicated *Plasmodium falciparum* infections. However, the emergence of multidrug resistant strains of *Plasmodium* has necessitated the identification of new biological targets as well as the development of antimalarial chemotherapeutics with novel modes of action. Despite intensive research towards the identification of novel antimalarial chemotherapeutics that can kill the parasite, there remains a significant knowledge gap regarding how antimalarial therapeutics affect the biology of *P. falciparum* parasites.

One functional genomics approach that can be used to identify the effects of drug perturbation on the biology of the parasite, is phenomics. Phenomics is defined as the collective characterization and quantification of the various phenotypes of an organism that describes the measurable physical and chemical interactions between genes and the environment and is expressed by either a cell, tissue or an organism. It aims to assess the global phenotypes in a set space and time under different environmental conditions. Phenomics provides an assessment of the biological pathways that are perturbed due to environmental conditions.

In this dissertation, the phenome of *P. falciparum* parasites was evaluated *in situ* in response to antimalarial compounds as environmental perturbations. Specifically, the phenome was determined by using Phenotype MicroArray (PM) technology to measure the real-time ability of *P. falciparum* parasites to use a variety of carbohydrate substrates for energy production. This was extended to evaluate parasites perturbed by antimalarial drug treatment including classically used drugs such as chloroquine (CQ) disulphate, pyrimethamine (PYR) and dihydroartemisinin (DHA). Substrate catabolism was used to identify global differences between treated and untreated trophozoite-stage *P. falciparum* parasites. The information obtained was subsequently

used to interrogate the presence of distinct phenotypic fingerprints consistent with the mode of action of each compound.

Significant variations in carbohydrate source utilization were identified with, untreated parasites catabolizing 56% of the carbohydrate substrates. By contrast, parasites treated with the antimalarials were metabolically severely affected as evident in a use of only 13% to maximally 40% of the substrates. Global analyses of the resultant phenomes revealed clear differences in the phenotypic profiles and modes of actions (MOAs) of parasites treated with either CQ disulphate, DHA or PYR. This study describes the first real-time phenotypic profile of treated and untreated trophozoite-stage *P. falciparum* parasites. The PM platform has displayed its utility in the identification of phenotypic profiles and distinguishing between variations in MOAs of classical antimalarial compounds. This study serves as a blueprint for future PM studies of drug perturbations in the asexual form of the parasite.

Table of contents

Acknowledgements	iii
Summary	iv
Table of contents	vi
List of figures	viii
List of tables	x
List of abbreviations	xii
Chapter 1	1
Introduction	1
1.1 Global impact of malaria.....	1
1.2 <i>Plasmodium</i> species	2
1.2.1 The life cycle of <i>P. falciparum</i> parasites	3
1.3 Uptake of glucose in <i>P. falciparum</i> parasites	5
1.4 Glucose metabolism in <i>P. falciparum</i> parasites	8
1.5 Antimalarial therapeutics.....	12
1.5.1 Antimalarial drug discovery	14
1.6 Functional genomics	22
1.7 Phenomics	24
1.7.1 The Phenotype MicroArray platform.....	24
Hypothesis	27
Aim	27
Objectives	27
Chapter 2	29
Materials and methods	29
2.1 Ethical clearance	29
2.1.1 <i>In vitro</i> maintenance of asexual stage <i>P. falciparum</i> parasite cultures...29	
2.1.2 Sorbitol synchronization of asexual NF54 <i>P. falciparum</i> parasites.....30	
2.1.3 Intraerythrocytic <i>P. falciparum</i> parasite <i>in vitro</i> proliferation inhibition assay	32
2.2 Magnetic enrichment of intraerythrocytic <i>P. falciparum</i> parasites with VarioMACS.....	33
2.3 Lactate dehydrogenase viability assay	34
2.4 Determination of carbohydrate substrate use in untreated and treated trophozoite-stage infected erythrocytes using the PM platform.....	35
2.5 Analyses of PM data.....	35

Chapter 3	38
Results	38
3.1 <i>In vitro</i> <i>P. falciparum</i> parasite culturing	38
3.2 CQ disulphate, DHA and PYR display nM activity against intraerythrocytic <i>P. falciparum</i> parasites	39
3.3 Enrichment of trophozoite stage intraerythrocytic <i>P. falciparum</i> parasites	42
3.4 Determination of the viability of enriched trophozoite stage infected erythrocytes under PM assay conditions.....	43
3.5 PM analyses of carbohydrate substrate use by enriched trophozoite stage infected erythrocytes in the absence or presence of CQ disulphate, DHA and PYR.....	44
3.6 A Comparison of the phenotypic profile of untreated trophozoites to literature.....	52
3.7 MOA analyses of the phenotypic profiles of untreated trophozoite-stage <i>P. falciparum</i> parasites in comparison to treated trophozoites.....	51
Chapter 4	70
Discussion	70
Chapter 5	74
Concluding discussion	74
References	76
Appendix:	77

List of figures

Figure 1.1: Global distribution and population at risk of contracting malaria	2
Figure 1.2: The life cycle of <i>P. falciparum</i> parasites	4
Figure 1.3: Transport processes that are involved in the uptake of hexose sugars in <i>P. falciparum</i> infected erythrocytes	7
Figure 1.4: Overview of glycolysis in <i>P. falciparum</i> parasites and the connection to the PPP	8
Figure 1.5: The pentose phosphate pathway in the cytoplasm of <i>Plasmodium</i>	9
Figure 1.6: The different modes of the PPP in <i>Plasmodium</i>	11
Figure 1.7: The differences between target based and phenotypic screening assays.....	16
Figure 1.8: The mechanism and mode of action of CQ disulphate.....	18
Figure 1.9: The principle of the PM platform for the identification of changes in the phenome of an organism.....	25
Figure 2.1: A schematic representation of a typical growth curve and the growth parameters that can be determined after performing a PM experiment.	36
Figure 3.1: Dose response curves of the <i>in vitro</i> proliferation inhibition of intraerythrocytic <i>P. falciparum</i> NF54 parasites.....	39
Figure 3.2: Morphology of NF54 <i>P. falciparum</i> parasites prior and post-enrichment	40
Figure 3.3: The viability of enriched trophozoite stage <i>P. falciparum</i> parasites over time in either CM or IF-M2+.	42
Figure 3.4: The effects of CQ disulphate, DHA or PYR against <i>P. falciparum</i> parasites in CM or IF-M2+.	43
Figure 3.5: Representative PM using the PM-M1 microplate, with measurements at 0 h and 12 h shown.....	45

Figure 3.6: Multi-scatterplot of PM data before and after normalisation	48
Figure 3.7: Comparison of PM phenotypic profiles of untreated trophozoites to published data.....	51
Figure 3.8: Phenotypic profiles of untreated and treated <i>P. falciparum</i> trophozoite-stage parasite after 12 h of treatment with either CQ disulphate, DHA or PYR...53	
Figure 3.9: A schematic representation of formazan production curves that have similar AUC values but differ in their curve shapes.....	58
Figure 3.10: Metabolic fingerprint of untreated and treated trophozoite-stage <i>P. falciparum</i> parasites.....	61

List of tables

Table 1: The use, mechanism of action and resistance of quinolones, artemisinins and antifolates.....	13
Table 2: Microscopic evaluation and characteristic traits of the various life cycle stages of <i>P. falciparum</i> (NF54) parasites.....	38
Table 3: A summary showing altered substrate use in untreated parasites (A) globally as well as when parasites are treated with (B) DHA, (C) CQ disulphate and (D) PYR.....	62
Appendix Table 1: Plate map of the mammalian phenotype microarray plate PM-M1.....	86
Appendix Table 2: Carbohydrate substrates that displayed a statistically significant decrease in metabolism in comparison to untreated trophozoites are displayed below for each treatment condition	88
Appendix Table 3: Kinetic parameters of trophozoite-stage <i>P. falciparum</i> parasites either untreated or treated with, CQ disulphate, DHA or PYR on different carbohydrate sources	90
Appendix Table 4: Comparison of the carbohydrate sources which produced a positive signal in untreated trophozoite-stage <i>P. falciparum</i> parasites in the PM system as compared to literature	93
Appendix Table 5: The average AIVs used to generate the map hit distribution.....	103

Abbreviations

ACTs	Artemisinin combination therapies
AIV	Activity index value
APAD	3-acetyl pyridine NAD
APAD⁺	Reduced 3-acetyl pyridine NAD
ART	Artemisinin
AUC	Area under the curve
CM	Complete culture medium
CNVs	Copy number variants
CQ	Chloroquine
DHA	Dihydroartemisinin
DHFR	Dihydrofolate reductase
DHPS	Dihydropteroate synthase
DMSO	Dimethyl sulfoxide
EPM	Erythrocyte plasma membrane
GC-MS	Gas chromatography-mass spectrophotometry
GLUT1	Glucose transporter 1
GLUT5	Glucose transporter 5
hpi	Hours post invasion
IDC	Intraerythrocytic developmental cycle
IRS	Indoor residual spraying
K13	Kelch 13
LC-MS	Liquid chromatography-mass spectrophotometry
LLINs	Long-lasting insecticide-treated nets
MOA	Mode(s) of action
MPMP	Malaria Parasite Metabolic Pathways
MS	Mass-spectrophotometry
NBT	Nitroblue tetrazolium
NMR	Nuclear magnetic resonance
PES	Phenazine ethosulfate
PfCRT	<i>Plasmodium falciparum</i> chloroquine resistant transporter protein
PfHT	<i>Plasmodium falciparum</i> hexose transporter

PfMDR1	<i>Plasmodium falciparum</i> multidrug resistant 1 gene
PGDB	Pathway genome database
PM	Phenotype MicroArray
PPM	Parasite plasma membrane
PPP	Pentose phosphate pathway
PVM	Parasitophorous vacuole membrane
PYR	Pyrimethamine
T	Time
TCA	Tricarboxylic acid cycle
UHPLC-MS	Ultra performance liquid chromatography
WHO	World Health Organization

Chapter 1

Introduction

1.1 Global impact of malaria

Malaria is a mosquito-borne infectious disease caused by parasitic protozoa of the genus *Plasmodium* (Cox, 2002). Records of fevers, chills, malaise and lethargy, which are characteristic traits of malaria, have been documented as far back as 2700 BC (Cox, 2010). The *Plasmodium* parasite is transmitted from mosquitoes to humans via the bite of an infected female *Anopheles* mosquito, which serves as the primary vector (Cox, 2002). Vector control strategies such as long-lasting insecticide-treated nets (LLINs) (Griffin *et al.*, 2010), indoor residual spraying (IRS) (Weiss, Crabb and Gilson, 2016) and chemotherapeutics targeting the *Plasmodium* parasites through the use of artemisinin combination therapies (ACTs), has dramatically decreased the incidence and death rate caused by malaria in the past decade, with a ~50% reduction in malaria cases observed [World Health Organization (WHO) World Malaria Report, 2015]. Approximately 216 million malaria cases were reported in 2016 with an estimated 445 000 deaths, compared to 446 000 deaths which occurred in 2015 (WHO World Malaria Report, 2017). However, the WHO has reported that approximately 3.2 billion people remain at risk of contracting the disease (Figure 1.1) (WHO World Malaria Report, 2016) due to factors such as a decrease in IRS protection, a decrease in the availability of LLINs and continued resistance of the parasites to clinically used antimalarials, including both components of ACTs (Dondorp *et al.*, 2009; Ashley *et al.*, 2014).

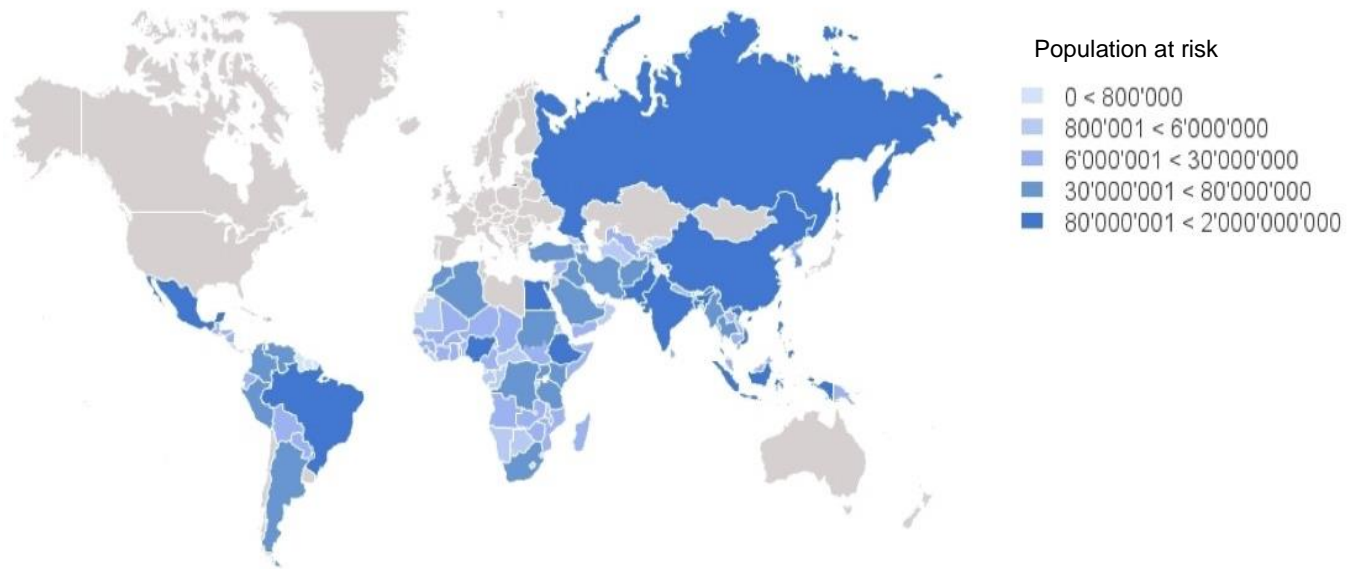


Figure 1.1: Global distribution of the population at risk of contracting malaria. Available from:http://www.who.int/malaria/publications/world_malaria_report/global_malaria_mapper/ [Date created: 21 February 2018].

1.2 *Plasmodium* species

Parasites that cause malaria are typically host specific with humans as the natural hosts for *P. falciparum*, *P. vivax*, *P. malariae* and *P. ovale* whereas, *P. knowlesi* and *P. cynomolgi* are simian specific parasites that can infect humans (Singh and Divis, 2008). *P. falciparum* is the most virulent and occurs predominantly in sub-Saharan Africa accounting for the majority of malaria deaths (WHO World Malaria Report, 2017). *P. vivax* has the greatest geographical distribution of the human infective *P. falciparum* species (Howes *et al.*, 2016), accounting for more than half of all malaria cases in Asia and Latin America (Kochar *et al.*, 2005). In contrast to *P. falciparum*, *P. malariae* and *P. knowlesi*, both *P. vivax* and *P. ovale* form hypnozoites which remain dormant in liver cells of the human host for either weeks or months. The dormant forms of both these parasites result in relapse in an infected individual, making it a challenge to eradicate infection by these parasites (Chu and White, 2016).

1.2.1 The life cycle of *P. falciparum* parasites

The life cycle of *P. falciparum* parasites is multifaceted with specific developmental processes occurring in either the mosquito vector or human host (Figure 1.2). *P. falciparum* parasites are transmitted when an infected female *Anopheles* mosquito injects sporozoites from the salivary glands of the mosquito vector into the subcutaneous tissue of the human host (Miller *et al.*, 2002). Exo-erythrocytic schizogony occurs when sporozoites penetrate hepatocytes and undergo asexual replication. Schizogony causes the formation of multinucleated hepatic schizonts, which rupture to release merozoites into the bloodstream of the human host, a process that takes ~16-days (Tuteja, 2007). The release of ~30 000 merozoites into the bloodstream initiates the intraerythrocytic developmental cycle (IDC), which maintains the reservoir of parasites in the human host (White, 2009).

Merozoites mature into haploid ring-stage parasites and thereafter, into highly metabolically active trophozoites (Dvorak *et al.*, 1975). Trophozoite-stage parasites are characterized by an increase in glucose consumption (100-fold increase), ingestion of host cytoplasm and the catabolism of host haemoglobin into its constituent amino acids. The degradation of haemoglobin into its constituent amino acids results in the release of haem, which is toxic to the parasite. Therefore, during the catabolism of haemoglobin, haem is polymerized into its non-toxic form, haemozoin, which is a crystalline substance that is stored within the parasitophorous food vacuole (Tuteja, 2007; Miller *et al.*, 2002). The end of the trophic stage is characterized by the initiation of schizogony as 3-4 rounds of DNA synthesis and mitosis occur. Mature schizonts burst to release merozoites into the bloodstream and this synchronous rupturing of schizonts results in the clinical symptoms of fever-chill cycles in infected individuals (Sherman, 1979).

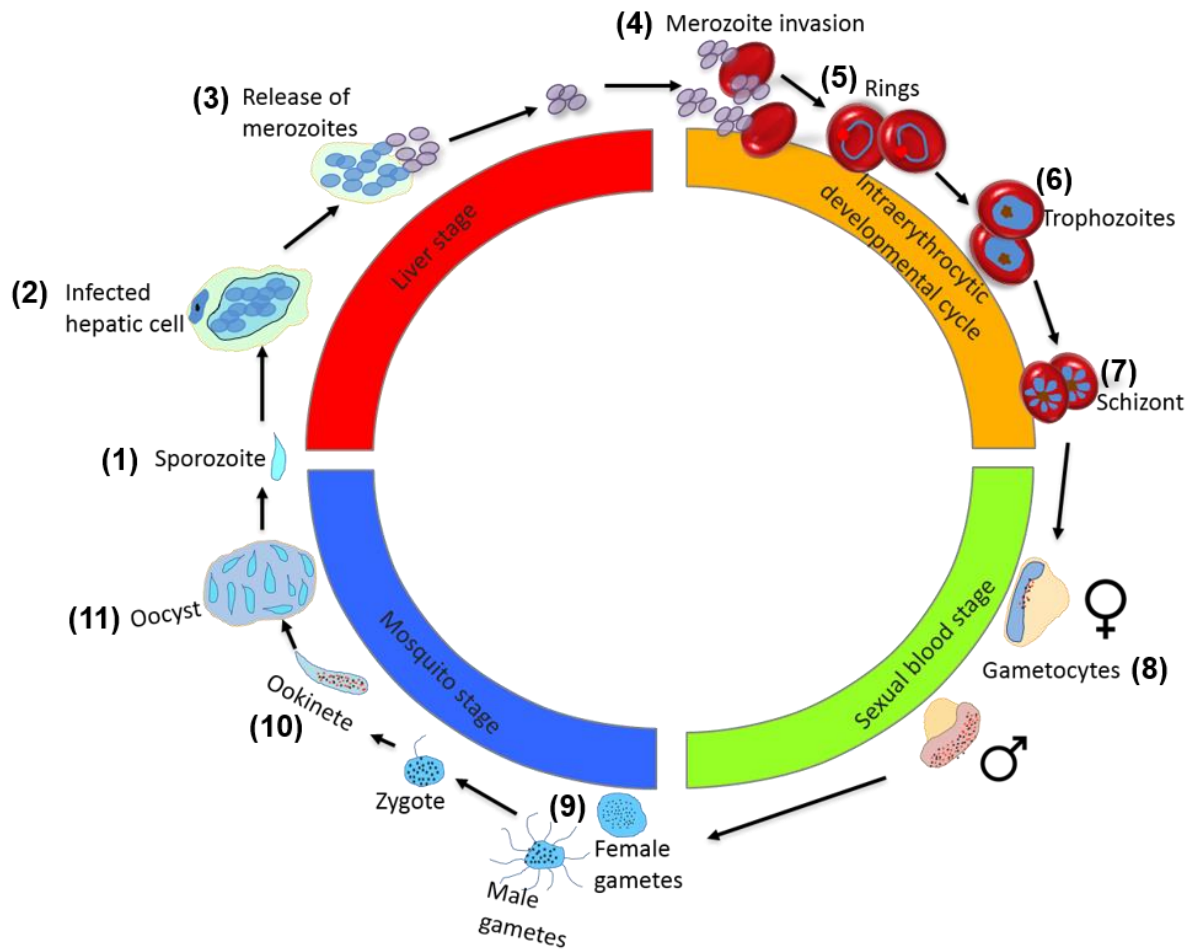


Figure 1.2: The life cycle of *P. falciparum* parasites. The life cycle of the *P. falciparum* parasite begins when a female *Anopheles* mosquito injects sporozoites into a human host (1). The sporozoites enter the bloodstream and migrate to liver where the formation of schizonts in hepatocytes occurs (2). Mature schizonts release merozoites into the bloodstream (3) and infect uninfected erythrocytes (4). Within the erythrocyte, the parasite develops through several developmental stages, from a ring-stage (5), to a trophozoite-stage (6) and finally into a schizont stage (7), which upon lysis release daughter merozoites to continue the intraerythrocytic developmental life cycle (3). A small proportion of merozoites commit to the transmissible sexual stage of the parasite and mature into gametocytes (8), which are taken up by the mosquito to develop into male and female gametes (9). Within the mosquito, fertilization of female gametes result in the formation of a motile ookinete (10). The motile ookinete migrates to the basal lamina of the mosquito and matures into an oocyst containing thousands of sporozoites (11). The subsequent lysis of the oocyst results in the migration of sporozoites to the mosquito salivary glands, re-initiating the life cycle of *Plasmodium*.

Sexual development of the parasite occurs when ring-stage parasites are committed to differentiating into either micro- or macrogametocytes (male and female respectively) (White, 2009). The proportion of parasites committed to sexual development is reliant on environmental stressors such as host immune cell activation and an increase in reticulocyte number (Field and Shute, 1956). Committed ring-stage

parasites complete asexual development and mature into schizonts. The subsequent merozoites that are released from a sexually committed schizont invade uninfected erythrocytes and develop into gametocytes (Bruce *et al.*, 1990). After developing for ~14 days sequestered in the bone marrow, mature gametocytes are released and taken up by female *Anopheles* mosquitoes during a blood meal from an infected human host, which allows the transfer of the parasite (Sherman, 1979).

In the mosquito midgut, gametocytes mature into gametes, fertilization occurs and zygotes penetrate the stomach wall through maturation into an ookinete. Ookinetes develop into oocysts, which contain thousands of sporozoites. Sporozoite maturation results in lysis of the oocyst and the migration of sporozoites to the salivary glands of the mosquito to continue transmission (Sherman, 1979).

1.3 Uptake of glucose in *P. falciparum* parasites

Blood stage *Plasmodium* parasites are highly reliant on glucose as their main energy source. Blood serves as a constant and abundant source of glucose for *Plasmodium* parasites residing within erythrocytes. *Plasmodium* parasites deprived of glucose display a decrease in intracellular ATP production with a concomitant decrease in cytoplasmic pH (Saliba and Kirk, 1999) and depolarization of the parasite plasma membrane (Allen and Kirk, 2004). Anaerobic respiration is less efficient than aerobic respiration, however, it provides the required glycolytic intermediates for rapid biomass production during schizogony. The remaining macromolecular biomass is obtained from purine precursors, amino acids, and lipids or fatty acids obtained from the human host (Salcedo-Sora *et al.*, 2014).

Glucose is transported to the intraerythrocytic malaria parasite by sugar transporters that are present on both the parasite and host's plasma membrane (Figure 1.3). Glucose is transported from the blood plasma into the cytosol of the host cell's erythrocyte by GLUT1, which is a facilitative glucose transporter. Facilitative glucose transporters such as GLUT1, transport glucose into the cytosol through passive transport of the molecule down its concentration gradient (Manolescu *et al.*, 2007).

Glucose is rapidly phosphorylated to glucose-6-phosphate by the host cell's hexokinase upon its transport into the erythrocytes cytosol, effectively rendering it membrane impermeant and trapping it within the host cell (McKee and McKee, 2015). In the parasite, the import of glucose across the parasitophorous vacuole membrane occurs through the dephosphorylation of the molecule by the enzyme, acid phosphatase, which cleaves phosphate bonds from a diversity of small molecules (Olszewski and Llinás, 2011). Thereafter, uptake of glucose into the parasite plasma membrane is mediated by the *P. falciparum* membrane hexose transporter (PfHT, Figure 1.3). *P. falciparum* trophozoite-stage infected erythrocytes display a greater activity of the glycolytic enzymes and of lactate dehydrogenase in comparison to their uninfected counterparts (Lang-Unnasch and Murphy, 1998). Differences in substrate interaction have been identified for both GLUT1 and PfHT, GLUT1 displays a preferential binding affinity towards D-glucose, whereas, PfHT can transport both D-glucose and D-fructose (Slavic *et al.*, 2011).

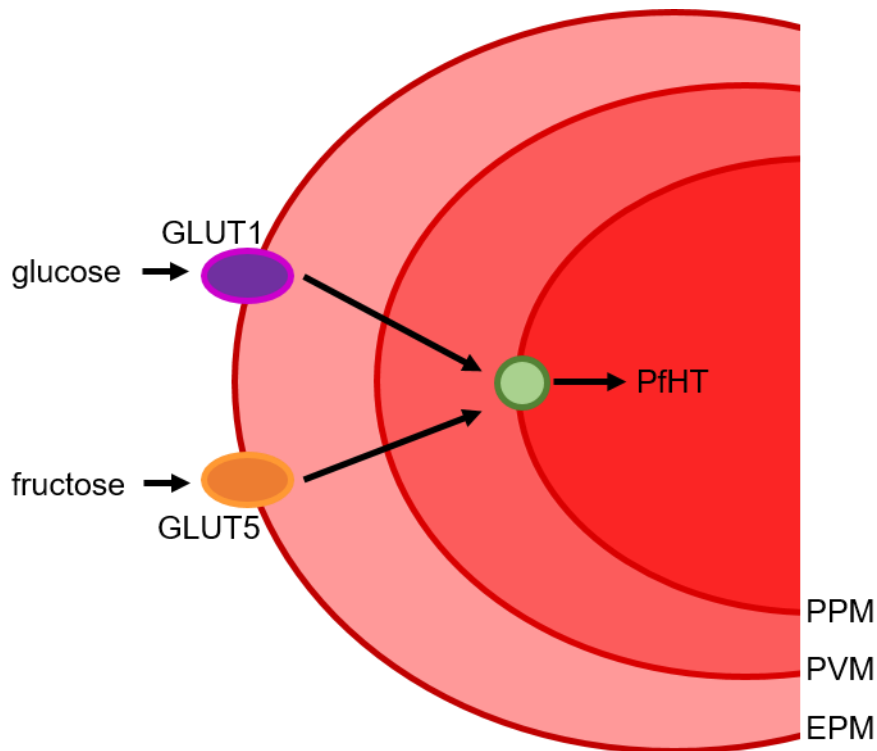


Figure 1.3: Transport processes that are involved in the uptake of hexose sugars in *P. falciparum* infected erythrocytes. Abbreviations used: Erythrocyte plasma membrane (EPM), parasitophorous vacuole membrane (PVM), parasite plasma membrane (PPM), *Plasmodium falciparum* hexose transporter (PfHT), Glucose transporter 1 (GLUT1) and Glucose transporter 5 (GLUT5). Created from (Slavic *et al.*, 2011).

1.4 Glucose metabolism in *P. falciparum* parasites

Two major pathways of glucose metabolism are prevalent in asexual intraerythrocytic, *P. falciparum* parasites. These pathways include glycolysis (Figure 1.4) and the pentose phosphate pathway (Figure 1.5). The primary source of ATP production in the asexual blood stages of the parasite is via glycolysis, which is subsequently followed by anaerobic fermentation of pyruvate to lactate (Slavic *et al.*, 2011).

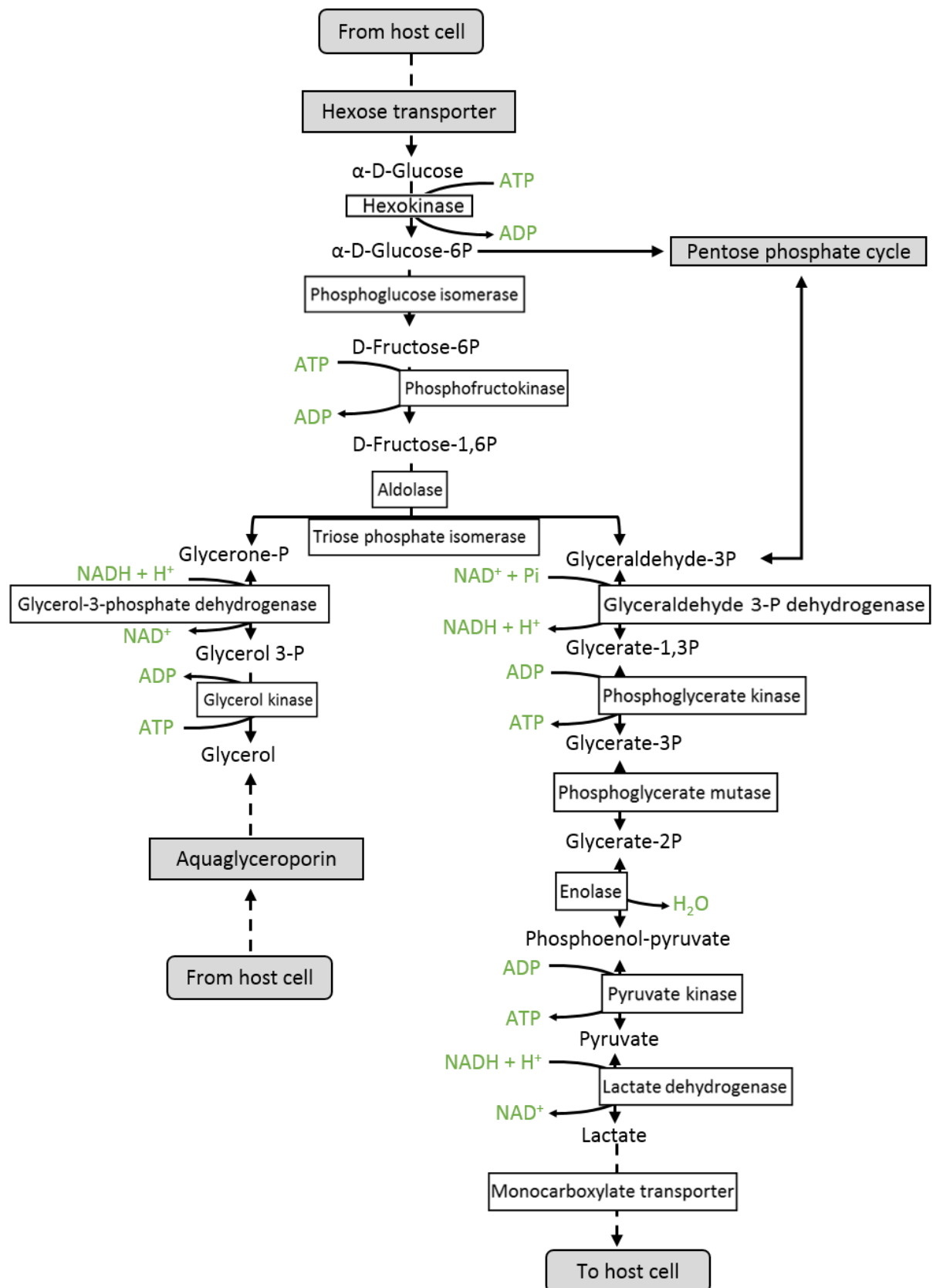


Figure 1.4: Overview of glycolysis in *P. falciparum* parasites and the connection to the PPP. Asexual *P. falciparum* parasites reside within erythrocytes of the human host and have a classic biochemical pathway, glycolysis and the PPP. Lactate is the major metabolic end

product of this process. Biochemical reactions that are indicated with double arrows indicate reversible reactions and those indicated with a single arrow are irreversible reactions. Created from (Ginsburg and Abdel-Haleem, 2017).

The primary function of the PPP is the reduction of NADP⁺ to NADPH, which is required by the parasites' antioxidant defence mechanism, for the conversion of ribonucleotides to deoxy-ribonucleotides for subsequent nucleotide biosynthesis (Ginsburg, 2016). In the infected erythrocyte (trophozoite-stage), the activity of PPP is 78-times greater than that of uninfected erythrocytes due to the highly proliferative nature of the parasite (Atamna, Pascarmona and Ginsburg, 1994).

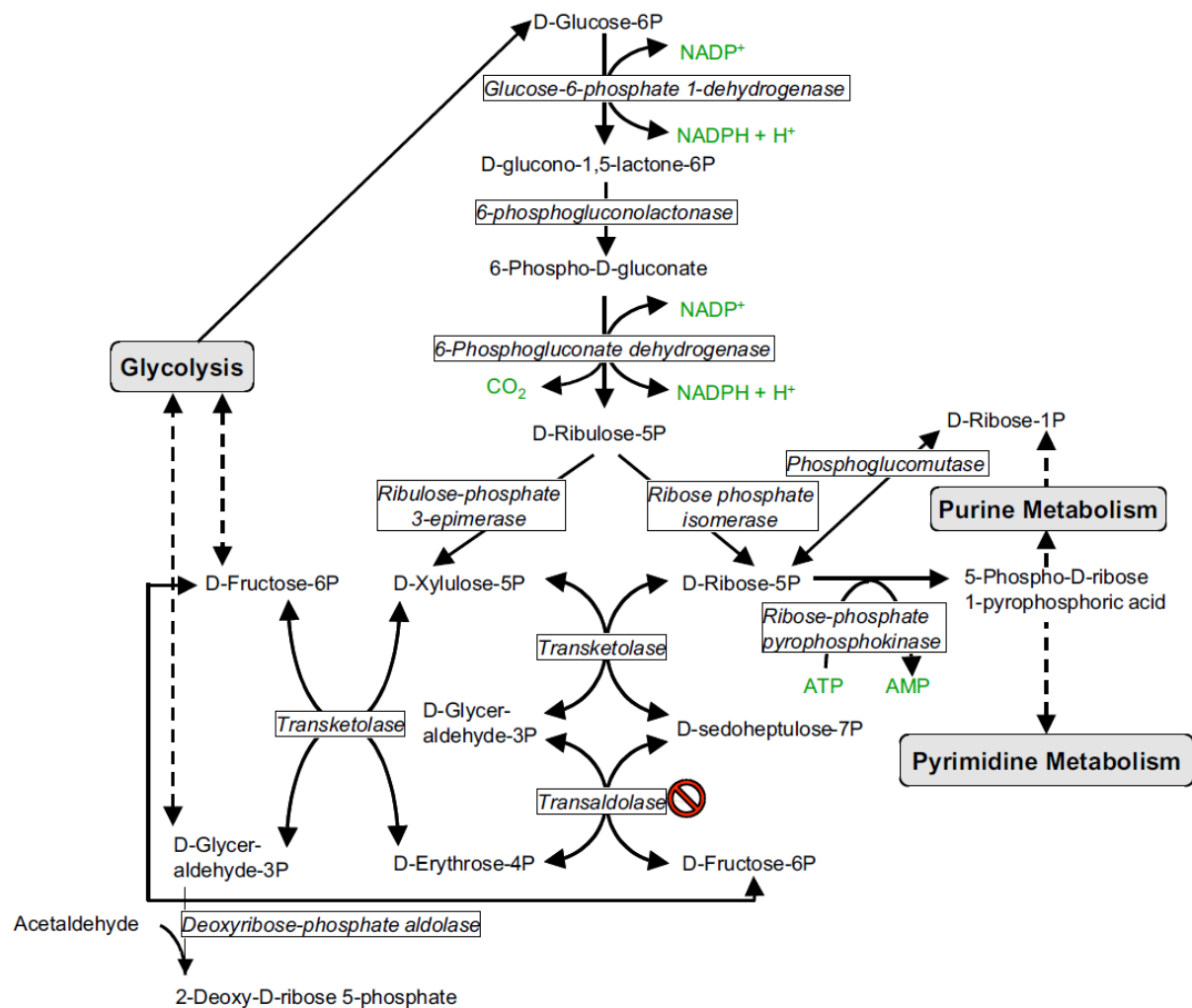


Figure 1.5: The pentose phosphate pathway in the cytoplasm of *Plasmodium*. The PPP is the predominant metabolic pathway that produces NADPH and 5-phospho- α -D-Ribose 1-pyrophosphoric acid. The no entry symbol represents that no gene could be identified for the enzyme transaldolase, however, biochemical evidence suggests that the activity of the enzyme is present in *Plasmodium*. Abbreviations used: phosphate (P). Created from (Bozdech and Ginsburg, 2005).

The enzymes required for a functional PPP have been identified in *P. falciparum* parasites with the sole exception of transaldolase for which no homolog has been identified (Figure 1.5). The PPP consists of two branches, an oxidative branch and a non-oxidative branch that exclusively occurs in the cytoplasm of the parasite. Enzymes catalysing reactions in the oxidative branch of the pathway utilize NADP⁺/NADPH as a cofactor pair. The non-oxidative branch of the PPP can also function in the reverse direction by using fructose-6-phosphate and glyceraldehyde-3-phosphate generated by glycolysis to produce D-ribose-5-phosphate (Bozdech and Ginsburg, 2005). Therefore, due to the reversibility of the PPP, it can function in different modes depending on the metabolic needs of the parasite when both D-ribose-5-phosphate and NADPH are required, only the oxidative branch of the PPP is activated (Figure 1.6, mode 1). When more D-ribose-5-phosphate than NADPH is required (Figure 1.6, mode 2), D-ribose-5-phosphate is produced through the reverse of the non-oxidative branch from fructose-6-phosphate and glyceraldehyde-3-phosphate generated by glycolysis. When more NADPH and ATP than D-ribose-5-phosphate is required, the oxidative and non-oxidative reactions occur and ribulose-5-phosphate is converted to fructose-6-phosphate and glyceraldehyde-3-phosphate for use in glycolysis to produce ATP and NADPH (Figure 1.6, mode 3) (Bozdech and Ginsburg, 2005). The production of NADPH during PPP in *Plasmodium* is critical in the defence against oxidative stress and detoxification of xenobiotics (Barrett, 1997) which aids in parasite survival.

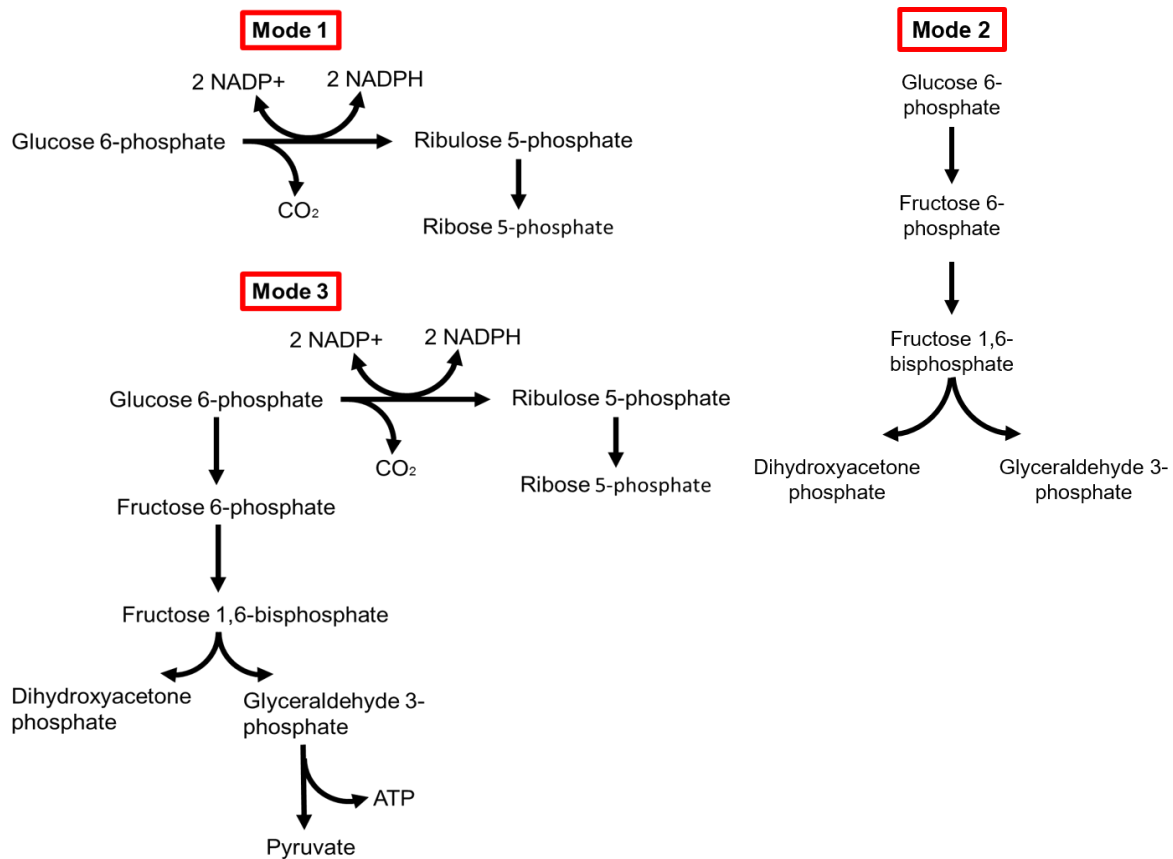


Figure 1.6: The different modes of the PPP in *Plasmodium*. In mode 1, the parasite requires both D-ribose-5-phosphate and NADPH. In mode 2, more ribose 5-phosphate is required than NADPH. Ribose 5-phosphate is synthesized by the non-oxidative branch of the PPP using fructose 6-phosphate and glyceraldehyde 3-phosphate, which are both supplied by glycolysis. Mode 3 involves the biosynthesis of NADPH and ATP but not D-ribose-5-phosphate. To generate both NADPH and ATP, ribulose-5-phosphate is converted to fructose-6-phosphate and glyceraldehyde-3-phosphate, which are directed into glycolysis. Adapted from (Bozdech and Ginsburg, 2005).

Metabolic differences observed between the host and parasite may provide insight into novel biochemical pathways or enzymes, which can be exploited quantitatively through the selection of metabolic pathways or enzymes that exert a high level of metabolic control in the parasite but much less control in the host. The exploitation of metabolic differences may result in the development of novel antimalarial therapeutics that target previously untargeted metabolic pathways (Verlinden *et al.*, 2001).

1.5 Antimalarial therapeutics

Antimalarial therapeutics aim to either prevent or eliminate dormant and circulatory forms of the *Plasmodium* parasite (Hobbs and Duffy, 2011). ACTs have proven effective in the treatment of uncomplicated cases of *P. falciparum* infections (WHO World Malaria Report, 2016). Their efficacy is due to the combination of a fast acting artemisinin component, which is responsible for rapid parasite clearance, and a slow acting drug partner, which eliminates remaining parasites and suppresses the selection of artemisinin resistant parasites (Lunev *et al.*, 2016). Antimalarial compounds can be classified into classes based on either the chemical structure or the mechanism of action: endoperoxides, 4- and 8-aminoquinolines amino alcohols, antifolate, antibiotics, sulphonamides and “other” antimalarial chemical compounds such as riboflavin, methylene blue and atovaquone (Table 1; Delves *et al.*, 2012).

Table 1: The use, mechanism of action and resistance of quinolones, artemisinins and antifolates.

Pharmacological class	Compound name	Use	Mechanism of action	Mechanism of resistance
Quinolines and derivatives	Quinine	Chemotherapy (severe malaria)	Inhibits the polymerization of toxic haem to haemozoin	Mutations in the chloroquine resistance transporter PfCRT and in the multidrug resistance 1 gene, PfMDR1
	Chloroquine disulphate	Chemotherapy (non- <i>falciparum</i> infections) and chemoprophylaxis		Mutations in PfCRT
	Mefloquine	Chemotherapy (non- <i>falciparum</i> infections) and chemoprophylaxis (non-severe <i>P. falciparum</i>)		Mutations in PfMDR1 and PfCRT
	Halofantrine	Treatment of suspected multi-drug resistant <i>P. falciparum</i> infections		
Artemisinins (ART)	Arteether	Treatment of multi-drug resistant <i>P. falciparum</i> infections	Antimalarial activity is due to the presence of an endoperoxide moiety	Mutations of the <i>Kelch 13</i> (K13) gene gives rise to delayed parasite clearance and recrudescence
	Artemether			
	Artesunate			
	Dihydroartemisinin			
Antifolates	Sulfonamides			

	Sulfones	Treatment of non-severe <i>P. falciparum</i> infections which are chloroquine resistant	Inhibition of dihydropteroate synthase (DHPS) which is essential for folate synthesis	Point mutations occurring in DHPS and DHFR genes
	Pyrimethamine	Targets the asexual erythrocytic life cycle and young gametocytes	Inhibition of the folate enzyme, dihydrofolate reductase (DHFR)	
	Biguanides			
	Quinazolines			

Compiled from: Viti, Tatti and Giovannetti, 2016; Warhurst, 2001; Foley and Tilley, 1997; Travassos and Laufer, 2009; Edwards and Odom John, 2016; Krishna, Uhlemann and Haynes, 2004; Mok *et al.*, 2015; Ndiaye *et al.*, 2005.

Despite the various antimalarial classes used therapeutically, the emergence of multidrug resistant strains of *Plasmodium* has hindered efforts to control and eliminate malaria (Cui *et al.*, 2015). Antimalarial resistance has been identified in both *P. vivax* and *P. falciparum* parasites against frequently administered antimalarials, such as chloroquine disulphate (CQ), pyrimethamine (PYR) (Warhurst, 2001; Travassos and Laufer, 2009) and more recently towards artemisinin (ART) (Cui *et al.*, 2015). The genome of *P. falciparum* encodes for multiple predicted transporters; polymorphisms that occur in these transporter proteins mediate resistance towards specific antimalarial compounds through an increase in efflux of the compound from the cell. *Plasmodium falciparum* chloroquine resistant transporter protein (PfCRT) (Table 1) encodes for a food vacuole membrane protein. A single mutation, K76T, mediates chloroquine resistance through an increase in the export of the compound from the food vacuole of the parasite. Parasites that display resistance towards the artemisinin family drugs may contain a Kelch 13 (K13) gene polymorphism (Table 1) which confers a delayed parasite clearance and recrudescence after artemisinin treatment (Cui *et al.*, 2015).

The emergence of artemisinin resistant strains of *P. falciparum* parasites in Southeast Asia (Fairhurst and Dondorp, 2016; Santos and Torres, 2013) and reported cases in Africa (Asia *et al.*, 2017; Sutherland *et al.*, 2017) has galvanised the need to advance the discovery of novel antimalarial compounds through preclinical pipelines and into clinical trials (Fairhurst and Dondorp, 2016). It has been estimated that if multidrug resistant parasites continue to emerge, the mortality rate will increase annually by 150 000 (Lytton, 2016). To reduce the emergence of multidrug resistant *Plasmodium* strains, novel antimalarial compounds with different mode(s) of action (MOA) to that of currently administered antimalarials are required.

1.5.1 Antimalarial drug discovery

Various strategies exist for the identification and development of novel antimalarial compounds, such as phenotypic-based or target-based assays (Figure 1.7). Phenotypic screening involves evaluating large libraries of compounds that cause an inhibition in the viability of the whole-cell parasite. In this case, the biochemical target

of the compound is unknown and is only further investigated during the lead optimisation phase of the drug discovery and development pipeline (Katsuno *et al.*, 2015). Alternatively, with target-based screening, compound libraries are screened against specific biochemical protein targets that were previously shown to be integral for the survival of the parasite (Flannery, Chatterjee and Winzeler, 2013). Subsequently, further studies are required to determine if the inhibition of a biochemical target translates to whole-cell inhibition of parasite proliferation (Flannery, Chatterjee and Winzeler, 2013; Figure 1.7).

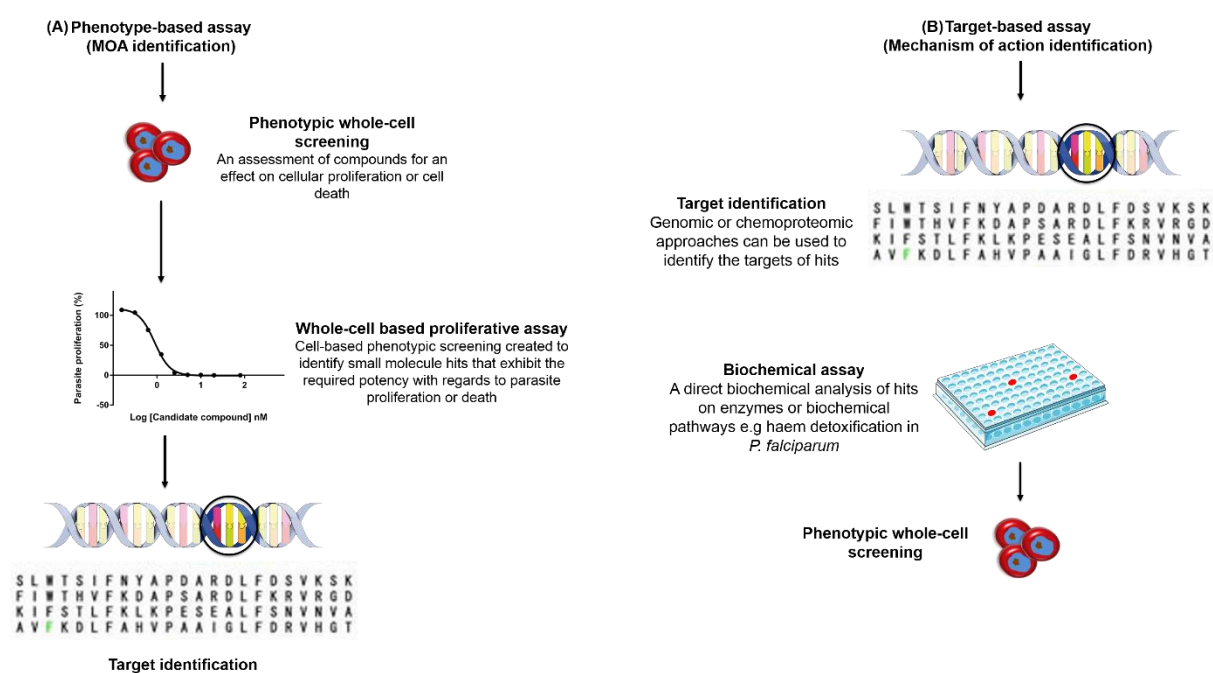


Figure 1.7: The differences between target-based and phenotypic-based assays. (A) Phenotype-based assays begin with whole-cell screening assays to identify if a candidate compound has an effect on biological processes (MOA) such as proliferation or parasite death (Hovlid and Winzeler, 2016). Thereafter; potential compound candidates undergo target identification assays such as affinity purification and metabolic profiling to identify the protein (target) inducing the phenotypic change (Hovlid and Winzeler, 2016). (B) Target-based approaches begin with a pre-identified target (mechanism of action); thereafter, candidate compounds that bind to the target of interest are identified through simple biochemical assays that mimic and miniaturize physiological events (Okombo and Chibale, 2017) and screened in whole-cell screening assays to validate the biological effects of the potential compound candidate.

The majority of antimalarial compounds currently used were identified through phenotypic screening, and not through the pre-identification of a specific target in

Plasmodium (Fidock *et al.*, 2004). This is mostly due to the fact that access to the parasite (and thus the biological target *in situ*) is restricted as the parasite is enclosed by three membrane systems (Bannister, 2001). Phenotypic screening therefore allows for the direct identification of compounds that are able to transgress the three membrane systems of the parasite, which allows for the identification of the MOA of these compounds. The MOA of a compound is defined here as the phenotypic result of a series of biological processes that occur upon exposure of an organism to a chemical entity resulting in either cellular injury, mortality or morbidity (Holsapple *et al.*, 2006; Swinney, 2015). By 2015, approximately 6 million compounds have been screened in this manner, resulting in 25 000 antimalarial compounds with a half maximal activity $<1 \mu\text{M}$ against *P. falciparum* parasites (Wells, van Huijsduijnen and Van Voorhis, 2015). Both phenotypic-based and target-based screening assays represent two complimentary approaches for the identification of viable medicinal chemistry starting points (Okombo and Chibale, 2017). Target-based screens specifically focus on the mechanism of action of a compound, which targets either a biological pathway or protein. The mechanism of action of an antimalarial compound is defined as the specific biochemical interaction between a compound and target to cause a pharmacological effect (Sipes, McQueen and Gandolfi, 1997). For example, the mechanism of action of chloroquine is attributed to the inhibition of the detoxification of haem (protoporphyrin-IX) to non-toxic haemozoin (Chou, Chevli and Fitch, 1980, Figure 1.8).

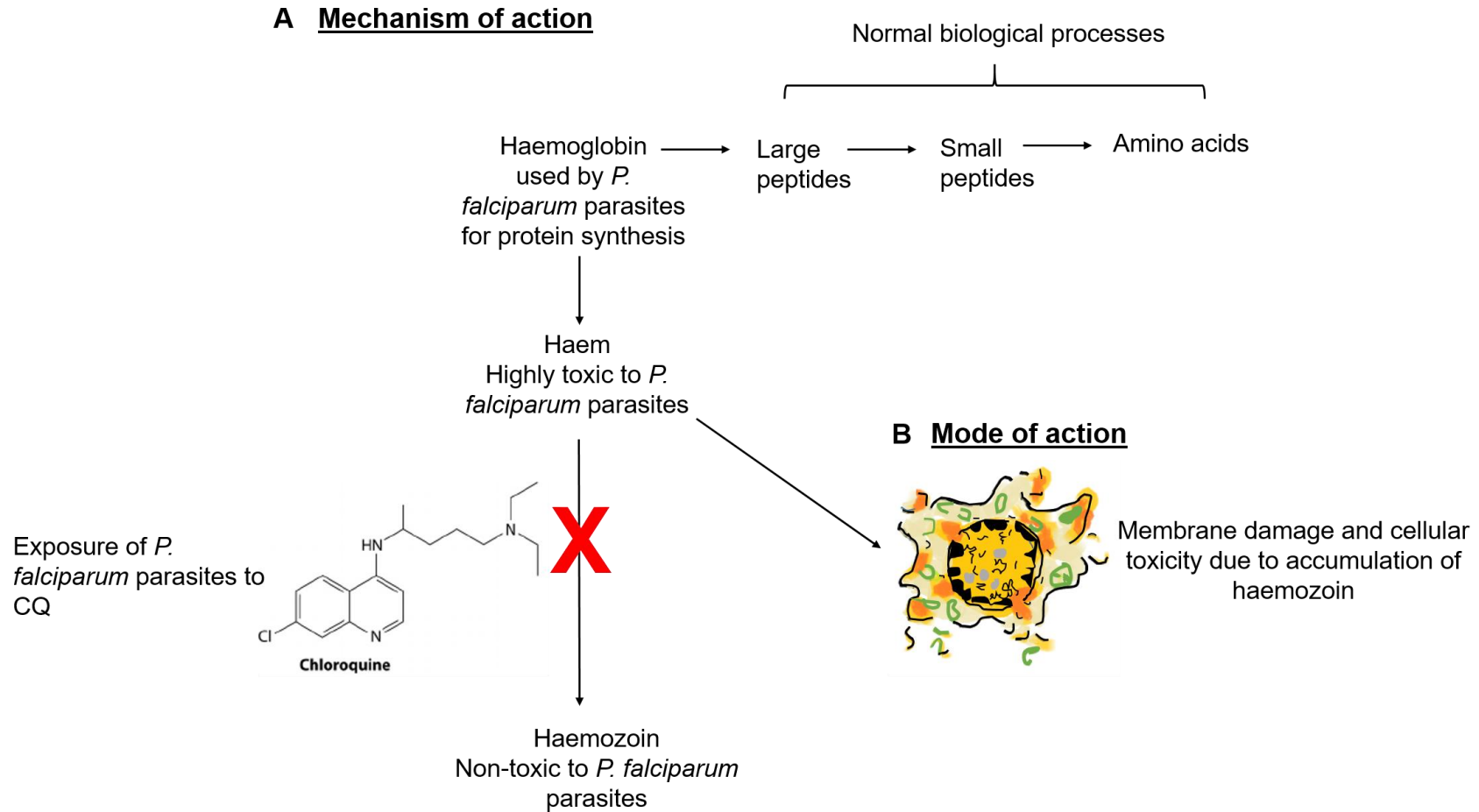


Figure 1.8: The mechanism and mode of action of CQ. In the malaria-infected erythrocyte, the intraerythrocytic parasite catabolizes haemoglobin into amino acids and haem which is its normal biological processes. Haem is a toxic by product of the catabolism of haemoglobin and is bio-mineralized by the parasite into its non-toxic form, haemozoin. However, exposure of the parasite to CQ causes an accumulation of both haem and CQ within the digestive vacuole. This is referred to as the mechanism of action of CQ as it inhibits the detoxification of haem to inert haemozoin (A) which consequently results in its mode of action (B) which is membrane damage and cellular toxicity (Goldberg *et al.*, 1991).

Several techniques have been used in malaria research to identify the mechanism of action of novel and pre-existing antimalarial compounds. Identifying the molecular targets that are responsible for the phenotypic effect observed in whole cell-based assays is often the most challenging and time-consuming step in antimalarial drug discovery (Edwards and Odom John, 2016). Mechanism of action determination techniques include, but are not limited to, resistance screening, metabolic labelling and affinity chromatography.

Resistance screening characterizes the mechanism of action of antimalarial compounds by generating *Plasmodium* parasites that have acquired resistance towards the compound (Erika, David and Winzeler, 2013). Parasites that display resistance towards the compound are cloned, the genomic DNA isolated and sequenced to identify genetic changes that are associated with resistance. Thereafter, the parental and mutant parasite lines are compared to each other to identify mutations or copy number variants (CNVs) (Erika, David and Winzeler, 2013). For example, Witkowski and colleagues (2010) successfully evolved a stable ART resistant line *in vitro* (Witkowski *et al.*, 2010). *P. falciparum* parasites were exposed to ART across a 3-year time frame, which produced a sub-culture of parasites that overcame the toxicity of ART through a quiescence mechanism. It was observed that ART resistant parasites stalled in the ring stage which is less susceptible to ART treatment. The quiescence mechanism is presumed to be a cause of the downregulation of a putative cell cycle regulator, PFE415w (Witkowski *et al.*, 2010).

Metabolic labelling has been frequently used to identify the mechanism of action of antimalarial compounds as it provides insight into unique biological pathways for the identification of novel targets. Traditionally, radiolabelled cysteine or methionine has been used to monitor protein synthesis, while the incorporation of radiolabelled hypoxanthine is used to monitor nucleic acid synthesis. For example, Rosenthal and colleagues (1996) evaluated the effects of vinyl sulfone cysteine protease inhibitors on the metabolic uptake of radiolabelled hypoxanthine and against the cysteine proteinase, falcipain, a

critical haemoglobinase. Several of the compounds inhibited the uptake of hypoxanthine, haemoglobin degradation and the development of the parasite. The effects observed supported the hypothesis that the antimalarial action of vinyl sulfone cysteine protease inhibitors is due to the inhibition of falcipain (Rosenthal *et al.*, 1996).

Affinity chromatography is often used to identify the targets of antimalarial compounds. The technique involves creating an affinity probe that contains both an active and inactive scaffold. The compound that displays drug-like activity is modified so that it can be attached to a column and the lysates of the organism of interest passed over the column. Thereafter, the different fractions are collected and analysed using mass spectrophotometry (Flannery, Fidock and Winzeler, 2013). This technique has been successful in identifying the targets for small molecules in *Plasmodium* such as casein kinase 1, a cyclin dependant kinase, responsible for proliferation of the parasite, which is the intracellular target of purvalanol, a cyclin dependant kinase inhibitor (Knockaert *et al.*, 2000; Kato *et al.*, 2008; Green *et al.*, 2016) .

Nevertheless, mechanism of action techniques have several caveats. The generation of resistant parasite lines results in numerous random mutations due to prolonged culturing and exposure of the parasite to an antimalarial compound (McNamara and Winzeler, 2011). Affinity chromatography methods rely on large quantities of lysates for the identification of a target posing a problem as lysates can be heavily contaminated with red blood cells (Flannery, Fidock and Winzeler, 2013). Target-based screens are limited since not all targets can be successfully purified or prepared in a manner that is suitable for biochemical evaluation. Furthermore, signals obtained from biochemical assays are solely capable of providing a physiological landscape that is either tissue-specific or involved in intracellular drug activity to a limited degree of accuracy (Okombo and Chibale, 2017). Target-based screens are solely used for the identification of the mechanism of action and target of an antimalarial compound. However, if the target cannot be identified through mechanism of

action studies, the MOA of the compound and its effects on the cell can be identified.

The MOA of an antimalarial compound is defined as the phenotypic outcome of a series of biological processes and events that occur upon exposure of an organism to a drug or chemical entity, which results in cellular injury, mortality or morbidity (Holsapple *et al.*, 2006; Swinney, 2015; Figure 1.7). The MOA of chloroquine is the damage to the lysosomal system which is the first morphological change that is observed after exposure of trophozoite-stage *P. falciparum* parasites to the drug (Slater, 1993). The swelling of lysosomes and the accumulation of endocytic vesicles in the central food vacuole containing undigested haemoglobin results in parasite death due to starvation, toxicity, subsequent membrane damage and the inhibition of biochemical reactions (Ginsburg and Golenser, 2003; Slater, 1993, Figure 1.7). MOA studies are performed using phenotypic-based assays instead of target-based assays as they have the advantage of identifying new protein targets unlike target-based screens which are reliant on known biochemical pathways and protein targets (Sykes and Avery, 2013). Antimalarial compounds may also affect multiple protein targets or biochemical pathways, which would not be identified in a typical biochemical screen.

Phenotypic-based methods are capable of identifying the MOA as the whole organism is exposed to the compound and therefore all the protein targets and biological pathways associated with it are subsequently affected. Cell membrane permeability and access to protein targets in their “natural” environment are taken into account in phenotypic screens (Sykes and Avery, 2013). Various strategies exist for the identification of the MOA of an antimalarial compound. The incorporation of [³H]-hypoxanthine by the parasite was the initial assay of choice due to its efficacy and cost-effectiveness (Sykes and Avery, 2013). However, alternative approaches such as, fluorescence based-assays which use stains such as Hoescht, SYBR Green (Johnson *et al.*, 2007) and 4',6-diamidino-2-phenylindole (DAPI) (Baniecki, Wirth and Clardy, 2007), which are incorporated into DNA have been used to measure the effects

of antimalarial compounds on parasite proliferation. Not all of these assays are suitable for high-throughput screening due to several factors such as cost, robustness and assay stability. To circumvent these factors, functional genomic tools which provide a global analyses of the MOA of an antimalarial compound are preferred.

1.6 Functional genomics

Functional genomics is defined as a field of study which aims to describe the functions and interactions of genes and proteins on a genome-wide scale (Bunnik and Roch, 2013). Functional genomic technologies are predominantly focused towards identifying cellular phenotypes, which arise from genome-wide perturbations (Ketteler, 2015). Data obtained from DNA sequencing, gene expression, protein function and metabolic profiling are combined to model dynamic networks that provide insight into gene expression, cell differentiation and cell cycle progression of an organism (Bunnik and Roch, 2013). Functional genomic tools that have been used to elucidate the MOA of antimalarial compounds include transcriptomics (Hu *et al.*, 2010; Siwo *et al.*, 2015) and metabolomics (Cobbold *et al.*, 2016; Allman *et al.*, 2016) which aim to describe the function and interactions of genes.

Transcriptomic analyses involves both the quantitative or qualitative study of RNA molecules on a genome-wide scale. Initially, transcriptomic studies were designed to quantify the expression levels of protein encoding genes with the assumption that it would provide insight into protein expression levels. However, with the progression of transcriptomic technologies, transcriptomics provides a deeper understanding of the complexities of alternate splicing events, the regulation of gene expression and allows for the accurate construction and annotation of complex genomes (Lee *et al.*, 2018). Transcriptomic data for *P. falciparum* MOA determination has been published by Hu *et al.* (2010) and Siwo *et al.* (2015).

Hu and colleagues (2010) identified changes in the gene expression of *P. falciparum* parasites induced by 20 different compounds that inhibit growth of the schizont stage of the intraerythrocytic development cycle. Inhibitors of calcium-dependant kinases and the calcineurin pathway inhibited the development of the schizont stage, whereas compounds such as trichostatin A and staurosporine cause an arrest in the development of the intraerythrocytic developmental cycle (Hu *et al.*, 2010). Siwo and colleagues (2015) transcriptionally profiled the effect of 31 chemically and functionally diverse small molecules on *P. falciparum*. This approach revealed transcriptional changes in specific metabolic pathways and supported the notion that ART targets the cell cycle and lipid metabolism, which leads to parasite death (Siwo *et al.*, 2015). Several intrinsic limitations are associated with transcriptomic techniques. For example, RNA sampling at specific time-points provides a static measurement and may not consider cyclical changes that occur in gene expression patterns of the parasite. Changes in gene expression levels at the transcript level cannot be directly correlated to changes in the levels of proteins. An increase or decrease in total RNA detected on microarrays is not indicative of the downstream processes of protein synthesis, post-transcriptional modification and protein stability in the parasite (Hu, 2016).

By contrast, metabolomics is the study of the entire complement of metabolites in a biological system. The complement of metabolites includes amongst others, sugars, amino acids and fatty acids, which perform critical functions such as energy storage, signal transduction, maintaining cellular structure and feedback regulation of gene expression (Lakshmanan, Rhee and Daily, 2011). Metabolomic-based techniques can measure the complement of metabolites of a cell in response to environmental perturbation such as compound treatment. For example, a dual gas chromatography, GC-MS and liquid chromatography, LC-MS approach was used to identify changes in metabolites induced by antimalarial compounds in asexual parasites (Cobbold *et al.*, 2016). The mechanism of action of several antimalarial compounds has been determined. For example, it was identified that DHA disrupts both haemoglobin catabolism and pyrimidine biosynthesis leading to parasite death. In addition, it was shown

that the mammalian target of rapamycin, Torin 2, affects haemoglobin catabolism in the parasite (Cobbold *et al.*, 2016). In a second study, ultra-high performance liquid chromatography mass-spectrophotometry (UHPLC-MS) was used to create a metabolic fingerprint of 189 antimalarial compounds including 169 drug-like antimalarial compounds. The generation of a metabolic fingerprint provided insight into the modes of action of each antimalarial compound through the generation of information on the biochemical pathways that are perturbed in the parasite subsequent to antimalarial treatment (Allman *et al.*, 2016).

A limitation to metabolomic studies includes the impact of antimalarial treatment on both parasite growth and viability, which may alter metabolite abundances, independent of the target of the compound. In addition, metabolomics approaches require multiple controls and time courses. Samples are destroyed at each time-point, the same sample cannot be measured at each time-point and multiple compound concentrations are required to delineate metabolic alterations from non-specific stress responses (Creek and Barrett, 2014). Taken together, these studies highlight the limitations of both transcriptomic and metabolomic analyses for the delineation of the MOA of antimalarial compounds.

For MOA studies to be routinely used in drug discovery programmes, cost effective, high-throughput and time-efficient platforms are required. Ideally, the platform must allow real-time, *in situ* evaluations of the biochemical perturbations that occur subsequent to compound treatment in the parasite. Phenomics, the study of the complete phenotype of a cell (or organism) in a given point in space and time, may provide such alternatives.

1.7 Phenomics

The phenotype of a cell or organism comprises the complete set of all observable cellular molecular traits manifested due to the combined influence of both genetic and environmental factors (Bilder *et al.*, 2009). Phenomics is

defined as the systematic study of different phenotypes of a cell on a genome wide scale (Bilder *et al.*, 2009). Phenomics has been established in the fields of neuropsychiatry (Bilder *et al.*, 2009; Manev and Manev, 2010), disease therapy (Hegele and Oshima, 2007) and plant phenotyping (Dhondt *et al.* 2013; Goggin *et al.* 2015).

The advent of high-throughput platforms for the analysis of metabolic phenotyping of mammalian cell lines has resulted in a decrease in both cost and time (Bochner *et al.*, 2011). For example, the Seahorse XF analyser (Ribeiro, Giménez-Cassina and Danial, 2015), measures the extracellular acidification rate of culture media as an assessment of glycolysis (Wu *et al.*, 2006) and the BioProfile Analyzer is used to measure the levels of glucose and lactate in cell culture media (Teslaa and Teitell, 2014). By contrast, the Phenotype MicroArray platform can be used to measure energy production by the catabolism of substrates such as carbohydrate sources to generate a phenotypic profile of the organism in real-time (Bochner *et al.*, 2011).

1.7.1 The Phenotype MicroArray platform

The Phenotype MicroArray (PM) platform measures the ability of an organism to use different substrates and measures the resultant NADH that is produced as a product of catabolic pathways (Bochner *et al.*, 2011). The platform aims to quantitatively assess an organism's physiological response to changes in environmental factors and metabolites. The system has medium-throughput capacity through 96-well plates, each pre-coated with either a carbon or nitrogen substrate per individual well (Bochner *et al.*, 2011). The ability of added cell suspensions to use metabolites and produce NADH is evaluated colourimetrically (detection of reduced formazan from tetrazolium) as a proxy of metabolic activity in the cell (Figure 1.9) (Bochner, 2001).

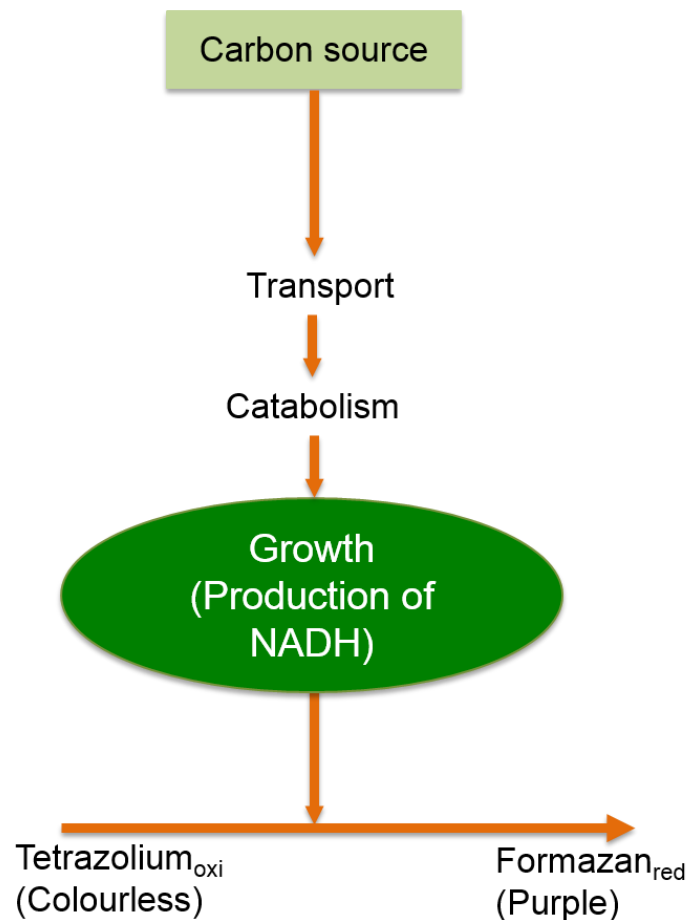


Figure 1.9: The principle of the PM platform for the identification of changes in the phenome of an organism. Normal cellular growth conditions permit the transport and catabolism of substrates resulting in the production of NADH. NADH causes a reduction in a tetrazolium dye from a colourless dye to purple formazan, with the intensity of the colour change of the tetrazolium dye directly related to the amount of NADH produced.

The PM platform has been used to determine bacterial cell metabolism and metabolic regulation (Scaria *et al.*, 2015) it has been used for the assessment of environmental perturbations (Baarda *et al.*, 2017), optimization of growth conditions for cell systems (Lei and Bochner, 2013) and the investigation of the effects of different compounds and chemical stimuli on metabolic pathways (Viti, Tatti and Giovannetti, 2016). The success of using PM in MOA analyses in the identification of novel antimicrobials (Bourne *et al.*, 2012) suggests that this technology may be applied to *P. falciparum* parasites to identify the MOA of antimalarial compounds, specifically the effect that antimalarial compounds have on substrate use by *Plasmodium* parasites.

Therefore, the goal of this project was to perform a proof of principle study of untreated *P. falciparum* parasites compared to parasites treated with known antimalarials. This was achieved by obtaining a phenotypic profile of untreated parasites compared to drug-treated *P. falciparum* parasites with the antimalarial compounds CQ disulphate, DHA and PYR as these compounds have distinctly different intracellular targets and known MOA.

Hypothesis

The Biolog Phenotype MicroArray platform can be used to detect differences in the MOA of antimalarial drugs on asexual *P. falciparum* parasites.

Aim

To establish and compare phenome profiles of *P. falciparum* parasites following drug treatment with the classical antimalarial drugs, CQ disulphate, DHA or PYR as descriptors of the MOA of these drugs.

Objectives

1. To confirm the *in vitro* proliferation inhibition of CQ disulphate, DHA and PYR against asexual forms of *P. falciparum* parasites.
2. To evaluate the viability of *P. falciparum* parasites under standard culturing conditions as well as PM-specific inoculation fluid.
3. Determine phenotypic profiles of treated and untreated parasites using the PM platform.

The results of this work have been presented as follows:

1. Investigating phenotypic differences of *Plasmodium falciparum* parasites following exposure to classical antimalarial drugs. Joshua A. van Biljon R, Birkholtz L.M. and Niemand, J. Medical Research Council's Office for Malaria Research (MOMR) South African Malaria Research Conference, July 2016, University of Pretoria. Poster presentation
2. Investigating phenotypic differences of *Plasmodium falciparum* parasites following exposure to classical antimalarial drugs. Joshua A. Birkholtz L.M. and Niemand J. University of Pretoria Postgraduate Biochemistry Symposium, August 2016 (poster), September 2017 (oral), University of Pretoria.

3. Investigating phenotypic differences of *Plasmodium falciparum* parasites following exposure to classical antimalarial drugs. Joshua A, Birkholtz L.M. and Niemand J. Medical Research Council's Office for Malaria Research (MOMR) South African Malaria Research Conference, November 2017, University of Pretoria. Poster presentation

Chapter 2

Materials and methods

2.1 Ethical clearance

P. falciparum (NF54) was obtained from MR4 (Malaria Research and Reference Reagent Resource Centre, Manassas, Virginia). All experiments were performed at the Malaria Parasite Molecular Laboratory (M²PL), under the supervision of Prof L. Birkholtz and Dr J. Niemand in an access controlled P2 facility. The M²PL has ethical clearance (EC 120821-077; 73/2015) from the Faculty of Natural and Agricultural Sciences as well as Health Sciences for the *in vitro* culturing of *P. falciparum* parasites in human erythrocytes (from volunteer donors) as well as for the handling of human blood.

2.1.1 *In vitro* maintenance of asexual stage *P. falciparum* parasite cultures

Continuous *P. falciparum* asexual cultures (NF54) were maintained (Trager and Jensen, 1976), in either type O⁺ or A⁺ human erythrocytes. Human blood was collected from consenting donors in a blood bag containing citrate phosphate adenine as an anticoagulant (Adcock Ingram, Johannesburg, South Africa) and incubated at 4°C for 12 h. The blood was transferred to centrifuge tubes, re-suspended in a phosphate buffered solution [1x PBS (10 mM Na₂HPO₄; 1.4 mM KH₂PO₄; 137 mM NaCl; 2 mM KCl, pH 7.4)] and centrifuged at 3500g (Boeco centrifuge c-28, Germany) for 10 min at ambient temperature. Thereafter, the supernatant was aspirated and the wash procedure repeated three to four times to remove serum and leukocytes. The washed erythrocytes were re-suspended in an equal volume of filter sterilized (0.2 µm) complete culture medium, (CM): [RPMI-1640 (Sigma-Aldrich, Missouri, USA); 23.81 mM Na₂CO₃; 80 mg/ml gentamycin; 25 mM HEPES, 20 mM glucose; 0.2 mM hypoxanthine and 0.5%

(w/v) Albumax II] resulting in a 50% haematocrit solution and stored at 4°C for no longer than 3-4 weeks.

P. falciparum (NF54) infected erythrocytes stored in cryotubes, were removed from liquid nitrogen storage, thawed and re-suspended in 0.2 ml of sterile 12% (w/v) NaCl solution which was added to increase the osmolarity of the solution, followed by the addition of 1.8 ml of a 0.6% (w/v) NaCl solution. The resultant suspension was centrifuged at 3500g for 5 min at ambient temperature and the supernatant aspirated. The pellet was re-suspended in complete CM supplemented with washed erythrocytes to a final haematocrit concentration of 5%. The culture was transferred to a 75 cm² Cellstar culture flask (Greiner bio-one, Frickenhausen, Germany) and gassed with a hypoxic gas mixture containing 5% O₂, 5% CO₂ and 90% N₂ (Afrox, Johannesburg, South Africa) for 40 s. Gassing the parasite culture with a hypoxic gas mixture mimics the *in vivo* microenvironment within human tissue cells during a *P. falciparum* infection. The flasks were sealed and incubated at 37°C with shaking at 60 rpm (Ratek, Orbital Mixer Incubator, Australia), to increase propagation rates and reduce the prevalence of multiple infections (Allen and Kirk, 2010).

Parasite growth was monitored daily by visual microscopic inspection of Giemsa stained thin blood smears on a microscopy slide at 1000x magnification (Nikon Digital Sight, Nikon, Japan, 100x oil immersion lens). The slides were fixed with methanol (Sigma-Aldrich) for 10 s and stained with a 10% (v/v) Giemsa stain solution (Merck, Darmstadt, Germany) for 5 min. The percentage parasitaemia (percentage of total erythrocytes infected with *P. falciparum* parasites) was maintained at 3-5%, with a 5% haematocrit, with daily replacement of CM.

2.1.2 Sorbitol synchronization of asexual NF54 *P. falciparum* parasites

Sorbitol synchronization was used to selectively lyse mature forms of *P. falciparum* (trophozoites and schizonts) without affecting uninfected erythrocytes or ring stage parasites (Lambros and Vanderberg, 1979). Majority

ring stage intraerythrocytic *P. falciparum* parasite cultures (3% parasitaemia, 5% haematocrit) were centrifuged at 3500g (Boeco centrifuge c-28, Germany) for 2 min at ambient temperature. The supernatant was aspirated and 10x the pellet volume of 5% (w/v) D-sorbitol (pre-heated to 37°C) was added, mixed and incubated at 37°C for 7 min. Thereafter, the suspension was centrifuged at 3500g for 2 min, the supernatant aspirated and 10x the pellet volume of a 1x PBS was used to wash the parasite pellet. The parasite pellet was washed 3x with PBS and then re-suspended in CM (3% parasitaemia, 5% haematocrit).

2.1.3 Intraerythrocytic *P. falciparum* parasite *in vitro* proliferation inhibition assay

The *in vitro* antiplasmodial activity of CQ disulphate, DHA or PYR were confirmed against intraerythrocytic *P. falciparum* NF54 parasites, using the SYBR Green I fluorescence assay (Bennett *et al.*, 2004; Smilkstein *et al.* 2004; Verlinden *et al.* 2015). Erythrocytes lack DNA, whereas *P. falciparum* parasites contain DNA, which can be measured as an indication of proliferation under different conditions. The DNA within the sample can be quantified following staining with a fluorescent dye like SYBR Green I, which selectively binds to double stranded DNA (Smilkstein *et al.*, 2004). A stock solution of CQ disulphate (Sigma-Aldrich, Missouri, USA) at 10 mM was prepared in 1x PBS, filter-sterilized (0.22 µm) and aliquots stored at -20°C. PYR and DHA (Sigma-Aldrich, Missouri, United States) were prepared to a final stock concentration of 10 mM in dimethyl sulfoxide (DMSO) and stored at -20°C. The parasites were synchronised as outlined in section 2.1.2 to obtain approximately 95% ring-stage parasites.

CQ disulphate (1 mM) was used as a positive drug control and was compared to untreated parasites which served as the 100% viable parasite control. Stock solutions of each antimalarial compound was serially diluted before use in CM to achieve desired range of concentrations. Parasite suspensions (1% parasitaemia, 1% haematocrit) were individually treated with the three antimalarial compounds in 96-well microtiter plates. Plates were incubated in a

sealed modular gas chamber, gassed with a hypoxic gas mixture and incubated for 96 h at 37°C. The contents of each well were re-suspended and transferred (100 µl) to a clean 96-well plate. To each well, 100 µl of SYBR Green I lysis buffer [0.2 µl /mL of 10 000 x SYBR Green I dye (Invitrogen); 20 mM Tris (pH 7.5); 5 mM EDTA; 0.008% (w/v) saponin and 0.08% (v/v) Triton X-100] and incubated in the dark at ambient temperature for 1 h. The fluorescence of each well was measured using a GloMax-Multi microplate fluorimeter (Promega, Wisconsin, USA) at an excitation wavelength of 490 nm and an emission wavelength of 540 nm. The proliferation of drug-treated parasites was expressed as a percentage of the untreated parasite proliferation after subtraction of the averaged fluorescence emitted by the negative control. The *in vitro* activity of all three antimalarial compounds was defined as the 50% inhibitory concentration (IC₅₀), which was determined from three independent biological experiments, performed in triplicate with the standard error of the mean indicated. Dose response curves were generated for each test compound using GraphPad Prism® version 6.0c (GraphPad Software, San Diego California, USA).

2.2 Magnetic enrichment of intraerythrocytic *P. falciparum* parasites with VarioMACS

Magnetic enrichment was used to isolate trophozoite and schizont-stage infected erythrocytes from uninfected erythrocytes and other *P. falciparum* life cycle stages. Magnetic-activated cell sorting is a technique used to separate cells by applying a magnetic field (Kim, Wilson and DeRisi, 2010). During the IDC, trophozoite-stage *P. falciparum* parasites catabolize haemoglobin, with concomitant accumulation of toxic haem, which is converted to insoluble haemozoin crystals (Moore *et al.*, 2006). Haemozoin crystals have paramagnetic properties due to the unpaired electrons of the Fe³⁺ iron (Coronado, Nadovich and Spadafora, 2014), which can be used to separate infected trophozoite and late stage trophozoites and schizonts from uninfected erythrocytes using magnetic separation systems (Spadafora, Gerena and Kopydlowski, 2011). A 3% parasitaemia, 5% haematocrit intraerythrocytic *P.*

falciparum parasite culture was centrifuged at 3500g for 3 min and re-suspended in 20 ml complete CM before loading the culture onto a CS column containing plastic coated ferromagnetic fibres placed into the VarioMACS magnetic separator (Miltenyi Biotec, Australia). Trophozoite-stage parasites were retained in the column matrix, while uninfected or ring-stage infected erythrocytes passed through. The CS column was washed with 2 column volumes of pre-warmed (37°C) complete CM. The column was removed from the magnetic field and a 2 column volume of pre-warmed (37°C) complete CM was added to elute the trophozoites. The eluent was centrifuged at 3500g (C-28, Boeco, Germany) for 3 min, the supernatant aspirated and the parasite pellet washed twice with 1x PBS, before re-suspending the parasite pellet in complete CM. Enriched trophozoites recovered from the eluent were counted using an improved-Neubauer, Bright-line haemocytometer (Sigma-Aldrich, Missouri, USA) for subsequent experiments requiring the estimation of parasite cell number. The percentage parasitaemia was estimated by microscopic examination of Giemsa-stained smears to determine the enrichment of the parasite culture.

2.3 Lactate dehydrogenase viability assay

Intraerythrocytic *P. falciparum* parasite viability was measured over time in either CM or in inoculation fluid medium 2 positive (IF-M2+, a proprietary RPMI 1640 without amino acids, phenol red and glutamine, Biolog Inc., Hayward, USA, supplemented with 80 mg/ml gentamycin and supplemented with glucose) in the absence or presence of CQ disulphate, DHA or PYR using the *Plasmodium* lactate dehydrogenase (pLDH) assay. The pLDH assay assesses the metabolic activity of the enzyme lactate dehydrogenase (Wiwanitkit, 2007). pLDH is an enzyme required in carbohydrate metabolism (Basco *et al.*, 1995) which causes the oxidation of lactate to pyruvate with concomitant reduction of 3-acetylpyridine adenine dinucleotide (APAD⁺) to APADH. APADH together with phenazine ethosulfate (PES) causes a reduction in a yellow tetrazolium dye, nitroblue tetrazolium (NBT), to a blue diformazan compound (Markwalter, Davis and Wright, 2016; Makler and Hinrichs, 1993).

The reduction of NBT can only occur if the cell is viable and metabolically active. Enriched trophozoite-infected erythrocytes (~95% parasitaemia, 10 000 cells/well, 50 μ l) were incubated in either CM (positive control for parasite viability) or IF-M2+ in the absence or presence of CQ disulphate (160 nM), DHA (8.8 nM) or PYR (160 nM) added at 10x the IC₅₀ to ensure parasite response, in triplicate. The 96 well microtiter plates were incubated in a sealed modular gas chamber, gassed with a hypoxic gas mixture for 24 h with sampling every 3 h at 37°C.

The signal produced by the samples, was measured every 3 h for 24 h and served as an indicator of pLDH activity. Malstat reagent (0.21 % v/v Triton-100; 222 mM L-(+)-lactic acid; 54.5 mM Tris; 0.166 mM ; APAD (Sigma-Aldrich, Missouri, USA); adjusted to pH 9 with 1 M NaOH) was added to the parasite suspension (1:5 v/v, 120 μ l final volume). Thereafter, 25 μ l PES/NBT (0.239 mM phenazine ethosulphate/1.96 mM NBT) was added to each well and the plates incubated in the dark at ambient temperature for 30 min. The end point reaction products were measured spectrophotometrically using a Multiskan Ascent 354 multiplate scanner (Thermo Labsystems, Finland) at 620 nm. All parameters were calculated from at least three independent experiments. Signal production was determined for parasites treated with CQ disulphate, DHA or PYR at 0 h and 12 h. The controls in each experiment were enriched trophozoites in either CM or IF-M2+ at time-point zero (T=0). Thereafter, background subtraction of either IF-M2+ or CM devoid of erythrocytes was performed. Results from each condition were expressed as the percentage viability compared to CM at T=0. Statistical significance between the means of the different culture medium conditions and antimalarial compounds across the 24 h incubation period was measured with an unpaired student-*t* test. All statistical analyses was generated with GraphPad Prism® version 6.0c (GraphPad Software, San Diego California, USA).

2.4 Determination of carbohydrate substrate use in untreated and treated trophozoite-stage infected erythrocytes using the PM platform

To measure the MOA that CQ disulphate, DHA or PYR treatment has on carbohydrate substrate use, the PM platform was used to obtain a phenotypic profile of treated and untreated trophozoite-stage *P. falciparum* parasite. (Bochner *et al.*, 2011). Untreated enriched trophozoite-stage *P. falciparum* parasites (95% parasitaemia) or parasites treated with 10x IC₅₀ CQ disulphate (160 nM), DHA (8.8 nM) or PYR (160 nM) were seeded at 10 000 cells per well (50 µl) in 96 well microtiter plates that were pre-coated with various carbohydrate substrates (PM-M1, Biolog Inc. Hayward, USA; see appendix table 1 for a complete list of metabolites) in IF-M2+. Following a 1 h incubation at 37°C, Biolog redox dye mix MA (final concentration of 500 µM) was added to each well, the plates placed in a glass desiccator with a lit candle and sealed until the flame burnt out as described previously to create hypoxic conditions (Jensen and Trager, 1977). Thereafter, the plates were sealed and formazan production measured at 37°C every 15 min for 12 h in Biolog's OmniLog® automated incubator-reader. Raw data files were supplied in the format of .oka files, which were subsequently converted to a .csv file using the kinetic module of the Omnilog® PM software (BiOLOG Inc, 2009) for further downstream analysis in RStudio (RStudio Team, 2016).

2.5 Analyses of PM data

PM data (given as “Omnilog values”, Figure 2.1) obtained from Biolog's OmniLog® automated incubator-reader was adjusted by subtracting the average values of the three negative control wells (devoid of carbohydrate substrates) at each time point. Thereafter normalization was performed to reduce variability amongst the different experiments using a modified version of the biolog decomposition script (Vehkala *et al.*, 2015) to analyse Phenotype MicroArray data, using RStudio (v 3.1.1) (R Core Team, 2016). Normalisation was achieved by assigning the array that is the most similar to all the other replicates in the experiment as a reference array, and adjusting the metabolic

profiles of the other replicates to the reference array. This was done by multiplying the non-reference arrays with a normalization factor, which is the ratio of the base curves of the reference array being investigated. The base curves are identified by fitting a linear model for non-active metabolic profiles or a logistic model for active metabolic profiles (Vehkala *et al.*, 2015). Omnilog values' can be graphed as a kinetic response curve to obtain kinetic growth parameters such as the area under the curve (AUC, total formazan production over time), slope (rate of formazan production), length of the lag phase (delay in formazan production) and the maximum formazan production (Figure 2.1) (Bochner, 2001; Vaas *et al.*, 2012).

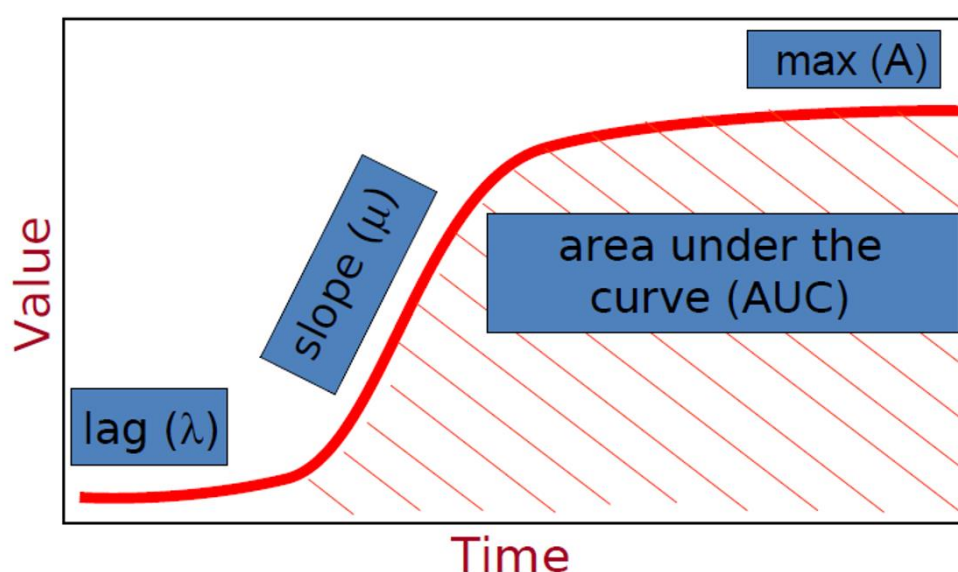


Figure 2.1: A schematic representation of a typical growth curve and the growth parameters that can be determined after performing a PM experiment. The descriptive growth curve parameters, slope, length of the lag phase, area under the curve (AUC), and maximum formazan production are indicated as described in (Vaas, Hofner and Göker, 2013).

Kinetic growth parameters, including the total formazan production (AUC), slope, lag phase and maximum formazan production (Figure 2.1) were subsequently calculated using DuctApe (Galardini *et al.*, 2014). Carbohydrate substrate use was compared between different experimental conditions using a single numerical parameter, termed the activity index value (AIV). The AIV was obtained using the dphenome module of the DuctApe software suite (Galardini *et al.*, 2014). *K*-means clustering of the normalized AUC, slope, lag phase and maximum formazan production generated clustered curves with

similar shapes together, which were then ranked according to the AUC. Both qualitative and quantitative information regarding substrate use is obtained, as an AIV of 0 indicates no metabolic activity and an AIV greater than 0 indicates an increase in metabolic activity, with a higher AIV given to substrates that are metabolized at a greater rate (Galardini *et al.*, 2014).

The AIVs were used to generate a metabolic fingerprint of both untreated and treated trophozoite-stage *P. falciparum* parasites using the supraHex package for R (Fang and Gough, 2014). The supraHex package creates a two-dimensional hexagonal fingerprint that arranges related metabolites into small hexagons or nodes that are arranged radially outward from the centre based on the weight of the vector. The organizational pattern places the most influential metabolite nodes on the outer edge of the suprahexagon while preserving the input data information such as the dimensionality, distribution, distance and clusters, which allows for the identification of metabolites.

A student's t-test was used to compare the normalized Omnilog values obtained for both treated and untreated trophozoites to identify differences in substrate utilization. A *P* value < 0.05 was defined as statistically significant between treated and untreated trophozoites. Multi-scatterplots were generated from the average of all three biological replicates for each treatment condition, using Perseus (Tyanova *et al.*, 2016) with *P*-values indicated.

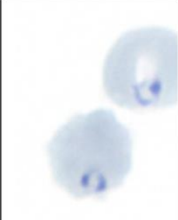

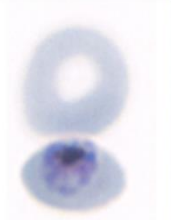
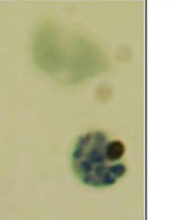
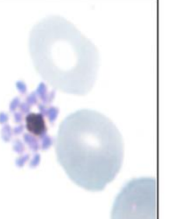
Chapter 3

Results

3.1 *In vitro* *P. falciparum* parasite culturing

Intraerythrocytic asexual *P. falciparum* (NF54) parasite cultures (3% parasitaemia, 5% haematocrit) were maintained *in vitro* and the average parasitaemia determined through light microscopy of Giemsa stained thin smears (Table 2).

Table 2: Microscopic evaluation and characteristic traits of the various life cycle stages of *P. falciparum* (NF54) parasites. The morphology, approximate hours post invasion (~hpi) and characteristic traits of each stage are depicted. Images were captured at a 1000x magnification after Giemsa staining of thin smear blood preparations.

Stage	Ring	Early trophozoite	Late trophozoite	Schizont	Merozoite
Morphology					
~hpi	4-6	10-14	24-28	36-38	46-48

Parasites completed their IDC as expected over 48 h, with each morphological stage observed and no abnormalities present. Ring-stage parasites appear as two small punctate densities containing a thick rim of cytoplasm containing the nucleus, mitochondrion, ribosomes and endoplasmic reticulum at 4-6 hpi (Bannister *et al.*, 2000). Approximately 10-14 hpi after the appearance of ring-stage parasites, early trophozoites are observed, characterized by the presence of a haemozoin crystal. During the next 24-28 hpi the early trophozoites mature into late trophozoites which contains an enlarged nucleus

and the haemozoin crystal (Sherman, 1979). Thereafter, schizogony occurs at ~30 hpi during which DNA synthesis, nuclear division and the formation of merozoite foci occur within the parasite (Bannister *et al.*, 2000). At 46-48 hpi, daughter merozoites were fully formed.

3.2 CQ disulphate, DHA and PYR display nM activity against intraerythrocytic *P. falciparum* parasites

The published inhibition of CQ disulphate, DHA and PYR of *in vitro* proliferation of *P. falciparum* (NF54) parasites was confirmed (Figure 3.1) using a fluorescence-based proliferation assay. Dose-response curves for each compound was obtained and the respective IC₅₀ values determined. IC₅₀ values were confirmed as 16 ± 2 nM for CQ disulphate; 0.88 ± 0.03 nM for DHA and 16 ± 2 nM for PYR, which are in agreement with previously published IC₅₀ values of 10 nM CQ, 0.4 nM DHA and 11 nM PYR (Delves *et al.* 2012; Flannery *et al.* 2013).

Therefore, these three antimalarial compounds were subsequently used to measure the MOA in *P. falciparum* parasites following exposure to these compounds.

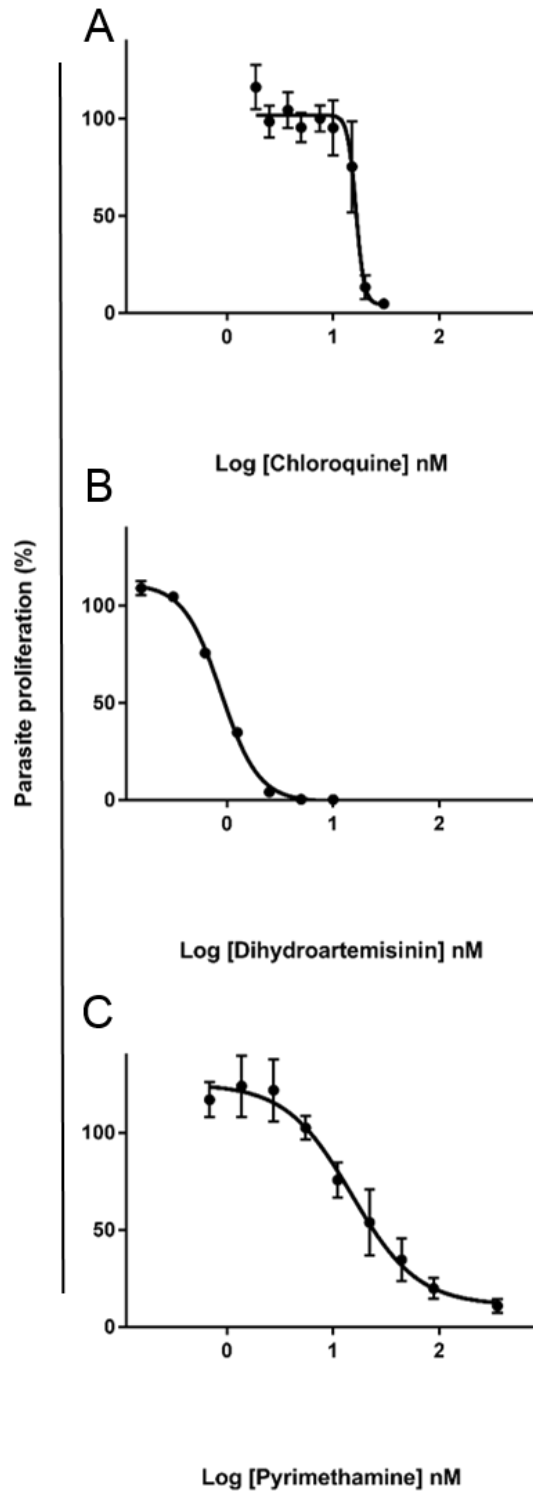


Figure 3.1: Dose response curves of the *in vitro* proliferation inhibition of intraerythrocytic *P. falciparum* NF54 parasites. Proliferation of asexual ring stage parasites (1% parasitaemia, 1% haematocrit) was determined following exposure to (A) CQ disulphate (16 ± 2 nM), (B) DHA (0.88 ± 0.03 nM) and (C) PYR (16 ± 2 nM). Parasite suspensions were incubated for 96 h at 37°C and SYBR Green I added after a 1 h incubation in the dark at ambient temperature. Data obtained are from 3 biological replicates (n=3), each performed in technical triplicate, \pm SEM. Where not shown, the error bars fall within the symbol.

3.3 Enrichment of trophozoite-stage intraerythrocytic *P. falciparum* parasites

To accurately measure the biological processes that occur in *P. falciparum* parasites following exposure to antimalarial compounds, the background erythrocyte signal had to be minimized. This was done by magnetic separation of the trophozoite-stage infected erythrocytes from uninfected erythrocytes. NF54 asexual *P. falciparum* parasite cultures (3% parasitaemia, 5% haematocrit, Figure 3.2 A) were enriched to a ~95% late-stage trophozoite culture (Figure 3.2 B). The morphology of parasite cultures post-enrichment was assessed through Giemsa-stained light microscopy, which revealed the presence of pyknotic forms of the parasite. These are characterised by a reduced cytoplasm volume around a punctate density (arrow in Figure 3.2 B), resulting in only 70-80% of the population being viable based on morphological evaluation. To compensate for this reduction in viability, all experiments were matched, so that a single parasite population was used for each biological repeat for simultaneous evaluation of CQ disulphate, DHA and PYR. Any observed differences were thus solely due to the different effects of the antimalarial compounds, and not due to differences in parasite viability between parasite populations.

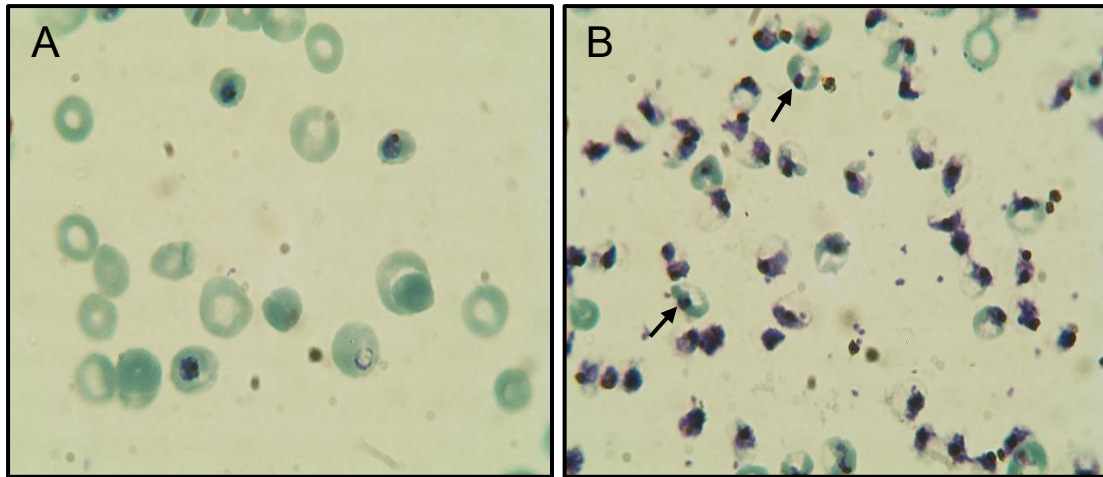


Figure 3.2: Morphology of NF54 *P. falciparum* parasites prior and post-enrichment. (A) Trophozoite parasite cultures (3% parasitaemia and 5% haematocrit) prior to enrichment and (B) post-enrichment (95% parasitaemia). Images were captured at a 1000x magnification after Giemsa staining of thin smear blood preparations. Pyknotic morphology are indicated by arrows.

3.4 Determination of the viability of enriched trophozoite-stage infected erythrocytes under PM assay conditions

One of the advantages of the PM platform for MOA determination is that a single population of live cells is used to measure the biological perturbations arising from compound exposure over time. This implies that one must ensure that the *P. falciparum* parasites remain viable under the assay conditions, so as to only measure biological effects due to compound exposure, and not general cell death responses due to the platform conditions. The viability of enriched trophozoites was assessed by measuring the enzymatic activity of pLDH to quantify parasite viability and metabolic activity (Makler and Hinrichs, 1993).

The first parameter that was assessed was the maximum time that enriched trophozoite-stage *P. falciparum* parasites remain viable in the substrate-poor IF-M2+ required for the PM assay. In this assay, enriched trophozoites were incubated in either CM or IF-M2+ for 24 h, with the pLDH activity measured at specific time points. Parasite viability was expressed as the percentage of untreated CM trophozoites at T=0, to compare differences in viability of parasites incubated in IF-M2+ in comparison to CM.

No difference was observed in parasite viability in either CM or IF-M2+ from 0-12 h ($P > 0.05$, $n = 3$, unpaired t-test). However, a significant reduction in parasite viability in both IF-M2+ and CM was observed after 24 h, in comparison to the 0 h time point (Figure 3.3, $P < 0.05$, $n=3$, unpaired t-test). This indicates that enriched trophozoite-stage parasites are equally viable in both CM and IF-M2+ and the viability is maintained up to 12 h of incubation. Therefore, for subsequent experiments, a 12 h incubation for enriched trophozoite-stage *P. falciparum* parasites was thus used.

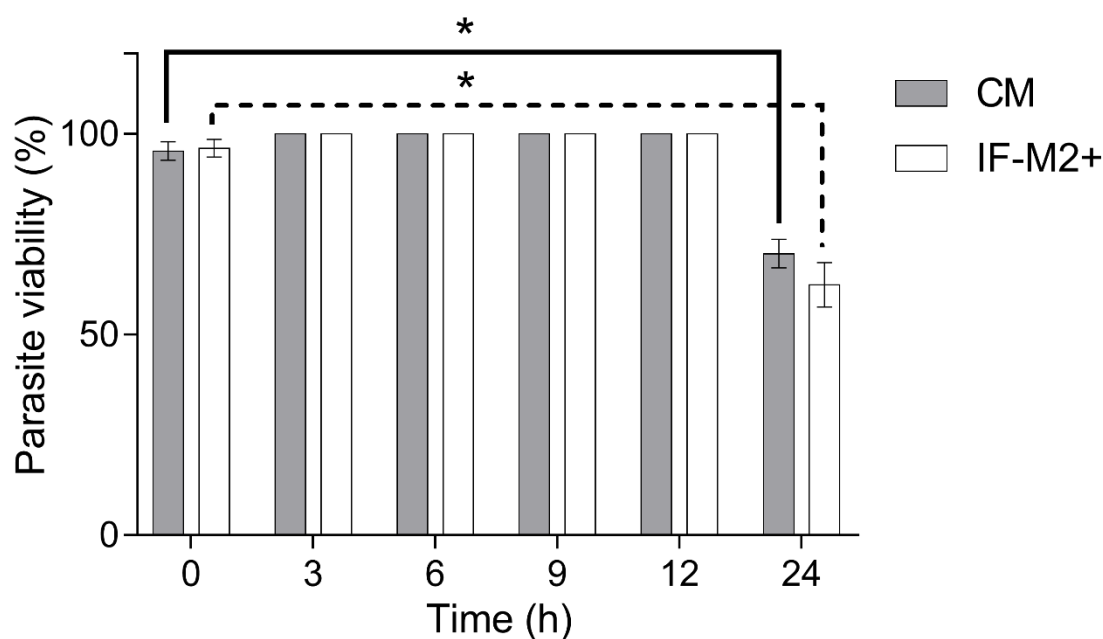


Figure 3.3: The viability of enriched trophozoite-stage *P. falciparum* parasites over time in either CM or IF-M2+. A ~95% enriched trophozoite *P. falciparum* culture (10 000 cells/well) was incubated for 24 h in either CM or IF-M2+. Column graphs represent parasite viability expressed as a percentage of the untreated CM control (T = 0) after background subtraction. Significance is indicated at $P < 0.05$ (*) as determined with a student-*t* test.

Subsequently, it was necessary to determine if each of the antimalarial compounds had a similar effect on parasite viability in IF-M2+ compared to CM (Figure 3.4). This analysis was performed as the available IC_{50} data obtained were derived from parasites incubated in CM and not IF-M2+. IC_{50} determinations cannot be performed in IF-M2+, as IF-M2+ is substrate-poor and will not support the continued proliferation of the parasite across a 96 h incubation time-frame used in the SYBR Green assay. Therefore, enriched

trophozoites were incubated in either CM or IF-M2+ with the antimalarial compounds, CQ disulphate (160 nM), DHA (8.8 nM) or PYR (160 nM) for 12 h, and the pLDH activity measured at 0 h and 12 h (Figure 3.4).

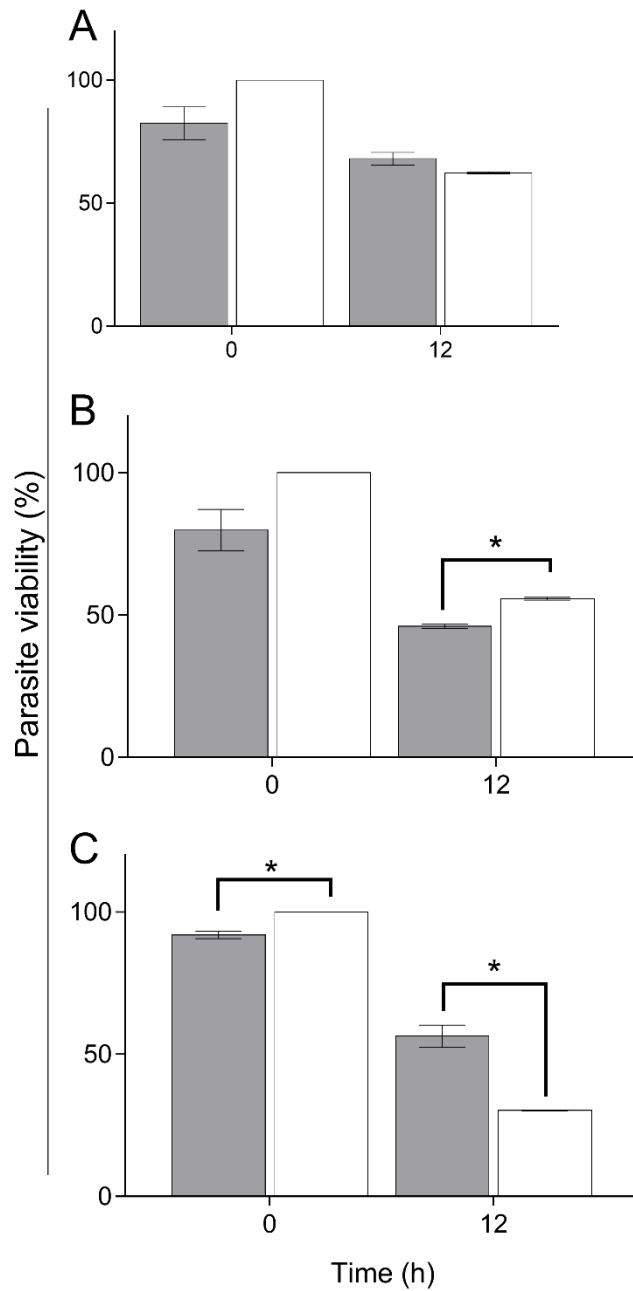


Figure 3.4: The effects of CQ disulphate, DHA or PYR against *P. falciparum* parasites in CM or IF-M2+. A ~95% enriched trophozoite *P. falciparum* parasite culture (10 000 cells/well) was incubated for 12 h in either CM or IF-M2+ with data collected at 0 h and 12 h. *P. falciparum* parasites were exposed to either (A) CQ disulphate (160 nM), (B) DHA (8.8 nM), or (C) PYR (160 nM) after which parasite viability was assessed. Grey bars, parasites incubated in CM; white bars, parasites incubated in IF-M2+ Column graphs represent parasite viability expressed as a percentage of the untreated control after background subtraction. Significance is indicated at $P < 0.05$ (*) as determined with a student-*t* test.

Parasites treated with CQ disulphate displayed no statistically significant difference in either CM or IF-M2+ at both 0 h and 12 h ($P > 0.05$, Figure 3.4 A). This may indicate that both CM and IF-M2+ has no effect on the *in vitro* toxicity of CQ disulphate. Parasites incubated in CM displayed a statistically significantly lower parasite viability in comparison to parasites incubated in IF-M2+, suggesting that the toxicity of DHA is greater in CM than in IF-M2+ ($P < 0.05$, Figure 3.4 B). By contrast, *P. falciparum* parasites exposed to PYR displayed statistically significant differences in parasite viability for both 0 h and 12 h. Parasites incubated in CM displayed a lower parasite viability than parasites incubated in IF-M2+ at 0 h, showing that PYR has a greater toxicity in CM than in IF-M2+ ($P < 0.05$, Figure 3.4 C). The results obtained from these experiments show that variable differences in the effects of each of the antimalarial compounds tested are present when *P. falciparum* parasites are incubated in IF-M2+. Because of these differences, the 10x IC₅₀ values measured against *P. falciparum* parasites in CM were used in the PM platform for phenotypic profile identification of each antimalarial compound.

3.5 PM analyses of carbohydrate substrate use by enriched trophozoite-stage infected erythrocytes in the absence or presence of CQ disulphate, DHA and PYR

To determine the effect that CQ disulphate, DHA or PYR exposure have on carbohydrate substrate use by *P. falciparum* parasites, enriched trophozoite-stage parasites were placed in the mammalian carbohydrate microplate, PM-M1 and formazan production measured every 15 min over 12 h as an indication of NADH production (Figure 3.5). Untreated enriched trophozoite-stage *P. falciparum* parasites served as the untreated control in this experiment. Compared with untreated trophozoite-stage *P. falciparum* parasites, parasites treated with either CQ disulphate, DHA or PYR displayed slight variations in

colour production (Figure 3.5) which may indicate a perturbation in NADH production of treated *P. falciparum* trophozoites.

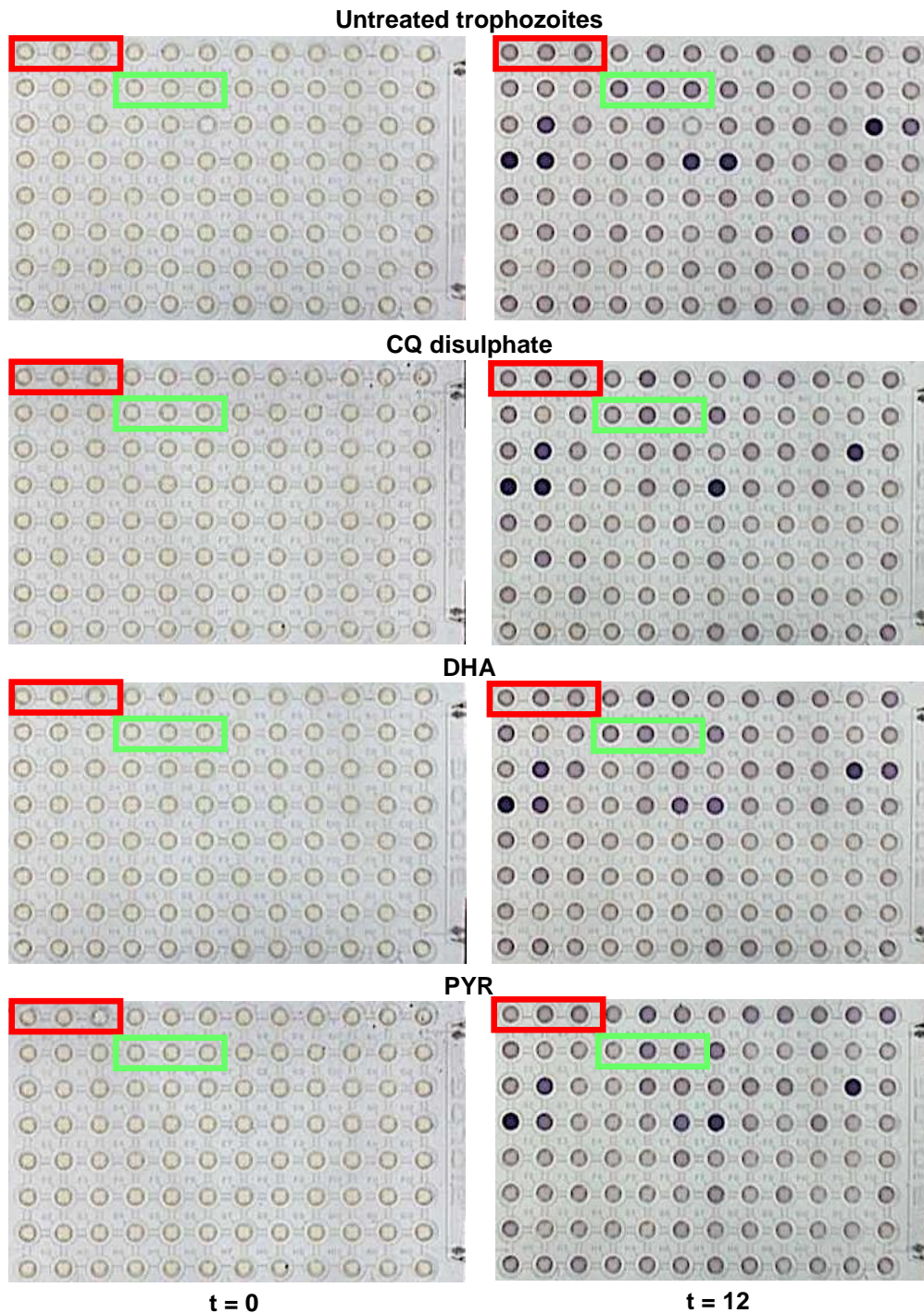
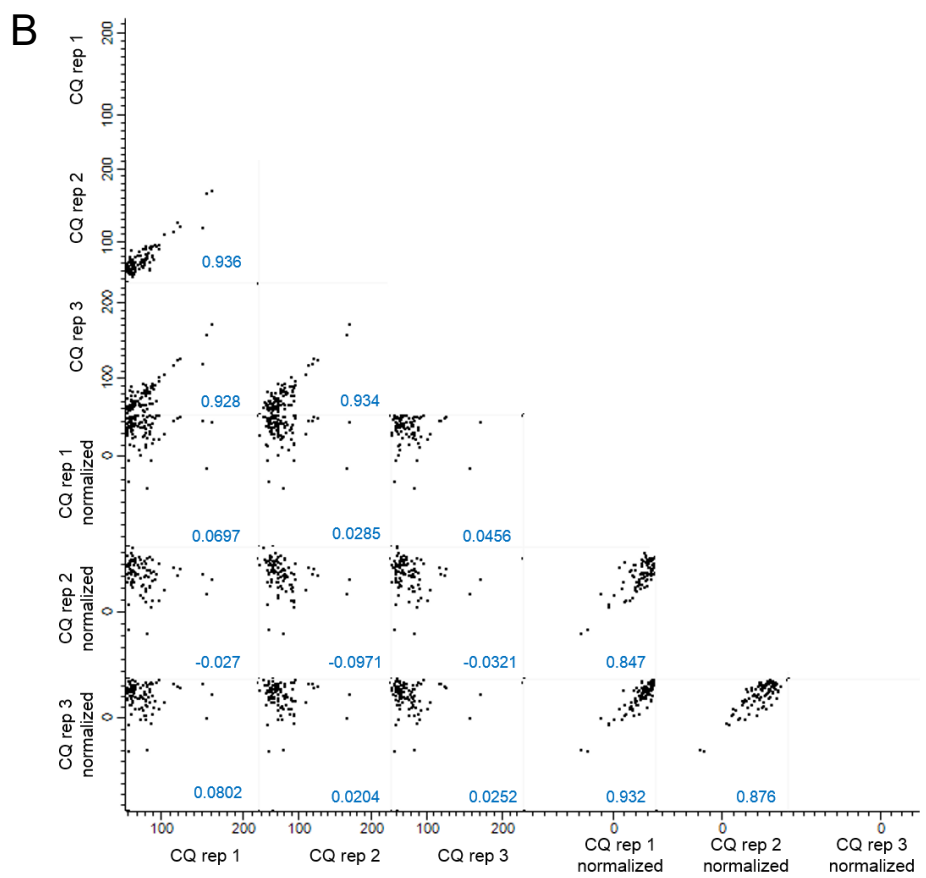
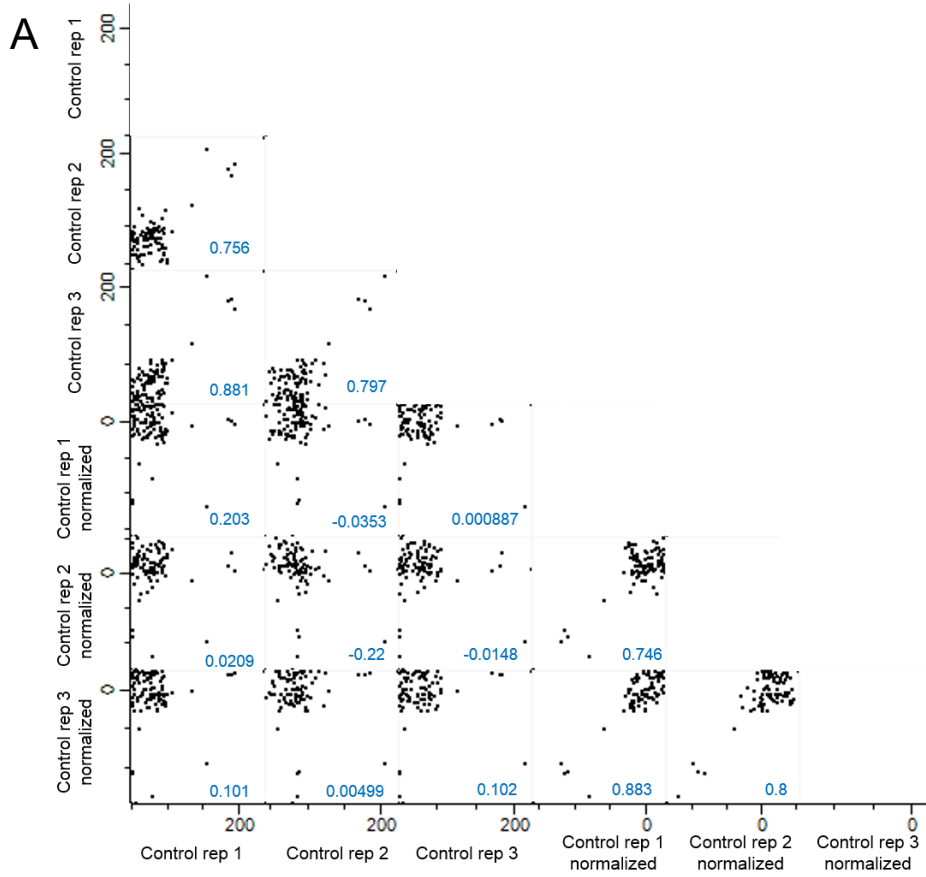


Figure 3.5: Representative PM using the PM-M1 microplate, with measurements at 0 h and 12 h shown. Enriched trophozoite-stage infected erythrocytes (~95% parasitaemia, 10 000 cells/well) in IF-M2+ with dye MA (final concentration 500 μ M) were incubated at 37°C for 12 h, during which formazan production was measured every 15 min. Green blocks indicate the positive control wells (glucose containing wells) and the red blocks the negative control wells (substrate free wells).

The average signal of the three negative control wells in PM-M1 (indicated in red in Figure 3.5), for each test condition was subtracted from the signal produced by the substrate-containing wells. Thereafter, normalisation was performed to ensure that the biological repeats are comparable to one another using a modified version of the Biolog decomposition script (Vehkala *et al.*, 2015). Normalisation is performed to make the arrays of PM experiments comparable with each other. In PM experiments, arrays are not comparable regardless of identical experimental condition, as one array may produce a systematically stronger or weaker signal than the others. Therefore, normalization is required to detect and remove these systematic errors derived from other sources such as differential responses to experimental conditions (Vehkala *et al.*, 2015). Subsequent to normalisation, a multi-scatterplot was generated for each array before and after normalisation to evaluate the outcome of the normalisation (Figure 3.6).

The level of marginal significance, which is indicated by P is provided on each plot. Prior to normalisation, the P values were variable between each array, with untreated trophozoites displaying a P value between the range of -0.03 and -0.02 (Figure 3.6 A). A similar observation was evident for CQ disulphate (Figure 3.6 B), DHA (Figure 3.6 C) and PYR (Figure 3.6 D) treated parasites. Following normalisation, P values ranged between 0.8 and 0.9 for all arrays belonging to a single condition, indicating a high correlation between each array (Figure 3.6).



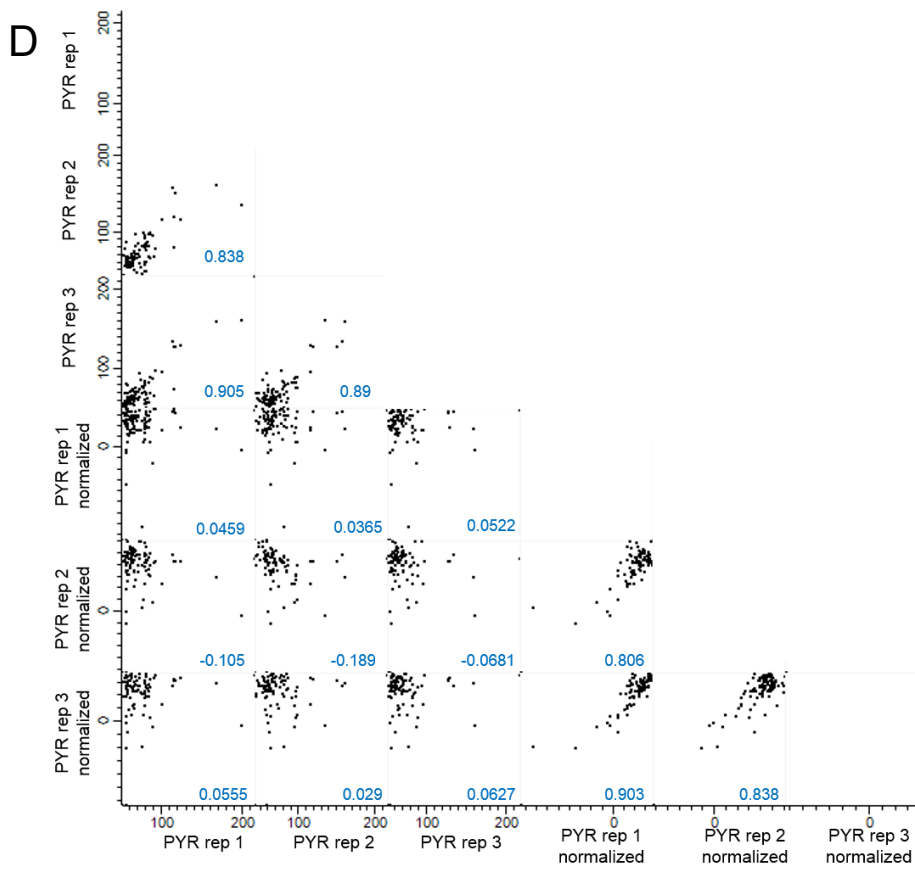
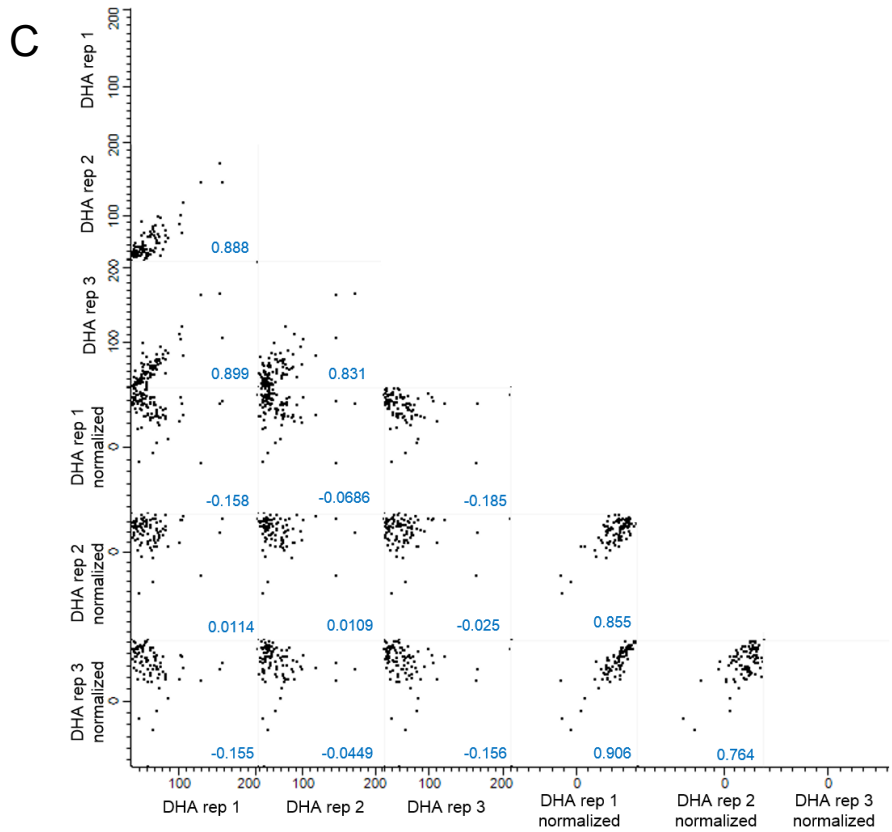


Figure 3.6: Multi-scatterplot of PM data before and after normalisation. The average Omnilog values from each biological replicate, following background

subtraction across the 12 h time-course were compared to one another for untreated trophozoite-stage parasites (A), CQ disulphate (B), DHA (C) and PYR treated (D) parasites. Multi-scatterplot's were generated using Perseus with the level of marginal significance indicated by P , $n = 3$.

The reduction in the variability between each of the treatment conditions subsequently allows each treatment condition to be comparable. The normalised datasets were thus deemed suitable to proceed with a comparative analysis of carbohydrate substrates which were expected to produce a positive signal based on literature relative to the experimental findings.

3.6 A Comparison of the phenotypic profile of untreated trophozoites to literature

The Phenotype MicroArray platform has not been used in enriched trophozoite-stage *P. falciparum* parasites to obtain a baseline phenotypic profile. Therefore, it was necessary to identify which carbohydrate substrates are expected to produce a positive signal, and compare that to the signals obtained for untreated trophozoite parasites. A positive signal was expected if there is evidence in literature that the substrate can be taken up by the parasite and/or evidence that it is metabolized in a biochemical pathway that results in the production of NADH.

To obtain a single quantitative and qualitative value of whether a substrate was metabolized by untreated trophozoite-stage *P. falciparum* parasites, a single AIV was calculated. The AIV provides quantitative information on the ability of an organism to metabolize a single substrate source in a specific culture condition. The parameter is obtained through a k -means clustering algorithm on four normalized growth parameters: the AUC, slope, lag phase and maximum formazan production (Galardini *et al.*, 2014).

The AIV values were calculated from the average of all three biological replicates for untreated *P. falciparum* trophozoites. An AIV value of zero indicated that a substrate did not cause formazan production (NADH production

absent). AIV values ranged from 1-9 (Appendix table 4) indicating an increase in formazan production with 1-4 classified as a weak positive signal, 5-6 a positive signal and 7-9 a very strong positive signal.

A literature analysis of the carbohydrate substrates in PM-M1 revealed that in the untreated trophozoites, 12 carbohydrate substrates were expected to produce a positive signal by untreated trophozoites.

The experimental data obtained from untreated trophozoites, revealed that 27 carbohydrate substrates displayed a positive signal, these substrates included monosaccharides (dextrin, D-glucuronic acid and D-glucosaminic acid), disaccharides (D-maltose, D-cellobiose and gentiobiose) as well as trisaccharides (maltotriose and D-melezitose), dicarboxylic acids (succinic Acid, L-malic Acid and D-malic Acid) and carboxylic acids (γ -Amino-N-Butyric Acid, α -Hydroxy-Butyric Acid, butyric Acid and hexanoic Acid) as shown in the Venn diagram (Figure 3.7) and appendix table 4 . These results reveal that both new and expected signals were identified in the experimental data.

Of the 27 carbohydrate substrates that displayed a positive signal, 12 of these substrates displayed an expected positive signal from the literature and included, glycerol, D-glucose-6-phosphate, α -D-glucose, D-fructose-6-phosphate and D-fructose which are intermediates in the glycolytic pathway (Ginsburg and Abdel-Haleem, 2017; Lian *et al.*, 2009), 3-O-methylglucose which is a non-metabolizable sugar that can be taken into cells via the parasite's glucose transporter system but not metabolized (Diribe and Warhurst, 1985) and adenosine which is required for the synthesis of nucleic acids (Downie, Kirk and Mamoun, 2008; Ginsburg and Abdel-Haleem, 2017). In addition, the reducing sugars, palatinose, D-tagatose and L-sorbose, which have been reported to cause abiotic colour development (Bochner *et al.*, 2011) resulted in the greatest AIV value and signal as expected (Figure 3.7; appendix table 4).

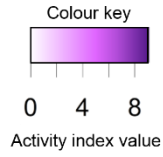


Figure 3.8: Phenotypic profiles of untreated and treated *P. falciparum* trophozoite-stage parasites after 12 h of treatment with either CQ disulphate, DHA or PYR. The average AIV values for each treatment condition were obtained through k-means clustering (four clusters) on five normalized curve parameters, length of the lag phase, total formazan production, maximum formazan production and slope using the dphenome module of DuctApe (Galardini *et al.*, 2014). Thereafter, AIVs were imported into R for the generation of a heat map. White represents a reduction in NADH production and purple represents an increase in NADH production. The colour intensity is directly proportional to the production of NADH. Carbohydrate substrates that have been discussed are indicated by black boxes. Abbreviations used: untreated trophozoites (UT), chloroquine disulphate (CQ), dihydroartemisinin (DHA) and pyrimethamine (PYR).

Overall, global differences and similarities were observed between untreated trophozoites and treated trophozoite-stage *P. falciparum* parasites. The use of 93 carbon sources (excluding the substrate-free wells) displaying diverse levels of complexity (monosaccharides, disaccharides, trisaccharide, polysaccharides and carboxylic acids) were tested. Clear phenotypic differences were observed between untreated trophozoites, CQ disulphate-, DHA- and PYR- treated parasites.

Untreated parasites displayed a highly active glycolytic pathway as evident by the AIV obtained for glucose in comparison to treated parasites (Figure 3.8) highlighting the parasite's dependency on glycolysis for the rapid growth and proliferation of the parasite (Olszewski and Llinás, 2011).

Of the 93 substrates in PM-M1 that displayed a positive signal, CQ disulphate-treated parasites displayed a 40% (37/93), DHA a 13% (12/93) and PYR an 18% (17/93) similarity to that of untreated trophozoite parasites. The differences in similarities for each antimalarial compound to that of untreated trophozoites highlights the differences in MOA of each compound.

DHA-treated parasites displayed the greatest difference in carbon source use whereas, CQ disulphate and PYR-treated parasites displayed minor differences in carbon source use compared to untreated parasites (Figure 3.8). Parasites treated with DHA displayed the greatest alteration in carbohydrate metabolism in comparison to untreated trophozoites. This was specifically

pronounced in tricarboxylic acid cycle intermediates such as succinic acid and D-malic acid as well as substrates that are required for fatty acid metabolism and for nucleic acid biosynthesis. AIVs were decreased for the pyrimidine analog, uridine, and the purine nucleoside, inosine, indicating that nucleic acid biosynthesis is affected by DHA treatment (Figure 3.8). The decreased signal observed for uridine, a glycosylated pyrimidine-analog containing uracil, is consistent with DHA-induced disruption of pyrimidine biosynthesis (Cobbold *et al.*, 2016). The pharmacological class of artemisinins have previously been shown to inhibit the enzyme adenylosuccinate synthase, which is essential for the biosynthesis of purines, therefore, the observed perturbed utilization of the purine inosine corroborates these findings (Ismail *et al.*, 2016).

The altered utilization patterns of DHA-treated parasites are consistent with previous literature reports on the pleiotropic nature of artemisinin compounds which is attributed to the potency of the endoperoxide bridge found in this pharmacological class of compounds (Cobbold *et al.*, 2016). Interestingly, DHA was the sole antimalarial compound that significantly ($P < 0.05$) altered N-acetylneuraminic acid and L-lactic acid utilization (Figure 3.8, Appendix table 2). N-acetylneuraminic acid is a monosaccharide that is found in glycoproteins and is found on the surface of human erythrocytes, commonly referred to as a sialic acid. Sialic acids expressed on the surface of human erythrocytes are involved in invasion by *P. falciparum* parasites (Klotz *et al.*, 1992). The altered utilization of N-acetylneuraminic acid is consistent with previous reports of DHA hindering parasite-host cell invasion (Ismail *et al.*, 2016).

Parasites treated with DHA displayed a decrease signal for the carbohydrate substrate, L-lactic acid, as evident by the decrease in AIV in comparison to untreated parasites (Figure 3.8). The decrease in signal observed may be attributed to a reduction in the interconversion of pyruvate to lactic acid during glycolysis. This may suggest that the enzymatic activity of pLDH is reduced due to an increase in oxidative stress and damage that occurs within the parasites membrane (Meshnick, 2002; Ismail *et al.*, 2016).

Differences in the utilization patterns of fructose phosphates were evident for each treatment condition (Figure 3.8). *P. falciparum* trophozoites treated with CQ disulphate and PYR displayed a significant decrease in signal ($P = 0.001$) in the utilization of D-fructose-6-phosphate (Appendix table 2). By contrast, DHA-treated parasites displayed a significant decrease in signal ($P = 0.01$) in D-fructose metabolism (Appendix table 2). This suggests that all three antimalarial compounds may inhibit the metabolism of fructose phosphates in distinct ways either by the alteration of homeostasis of the digestive vacuole or through the inhibition of transporters on the digestive vacuolar membrane (Cobbold *et al.*, 2016). Compared with CQ disulphate-treated parasites, parasites treated with PYR displayed a decrease signal in the use of the ribonucleoside, adenosine. Adenosine is involved in the process of purine metabolism which is required for the biosynthesis of nucleic acids (Berg, Tymoczko and Stryer, 2002). However, it has been shown that PYR causes an accumulation of NADPH and deoxyuridine monophosphate due to the inhibition of the folate enzyme DHFR (Allman *et al.*, 2016). Therefore, the altered utilization of adenosine may be an effect of the inhibition of DHFR.

Previous changes in substrate metabolism were based on the AIV values for each treatment condition, therefore, to further delineate the phenotypic alterations observed between untreated trophozoites and treated trophozoite-stage *P. falciparum* parasites, the three kinetic parameters, AUC, length of the lag phase and rate of NADH production were assessed (Appendix table 3). Globally, the carbon sources that were identified as displaying alterations in NADH production, was indicated by a statistically significant difference in AIVs compared to untreated trophozoites for the kinetic parameter, AUC. Therefore, both the AIVs and AUC values obtained corroborate each other. Significant differences were identified in the rate of colour production and the length of the lag phase, which distinguishes each antimalarial compound into a specific phenotypic profile (Appendix table 3).

The AIVs obtained for each of the treatment conditions, identified DHA-treated parasites as displaying the greatest perturbation in carbon use. However,

investigation of the kinetic parameters has shown that DHA treatment significantly affects the lag phase of three carbon sources, D-glucuronic acid, D-tagatose and tricarballylic acid (Appendix table 3). This shows that the AIVs obtained are useful to globally compare large datasets, however, information on kinetic parameters such as the rate of colour production and length of the lag phase are masked from analysis. Formazan production curves may have similar AIVs due to similar AUC values, but differ in their curve shapes (Figure 3.9). For example, a formazan production curve with a low rate of colour production but a high final maximum value may have the same AUC as a curve with no lag phase, a high rate of colour production but a low maximum value of final colour production (Figure 3.9).

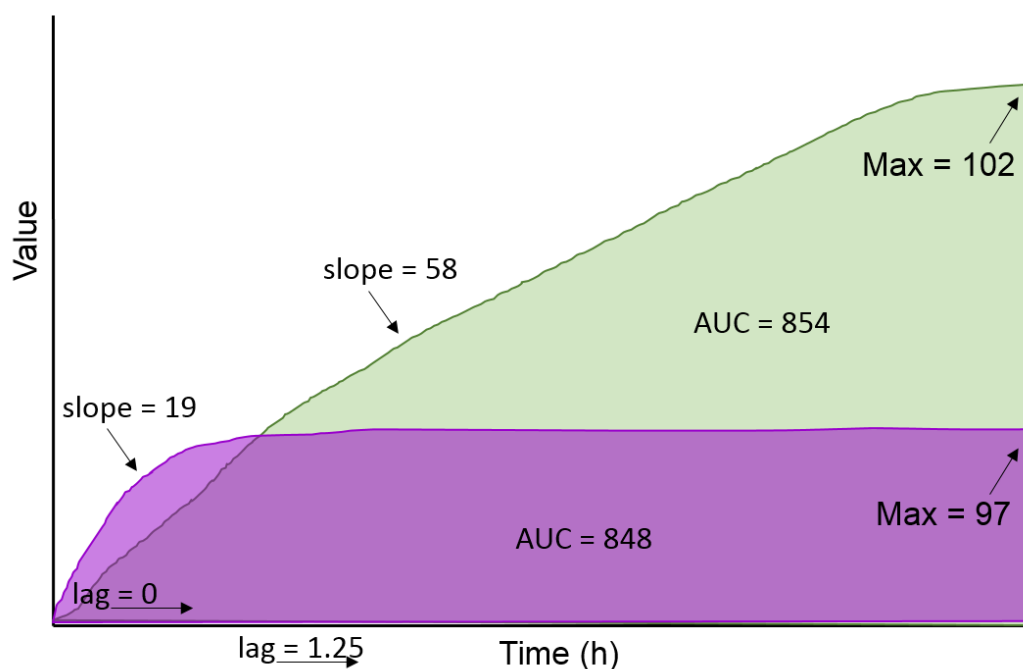


Figure 3.9: A schematic representation of formazan production curves that have similar AUC values but differ in their curve shapes.

This means that each parameter must be investigated individually to obtain a clear profile of carbohydrate substrate use. DHA-treated parasites displayed no statistically significant differences, for all three kinetic parameters ($P > 0.05$) in the catabolism of D-fructose and the tricarboxylic acid cycle intermediates (tricarballylic acid, succinic acid and D-malic acid) to that of untreated trophozoites parasites (Appendix table 3). However, DHA-treated parasites

displayed lower rates of colour production on the carbon sources, α -D-glucose and D-fructose-6-phosphate, an observation that corroborates with previous findings on the multiple molecular targets (Ismail *et al.*, 2016) and pleiotropic nature of DHA (Cobbold *et al.*, 2016). Subsequently DHA does not affect the rate of colour production nor lag phase of the monosaccharides (D-glucuronic acid, D-tagatose, N-acetylneuraminic acid and β -methyl-D-xylopyranoside), disaccharide (α -D-lactose) and complex carbohydrate substrates such as polyalcohols, dicarboxylic acids and alpha-keto acids. However, a statistically significant difference ($P < 0.001$) was observed in the AUC values for each substrate, an observation reflective of the AIVs obtained.

Neither untreated trophozoites nor CQ disulphate-treated parasites were able to produce a colour change on plant-derived carbohydrates such as pectin and arabinose (Appendix table 3). Neither untreated trophozoites nor PYR-treated parasites were capable of producing NADH on the plant-derived carbon sources, melibionnic acid and pectin, a similar result was observed for both CQ disulphate and DHA-treated parasites. The lack of colour formation observed for these carbon sources may be a result of a lack of enzymes responsible for the cleavage of these substrates. CQ disulphate-treated parasites exhibited a prolonged lag phase for the carbon sources L-sorbose and D-fructose. The prolonged lag phase observed for the carbon sources, L-sorbose and D-fructose could be a result of a perturbed adaption period of the parasite to these carbon sources. A significant reduction in the rate of colour production was observed for α -D-glucose and D-fructose-6-phosphate (Appendix table 3), both of these substrates are essential for glycolysis. The perturbed NADH production observed for both α -D-glucose and D-fructose-6-phosphate could be a result of CQ disulphate displaying a broad range of molecular targets in addition to perturbed haemoglobin-derived peptide and amino acid derivatives (Allman *et al.*, 2016)

PYR-treated parasites displayed a significantly lower rate of colour production on the monosaccharide, L-sorbose, with a concomitant prolonged lag phase (Appendix table 3). The significantly lower rate of colour production and

prolonged lag phase ($P < 0.05$) compared to that of untreated trophozoites parasites could be a result of a general decrease in catabolism of L-sorbose subsequent to PYR treatment due to an alteration in glycolysis. PYR-treated parasites displayed no significant perturbations ($P > 0.05$) in the rate of colour production for carbon sources that are essential for glycolysis (α -D-glucose, D-fructose and D-fructose-6-phosphate) showing that PYR-treated parasites have a functional glycolytic pathway in comparison to CQ disulphate and DHA-treated parasites. A global summary of the experimental findings for UT parasites and DHA, CQ disulphate and PYR treated parasites can be found below (Table 3).

Table 3: A summary showing altered substrate use in untreated parasites (A) globally as well as when parasites are treated with (B) DHA, (C) CQ disulphate and (D) PYR.

A.	Untreated parasites	DHA	CQ disulphate	PYR	Biological interpretation
Substrate use out of a total of 93	52 (56%)	12 (13%)	37 (40%)	17 (18%)	DHA and PYR-treated parasites display distinct substrate use to that of untreated parasites, whereas CQ disulphate-treated parasites display the most similar substrate use to that of untreated parasites. The metabolic fingerprint of CQ disulphate-treated parasites more closely resembles the fingerprint obtained for untreated parasites

B. Parameter measured	DHA treatment	Biological interpretation relative to untreated parasites
AIV/AUC	Low α -D-glucose AIV - 2	A low AIV for glucose indicates a perturbation in glycolysis
	Low pyrimidine/purine AIV – uridine (1); inosine (1)	DHA-induced disruption of pyrimidine synthesis

	Low N-acetylneuraminic acid AIV - 1	DHA hinders parasite-host cell invasion
	Low lactic acid AIV - 1	Reduced LDH activity resulting in an increase in oxidative stress and subsequent damage to the parasite membrane
	Low glycerol AIV - 1	DHA alters the metabolism of glycerol which is required for membrane biogenesis during parasite proliferation
	<ul style="list-style-type: none"> • TCA intermediates • Fatty acid metabolism • Nucleic acid biosynthesis 	Parasites treated with DHA display alterations in fatty acid metabolism, nucleic acid biosynthesis and in the metabolism of TCA intermediates
Kinetic parameters	No significant difference in the AUC, lag and rate of colour production for D-fructose and TCA intermediates	No alterations in fructose and TCA intermediate substrate catabolism

	Low colour production of glycolytic intermediates	Perturbation in glycolysis observed
<p>Conclusion: Overall DHA-treatment results in a low AIV and/or kinetic parameters for glycolytic intermediates. DHA is known to cause oxidative stress and damage resulting in a pleiotropic effect. That fact that we observe alterations in metabolic pathways such as glycolysis, fatty acid metabolism and the TCA, is in line with the fact that DHA acts in a pleiotropic nature, confirming the MOA of this drug</p>		

C. Parameter measured	CQ disulphate	Biological interpretation relative to untreated parasites
AIV/AUC	Low D-fructose-6-phosphate AIV - 7	A low AIV may indicate perturbations in the homeostasis of the digestive vacuole of the parasite upon CQ disulphate treatment or inhibition of fructose transporters on the digestive vacuolar membrane of the parasite
Kinetic parameters	Low colour production and prolonged lag phase observed for L-sorbose and D-fructose	Prolonged lag phase observed in these substrates may be due to a prolonged adaptation period of the parasite on these substrates
	Reduction in the rate of colour production observed	Reduction in glycolysis

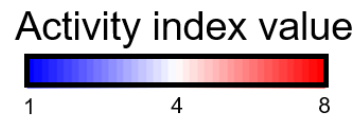
	for α -D-glucose and D-fructose-6-phosphate	
Conclusion: CQ disulphate generally shows a decrease in AIV and/or kinetic parameters for the glycolytic intermediates, D-fructose and D-fructose-6-phosphate. The fact that we observe alterations in glycolysis is in line with the fact that CQ disulphate acts on a broad range of molecular targets confirming the MOA of this drug		

D. Parameter measured	PYR	Biological interpretation relative to untreated parasites
AIV/AUC	Low adenosine AIV - 1	Low AIV implies a reduction in nucleic acid biosynthesis
Kinetic parameters	Lower rate of colour production observed for L-sorbose	Overall decrease in L-sorbose metabolism due to PYR treatment
	Rate of colour production unaffected for α -D-glucose, D-fructose and D-fructose-6-phosphate	PYR-treated parasites display a functional glycolytic pathway

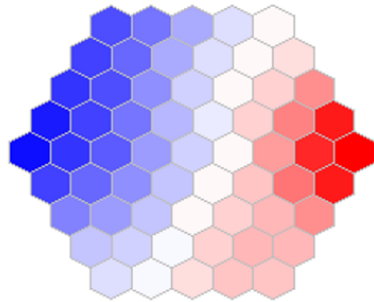
Conclusion: PYR generally shows a decrease in the AIV and/or kinetic parameters for adenosine and L-sorbose. The fact that we do not observe any alterations in glycolytic intermediates is in line with the fact that PYR does not affect glycolysis and solely targets the enzyme. DHFR which is essential for folate biosynthesis, confirming the MOA of this drug.

To visualize the different phenotypic profiles of both treated and untreated trophozoite-stage parasites, the AIVs were projected onto a suprahexagonal landscape. The landscape displays a metabolic fingerprint for a specific treatment condition and serves as a visualization aid to display carbohydrate source utilization perturbations induced by any of the antimalarial compounds studied. It also allows one to easily distinguish and compare the phenotypic profiles between the compounds (Figure 3.10 A). Thereafter, a cluster index (Figure 3.10 B) and cluster hit count map (Figure 3.10 C) were generated to identify which node corresponds to a specific carbohydrate substrate (Appendix table 5). The MetaPrints generated place the most influential nodes on the outer portion of the larger hexagon as observed in Figure 3.10 A.

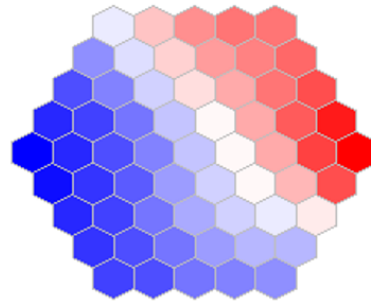
The resulting metabolic fingerprints from treatment with an individual compound may have similar patterns of metabolic perturbation that may resemble the responses observed in other compounds, however, no two compound responses are exactly the same, just as no two fingerprints are identical (Allman *et al.*, 2016).



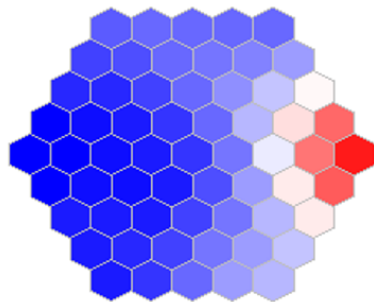
(A) Untreated trophozoites



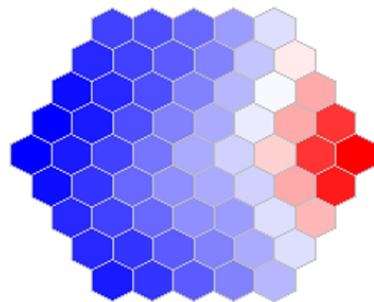
Chloroquine disulphate



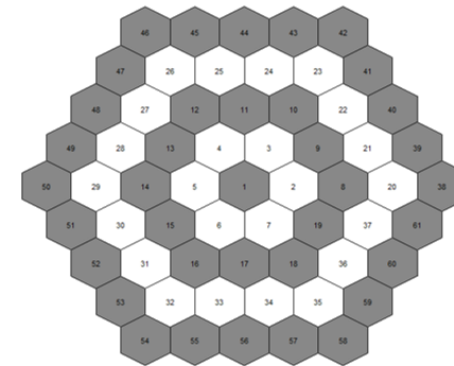
Dihydroartemisinin



Pyrimethamine



(B) Cluster Index



(C) Cluster Hits

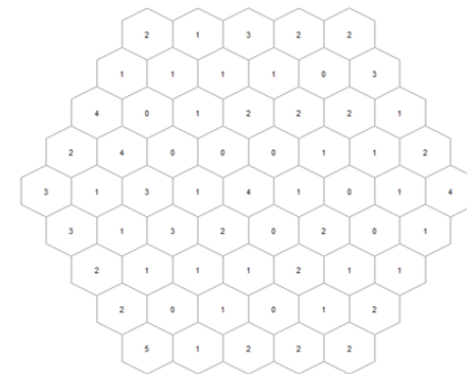


Figure 3.10: Metabolic fingerprint of untreated and treated trophozoite-stage *P. falciparum* parasites. (A) Metabolic fingerprints were assembled based on the phenotypic profiles for each compound and untreated trophozoites, as determined from the average AIVs. (B) Map index demonstrating the MetaPrint node layout, consisting of 61 nodes which are arranged radially outward within a larger hexagon. 96 carbohydrate substrates were used to generate a suprahexagon of optimal size, in this case a hexagon containing 61 smaller hexagons (Appendix table 5). (C) A cluster hit count map corresponding to the number of metabolites mapping to each node was generated.

Examination of the metabolic fingerprints revealed that untreated trophozoites display a greater amount of carbon source utilization in comparison to parasites treated with CQ disulphate, DHA and PYR. This finding corroborates with the AIV values obtained for glycolytic and fructose intermediates. Of the treatments, DHA and PYR resulted in the greatest perturbation in carbon source utilization, however, distinct differences in carbon source perturbation were apparent for each treatment condition (Figure 3.10 A). DHA consistently causes the greatest perturbation in carbon source use in trophozoite-stage *P. falciparum* parasites. CQ disulphate treatment resulted in a metabolic fingerprint similar to that of untreated trophozoites however, a greater proportion of carbon sources were perturbed.

Chapter 4

Discussion

The phenome of an organism refers to the complete set of phenotypes resulting from genetic variation in an organism population (Samuels, 2010). Until recently, the phenotype has been inaccessible with high-throughput techniques, such as DNA microarray, proteomics, transcriptomics and metabolomics (Vaas *et al.*, 2012). This is unfortunate as it is the phenotype that is the object of selection, as every genotype interacts with its environment to produce a range of phenotypes (Ernst, 1997). Limitations of the aforementioned functional genomic techniques for studying the parasite have resulted in static snapshots of the physiological response of the parasite towards environmental perturbations.

The PM system aims to identify the phenome of an organism in response to varying environmental conditions. Previous PM studies have identified the phenome of microbial cells (Blin *et al.*, 2017), mammalian cells (Bochner *et al.*, 2011) and yeast/fungi (Wang *et al.*, 2016). However, to date the platform has not yet been used to determine the phenome of untreated and treated *P. falciparum* parasites with classical antimalarial compounds. This study aimed to identify the phenotypic profiles and MOA of parasites treated with the classical antimalarial compounds, CQ disulphate, DHA or PYR. In doing so, the first experimental data was generated showing that the PM platform can be used for the identification of differences in the MOA of these compounds as well as the phenotypic profiles of treated trophozoite-stage parasites.

The PM platform was used in this study to identify if a phenotypic profile of untreated and treated *P. falciparum* trophozoites can be obtained for subsequent MOA determination. Central carbohydrate metabolism of *P. falciparum* parasites has been extensively reviewed and studied (Olszewski and Llinás, 2011; Sylke *et al.*, 2016; Ginsburg, 2016) as it is the primary energy producing pathway in the parasite during the IDC, while the sexual stages of the parasite rely predominantly on mitochondrial activity (Muller, Cerdan and

Radulescu, 2016). *Plasmodia* inhabit uninfected erythrocytes at the expense of which they undergo rapid and extensive changes in both size and structure. The efficient asexual reproduction and concomitant expansion of the parasite food vacuole during this life stage requires a significant amount of nutritional import and biomass synthesis within the parasite. In addition, the bioenergetics demands of the parasite are likely adjusted to compensate for nutritional cues in the surrounding host cell environment that it encounters during its natural life cycle. Therefore, it is not surprising that glucose metabolism is highly up regulated in *Plasmodia* and because of this, glucose consumption increases drastically, suggesting a dependency of the parasite on the metabolic processes of the host cell (Wendel, 1943). This observation was highlighted by the increased rate of colour production, decreased lag phase and total formazan production of untreated trophozoites (Appendix table 2) in comparison to treated trophozoites.

The phenotypic profiles obtained for each experimental test condition, displayed global differences in carbon utilization between untreated trophozoite and treated parasites. The phenotypic profiles obtained for treated *P. falciparum* trophozoite-stage parasites show that subtle changes are apparent in NADH production, for example, CQ disulphate-treated parasites display a decrease in the rate of colour production of the glycolytic intermediates, α -D-glucose and D-fructose-6-phosphate, in comparison to PYR-treated parasites which retain the ability to produce NADH on glycolytic intermediates.

CQ disulphate treatment resulted in a decrease in glycolysis of *P. falciparum* trophozoite-stage parasites as evident by the decrease in the rate of colour production of glycolytic intermediates. This is an observation which correlates with the reported broad range of molecular targets of the quinoline class of antimalarial compounds (Allman *et al.*, 2016; Penna-Coutinho *et al.*, 2011). CQ disulphate has been reported to interact with the glycolytic enzyme, pLDH, an enzyme critical for the interconversion of pyruvate to lactic acid during glycolysis. CQ disulphate act as a competitive inhibitor for pLDH by binding in the NADH binding pocket. Haem, a by-product of the catabolism of

haemoglobin by *Plasmodium* parasites intoxicates the parasite by competing with NADH for the active site of pLDH. The survival of the parasite is reliant on the ability of it to effectively bio-mineralized haem to inert haemozoin. The quinoline derivatives form complexes with haem preventing the formation haemozoin, which affects energy production in the parasite (Penna-Coutinho *et al.*, 2011). The observation that PYR-treated parasites retain the ability to catabolise glycolytic intermediates correlates with previous findings on the MOA of PYR. PYR targets the bifunctional enzyme DHFR which catalyses the conversion of deoxyuridine monophosphate (dUMP) to deoxythymidine monophosphate (dTMP) (Allman *et al.*, 2016). Therefore, treatment with PYR causes an accumulation of dUMP, showing that glycolysis is not the molecular target of PYR.

Similarly to CQ disulphate-treated parasites, DHA treatment resulted in a lower production of NADH when α -D-glucose and D-fructose-6-phosphate were the sole carbon sources. This has previously been shown by Ismail and colleagues (2016) that identified multiple molecular targets of DHA including the inhibition of the enzymes hexokinase and fructose-bisphosphate aldolase (Ismail *et al.*, 2016). An overview of the phenotypic profiles of CQ disulphate, DHA and PYR treated parasites has shown that variations in carbon use are apparent between each treatment condition, highlighting that the PM platform can be used to identify differences in the MOA of classical antimalarial compounds. The identification of the biological effects of target inhibition may lead to the discovery of novel antimalarial compounds or related protein targets in a biological network. Understanding the cascades that are involved in the action of a drug can aid in the identification of lead compounds that act on different biochemical pathways and for the identification of parent and daughter compounds that may share either the same or different MOA (Kramer and Cohen, 2004). Therefore, the importance of understanding the MOA of a lead or candidate compound cannot be over-stated in the field of malaria research (Birkholtz *et al.*, 2008).

In conclusion, we have demonstrated the potential of the PM platform for the study of real-time phenotypic profiles in trophozoite-stage *P. falciparum* parasites. The identification of carbohydrate substrates that are metabolized by untreated trophozoites, the significant perturbations induced by classical antimalarial compounds coupled with our understanding of carbohydrate metabolism of the parasite have been shown.

As functional genomic tools advance, an increased implementation of high-throughput, time efficient and cost effective techniques will facilitate our understanding of the various biochemical pathways in *P. falciparum* parasites in different life stages. For the purpose of identifying biochemical pathways or targets for the development of novel antimalarial compounds. The PM platform has displayed its utility in the identification of variable MOA between classical antimalarial compounds and the successful generation of phenotypic profiles for treated trophozoite-stage parasites. Additionally, this study serves as a blueprint for future PM studies of drug perturbations in the asexual form of the parasite.

Chapter 5

Concluding discussion

The primary obstacle towards malaria elimination has been the development of resistance of *Plasmodium* parasites towards antimalarial therapeutics (Travassos and Laufer, 2009). Antimalarial compounds have two roles to aid in the elimination of malaria. Firstly, treatment has to prevent the progression of the disease, inhibit the development of gametocytes thereby inhibiting the transmission of the parasite from the human host to the mosquito vector. Secondly, the compounds have to serve as effective forms of chemoprophylaxis and contain transmission blocking properties (Cui *et al.*, 2015). The development of novel antimalarials with different MOA are required to overcome the spread of antimalarial resistant *Plasmodium* species.

The objective of this study was to identify the phenotypic profiles of trophozoite-stage parasites in the absence and presence of classical antimalarial compounds. We aimed to assess the interplay between the environment and drug pressure on *P. falciparum* trophozoite-stage parasites by delineating the MOAs of the classical antimalarial compounds, DHA, CQ disulphate, and PYR. The conventional functional genomic methods implemented provide a static snapshot of an organism in response to environmental perturbations. However, the PM platform has provided a means to obtain a highly dynamic phenotypic profile to identify carbon phenotypes in treated and untreated trophozoites trophozoite-stage *P. falciparum* parasites. Differential phenotypic profiles of carbohydrate metabolism for treated and untreated trophozoite parasites was successfully obtained, as well as, the identification of variations in the MOA of classical antimalarial compounds.

The Phenotype MicroArray platform has indeed provided a means for the identification of global differences and similarities in untreated trophozoites and treated trophozoite-stage *P. falciparum* parasites on several complex and highly diverse carbohydrate sources. Carbohydrate sources were specifically

investigated in this study, due to the parasite's high dependency on glycolysis for maturation and development.

It has been established that *Plasmodium* metabolism is a functional consequence of the “hard-wired”, just in time regulation of gene expression (Hu *et al.*, 2010; Le Roch *et al.*, 2003). *P. falciparum* parasites are highly proliferative and require glucose to support biomass generation through the redirection of glycolytic intermediates into anabolic reactions while maintaining an approximate 90% fermentation flux to lactate (Salcedo-Sora *et al.*, 2014).

The data obtained in this study report the first phenotypic profiles of trophozoite-stage *P. falciparum* parasites in the absence and presence of classical antimalarial compounds. The PM system aims to provide insight into the physiology of an organism at a cellular level (Viti, Tatti and Giovannetti, 2016). Taken together, these results clearly show that the PM platform can be used to obtain a phenotypic profile of parasites treated with CQ disulphate, DHA or PYR and can be used for the identification of differences in the MOA of antimalarial compounds on asexual *P. falciparum* parasites.

Future studies would be aided by incorporating data sets from functional genomic techniques such as transcriptomics and DNA microarray analysis to serve as a comparative analysis for the data obtained from PM experiments, towards the investigation of phenotypic profiles of the parasite for the identification of novel biochemical pathways that may serve as potential drug targets.

References

- Allen, R. J. W. and Kirk, K. (2004) 'The Membrane Potential of the Intraerythrocytic Malaria Parasite *Plasmodium falciparum*.', *The Journal of Biological Chemistry*, 279(12), pp. 11264–11272.
- Allen, R. J. W. and Kirk, K. (2010) '*Plasmodium falciparum* culture : The benefits of shaking.', *Molecular & Biochemical Parasitology*, 169, pp. 63–65.
- Allman, E. L., Painter, H. J., Samra, J., Carrasquilla, M. and Llinás, M. (2016) 'Metabolomic Profiling of the Malaria Box Reveals Antimalarial Target Pathways', *Antimicrobial Agents and Chemotherapy*, pp. 6635-6649.
- Ashley, E. a., Dhorda, M., Fairhurst, R. M., Amaratunga, C., Lim, P., Suon, S., Sreng, S., Anderson, J. M., Mao, S., Sam, B., Sopha, C., Chuor, C. M., Nguon, C., Sovannaroeth, S., Pukrittayakamee, S., Jittamala, P., Chotivanich, K., Chutasmit, K., Suchatsoonthorn, C., Runcharoen, R., Hien, T. T., Thuy-Nhien, N. T., Thanh, N. V., Phu, N. H., Htut, Y., Han, K.-T., Aye, K. H., Mokuolu, O. a., Olaosebikan, R. R., Folaranmi, O. O., Mayxay, M., Khanthavong, M., Hongvanthong, B., Newton, P. N., Onyamboko, M. a., Fanello, C. I., Tshefu, A. K., Mishra, N., Valecha, N., Phyto, A. P., Nosten, F., Yi, P., Tripura, R., Borrmann, S., Bashraheil, M., Peshu, J., Faiz, M. A., Ghose, A., Hossain, M. A., Samad, R., Rahman, M. R., Hasan, M. M., Islam, A., Miotto, O., Amato, R., MacInnis, B., Stalker, J., Kwiatkowski, D. P., Bozdech, Z., Jeeyapant, A., Cheah, P. Y., Sakulthaew, T., Chalk, J., Intharabut, B., Silamut, K., Lee, S. J., Vihokhern, B., Kunasol, C., Imwong, M., Tarning, J., Taylor, W. J., Yeung, S., Woodrow, C. J., Flegg, J. a., Das, D., Smith, J., Venkatesan, M., Plowe, C. V., Stepniewska, K., Guerin, P. J., Dondorp, A. M., Day, N. P. and White, N. J. (2014) 'Spread of Artemisinin Resistance in *Plasmodium falciparum* Malaria.', *New England Journal of Medicine*, 371(5), pp. 411–423.
- Atamna, H., Pascarmona, G. and Ginsburg, H. (1994) 'Hexose-monophosphate shunt activity in intact *Plasmodium falciparum*-infected erythrocytes and in free parasites.', *Molecular and Biochemical Parasitology*, 67(1), pp. 79–89.
- Baarda, B. I., Emerson, S., Proteau, P. J. and Sikora, A. E. (2017) 'Deciphering the function of new gonococcal vaccine antigens using phenotypic microarrays.', *Journal of Bacteriology*, 199(17), pp. 1–24.

Baniecki, M. L., Wirth, D. F. and Clardy, J. (2007) 'High-throughput *Plasmodium falciparum* growth assay for malaria drug discovery.', *Antimicrobial Agents and Chemotherapy*, 51(2), pp. 716–723.

Bannister, L. H. (2001) 'Looking for the exit: How do malaria parasites escape from red blood cells?', *Proceedings of the National Academy of Sciences*, 98(2), pp. 383–384.

Bannister, L. H., Hopkins, J. M., Fowler, R. E., Krishna, S. and Mitchell, G. H. (2000) 'A brief illustrated guide to the ultrastructure of *Plasmodium falciparum* asexual blood stages', *Parasitology Today*, 16(10), pp. 427–433.

Barrett, M. (1997) 'The pentose phosphate pathway and parasitic protozoa.', *Parasitology Today*. Elsevier, 13(1), pp. 11–16.

Basco, L. K., Marquet, F., Makler, M. M. and Le Bras, J. (1995) '*Plasmodium falciparum* and *Plasmodium vivax*: lactate dehydrogenase activity and its application for *in vitro* drug susceptibility assay.', *Experimental parasitology*, 80(2), pp. 260–71.

Bennett, T. N., Paguio, M., Gligorijevic, B., Seudieu, C., Kosar, A. D., Davidson, E., Roepe, P. D., Bennett, T. N., Paguio, M., Gligorijevic, B., Seudieu, C., Kosar, A. D., Davidson, E. and Roepe, P. D. (2004) 'Novel , Rapid , and Inexpensive Cell-Based Quantification of Antimalarial Drug Efficacy Novel , Rapid , and Inexpensive Cell-Based Quantification of Antimalarial Drug Efficacy', *Antimicrobial Agents and Chemotherapy*, 48(5), pp. 1807–1810.

Berg, J., Tymoczko, J. and Stryer, L. (2002) *Biochemistry*. 5th edition. New York: W H Freeman. 2002. Section 16.1, Glycolysis Is an Energy-Conversion Pathway in Many Organisms. Available from: <https://www.ncbi.nlm.nih.gov/books/NBK22593/>.

Bilder, R. M., Sabb, F., Cannon, T. D., London, E. D., Jentsch, J. D., Parker, S., Poldrack, R. a, Evans, C. and Freimer, N. B. (2009) 'Phenomics: The systematic study of phenotypes on a genome- wide scale.', *Neuroscience*, 164(1), pp. 30–42.

Bilder, R., Sabb, F., Parker, S., Kalar, D., Chu, W., Fox, J., Freimer, N. and Poldrack, R. (2009) 'Cognitive Ontologies for Neuropsychiatric Phenomics

Research.', *The Journal of Cognitive Neuropsychiatry.*, 14(4), pp. 419–450.

Biolog Inc (2009) *Converter, file management software, parametric software, phenotype microarray, user guide, part # 90333*. Hayward, CA: Biolog Inc.

Birkholtz, L., van Brummelen, A. C., Clark, K., Niemand, J., Maréchal, E., Llinás, M. and Louw, A. I. (2008) 'Exploring functional genomics for drug target and therapeutics discovery in *Plasmodia*', *Acta Tropica*, 105(2), pp. 113–123.

Blin, C., Passet, V., Touchon, M., Rocha, E. P. C. and Brisse, S. (2017) 'Metabolic diversity of the emerging pathogenic lineages of *Klebsiella pneumoniae*', *Environmental Microbiology*, pp. 1881-1898.

Bochner, B. R. (2001) 'Phenotype MicroArrays for High-Throughput Phenotypic Testing and Assay of Gene Function', *Genome Research*, 11(7), pp. 1246–1255.

Bochner, B. R. (2003) 'Phenotype MicroArrays', *Microbial Genomics and Drug Discovery*, pp. 135–146.

Bochner, B. R., Siri, M., Huang, R. H., Noble, S., Lei, X. H., Clemons, P. A. and Wagner, B. K. (2011) 'Assay of the multiple energy-producing pathways of mammalian cells.', *PLoS ONE*, 6(3), pp. 1–8.

Bourne, C. R., Wakeham, N., Bunce, R. A., Berlin, K. D. and W., B. W. (2012) 'Classifying compound mechanism of action for linking whole cell phenotypes to molecular targets', *Journal of Molecular Recognition.*, 25(4), pp. 216–223.

Bozdech, Z. and Ginsburg, H. (2005) 'Data mining of the transcriptome of *Plasmodium falciparum*: The pentose phosphate pathway and ancillary processes.', *Malaria Journal*, 4, pp. 1–12.

Bruce, M. C., Alano, P., Duthie, S. and Carter, R. (1990) 'Commitment of the malaria parasite *Plasmodium falciparum* to sexual and asexual development.', *Parasitology*, 100(2), pp. 191–200.

Bunnik, E. M. and Roch, K. G. Le (2013) 'An Introduction to Functional Genomics and Systems Biology.', *Advances in wound care*, 2(9), pp. 490–498.

- Chou, A. C., Chevli, R. and Fitch, C. D. (1980) 'Ferriprotoporphyrin IX fulfills the criteria for identification as the chloroquine receptor of malaria parasites.', *Biochemistry*, 19(8), pp. 1543–1549.
- Chu, C. S. and White, N. J. (2016) 'Management of relapsing *Plasmodium vivax* malaria.', *Expert Review of Anti-Infective Therapy*. Taylor & Francis, 14(10), pp. 885–900.
- Cobbold, S. a., Chua, H. H., Nijagal, B., Creek, D. J., Ralph, S. a. and McConville, M. J. (2016) 'Metabolic Dysregulation Induced in *Plasmodium falciparum* by Dihydroartemisinin and Other Front-Line Antimalarial Drugs.', *Journal of Infectious Diseases*, 213(2), pp. 276–86.
- Coronado, L. M., Nadovich, C. T. and Spadafora, C. (2014) 'Malarial Hemozoin: From target to tool.', *Biochimica et Biophysica Acta.*, 1840(6), pp. 2032–2041.
- Cox, F. E. (2002) 'History of Human Parasitology.', *Proceedings of the National Academy of Sciences*, 19(September 2004), pp. 147–153.
- Cox, F. E. (2010) 'History of the discovery of the malaria parasites and their vectors.', *Parasites & vectors*, 3(1), pp. 5.
- Crandall, I. E., Szarek, W. A., Vlahakis, J. Z., Xu, Y., Vohra, R., Sui, J. and Kisilevsky, R. (2007) 'Sulfated cyclodextrins inhibit the entry of *Plasmodium* into red blood cells. Implications for malarial therapy.', *Biochemical Pharmacology*, 73(5), pp. 632–642.
- Creek, D. J. and Barrett, M. P. (2014) 'Determination of antiprotozoal drug mechanisms by metabolomics approaches.', *Parasitology*, 141(1), pp. 83–92.
- Cui, L., Mharakurwa, S., Ndiaye, D., Rathod, P. K. and Rosenthal, P. J. (2015) 'Antimalarial drug resistance: Literature review and activities and findings of the ICEMR network.', *American Journal of Tropical Medicine and Hygiene*, 93(Suppl 3), pp. 57–68.
- Delves, M., Plouffe, D., Scheurer, C., Meister, S., Wittlin, S., Winzeler, E. A., Sinden, R. E. and Leroy, D. (2012) 'The activities of current antimalarial drugs on the life cycle stages of *Plasmodium*: A comparative study with human and rodent parasites.', *PLoS Medicine*, 9(2), pp. e1001169.

Dhondt, S., Wuyts, N. and Inzé, D. (2013) 'Cell to whole-plant phenotyping: The best is yet to come', *Trends in Plant Science*, 18(8), pp. 1360–1385.

Diribe, C. . and Warhurst, D. C. (1985) 'A study of the uptake of chloroquine in malaria-infected erythrocytes.', *Biochemical Pharmacology*, 34(17), pp. 3019–3027.

Divo, A. A., Geary, T. G., Davis, N. L. and Jensen, J. B. (1985) 'Nutritional Requirements of *Plasmodium falciparum* in Culture. I. Exogenously Supplied Dialyzable Components Necessary for Continuous Growth.', *The Journal of Protozoology*, 32(1), pp. 59–64.

Dondorp, A. M., Nosten, F., Yi, P., Das, D., Phyo, A. P., Tarning, J., Ph, D., Lwin, K. M., Ariey, F., Hanpithakpong, W., Lee, S. J., Ringwald, P., Silamut, K., Herdman, T., An, S. S., Yeung, S., Socheat, D. and White, N. J. (2009) 'Artemisinin resistance in *Plasmodium falciparum* malaria.', *Drug Therapy*, 361(5), pp. 455–467.

Downie, M. J., Kirk, K. and Mamoun, C. Ben (2008) 'Purine salvage pathways in the intraerythrocytic malaria parasite *Plasmodium falciparum*.', *Eukaryotic Cell*, 7(8), pp. 1231–1237.

Dvorak, J. A., Miller, L. H., Whitehouse, W. C. and Shiroishi, T. (1975) 'Invasion of erythrocytes by malaria merozoites.', *Science*, 187(4178), pp. 748-750.

Edwards, R. L. and Odom John, A. R. (2016) 'Muddled mechanisms: recent progress towards antimalarial target identification.', *F1000Research*, 5(0), pp. 2514.

Erika, F., David, F. and Winzeler, E. (2013) 'Using genetic methods to define the targets of compounds with antimalarial activity.', *Journal of Medicinal Chemistry*, 56(20), pp. 1–21.

Ernst, M. (1997) 'The objects of selection', *Proceedings of the National Academy of Sciences of the United States of America*, 94(March), pp. 2091–2094.

Fairhurst, R. M. and Dondorp, A. M. (2016) 'Artemisinin-resistant *Plasmodium falciparum* malaria.', *Microbiology Spectrum*, 4(3), pp. 1–25.

Fang, H. and Gough, J. (2014) 'SupraHex: An R/Bioconductor package for tabular omics data analysis using a supra-hexagonal map.', *Biochemical and Biophysical Research Communications*. Elsevier Inc., 443(1), pp. 285–289.

Feng, L., Culleton, R., Zhang, M., Ramaprasad, A. and von Seidlein, L. (2017) 'Emergence of Indigenous Artemisinin-Resistant *Plasmodium falciparum* in Africa.', *The New England Journal of Medicine*, 376(10), pp. 1–3.

Fidock, D. a, Rosenthal, P. J., Croft, S. L., Brun, R. and Nwaka, S. (2004) 'Antimalarial drug discovery: efficacy models for compound screening.', *Nature reviews. Drug discovery*, 3(6), pp. 509–520.

Field, J. W. and Shute, P. G. (1956) *The Microscopic Diagnosis of Human Malaria. II. A Morphological Study of the Erythroeytic Parasites.*, *Studies from the Institute for Medical Research, Federated Malay States*. Kuala Lumpur: Govt. Press.

Flannery, E., Fidock, D. and Winzeler, E. (2013) 'Using genetic methods to define the targets of compounds with antimalarial activity.', *Journal of Medicinal Chemistry.*, 56(20), pp. 1–21.

Flannery, E. L., Chatterjee, A. K. and Winzeler, E. A. (2013) 'Antimalarial Drug Discovery: Approaches and Progress towards New Medicines.', *Nature Reviews Microbiology Rev Microbiol.*, 11(12), pp. 849–862.

Foley, M. and Tilley, L. (1997) 'Quinoline antimalarials: Mechanisms of action and resistance', *International Journal for Parasitology*, 27(2), pp. 231–240.

Galardini, M., Mengoni, A., Biondi, E. G., Semeraro, R., Florio, A., Bazzicalupo, M., Benedetti, A. and Mocali, S. (2014) 'DuctApe : A suite for the analysis and correlation of genomic and OmniLog™ Phenotype Microarray data.', *Genomics*. Elsevier Inc., 103(1), pp. 1–10.

Ginsburg, H. (2016) *The biochemistry of Plasmodium falciparum: An updated overview.*, *Recent Advances in Malaria*.

Ginsburg, H. and Abdel-Haleem, A. M. (2017) 'Malaria Parasite Metabolic Pathways (MPMP) Upgraded with Targeted Chemical Compounds.', *Trends in Parasitology*. Elsevier, 32(1), pp. 7–9.

Ginsburg, H. and Golenser, J. (2003) 'Glutathione is involved in the antimalarial action of chloroquine and its modulation affects drug sensitivity of human and murine species of *Plasmodium*.' , *Redox report : communications in free radical research*, 8(5), pp. 276–9.

Ginsburg, H., Krugliak, M., Eidelman, O. and Ioav Cabantchik, Z. (1983) 'New permeability pathways induced in membranes of *Plasmodium falciparum* infected erythrocytes.' , *Molecular and Biochemical Parasitology*, 8(2), pp. 177–190.

Goldberg, D. E., Slater, A. F., Beavis, R., Chait, B., Cerami, A. and Henderson, G. B. (1991) 'Hemoglobin degradation in the human malaria pathogen *Plasmodium falciparum*: a catabolic pathway initiated by a specific aspartic protease.' , *The Journal of Experimental Medicine*, 173(4), pp. 961–9.

Green, J. L., Moon, R. W., Whalley, D., Bowyer, P. W., Wallace, C., Rochani, A., Nageshan, R. K., Howell, S. A., Grainger, M., Jones, H. M., Ansell, K. H., Chapman, T. M., Taylor, D. L., Osborne, S. A., Baker, D. A., Tatu, U. and Holder, A. (2016) 'Dependent Protein Kinase 1 Also Target Cyclic GMP-Dependent Protein Kinase and Heat Shock Protein 90 To Kill the Parasite at Different Stages of Intracellular Development.' , *Antimicrobial agents and chemotherapy*, 60(3), pp. 1464–1475.

Griffin, J. T., Hollingsworth, T. D., Okell, L. C., Churcher, T. S., White, M., Hinsley, W., Bousema, T., Drakeley, C. J., Ferguson, N. M., Basáñez, M.-G. and Ghani, A. C. (2010) 'Reducing *Plasmodium falciparum* malaria transmission in Africa: A model-based evaluation of intervention strategies.' , *PLoS Medicine*, 7(8), pp. e1000324.

Hegele, R. A. and Oshima, J. (2007) 'Phenomics and lamins: From disease to therapy' , *Experimental Cell Research*, 313(10), pp. 2134–2143.

Hobbs, C. and Duffy, P. (2011) 'Drugs for malaria: something old, something new, something borrowed' , *F1000 Biology Reports*, 3(November), pp. 1–9.

Holsapple, M. P., Pitot, H. C., Cohen, S. H., Boobis, A. R., Klaunig, J. E., Pastoor, T., Dellarco, V. L. and Dragan, Y. P. (2006) 'Mode of action in relevance of rodent liver tumors to human cancer risk' , *Toxicological Sciences*, 89(1), pp. 51–56.

Hovlid, M. L. and Winzeler, E. A. (2016) 'Phenotypic Screens in Antimalarial Drug Discovery.', *Trends in Parasitology*. Elsevier Ltd, 32(9), pp. 697–707.

Howes, R. E., Battle, K. E., Mendis, K. N., Smith, D. L., Cibulskis, R. E., Baird, J. K. and Hay, S. I. (2016) 'Global epidemiology of *Plasmodium vivax*.', *American Journal of Tropical Medicine and Hygiene*, 95(Suppl 6), pp. 15–34.

Hu, G., Cabrera, A., Kono, M., Mok, S., Chaal, B. K., Haase, S., Engelberg, K., Cheemadan, S., Spielmann, T., Preiser, P. R., Gilberger, T.-W. and Bozdech, Z. (2010) 'Transcriptional profiling of growth perturbations of the human malaria parasite *Plasmodium falciparum*.', *Nature Biotechnology*, 28(1), pp. 91–98.

Hu, W. (2016) 'Microarray analysis of PBMC after *Plasmodium falciparum* infection: Molecular insights into disease pathogenesis.', *Asian Pacific Journal of Tropical Medicine*. Elsevier B.V., 9(4), pp. 313–323.

Ismail, H. M., Barton, V., Phanchana, M., Charoensutthivarakul, S., Wong, M. H. L., Hemingway, J., Biagini, G. A., O'Neill, P. M. and Ward, S. A. (2016) 'Artemisinin activity-based probes identify multiple molecular targets within the asexual stage of the malaria parasites *Plasmodium falciparum* 3D7.', *Proceedings of the National Academy of Sciences of the United States of America*, 113(8), pp. 2080–5.

Jensen, J. B. and Trager, W. (1977) '*Plasmodium falciparum* in Culture: Use of Outdated Erythrocytes and Description of the Candle Jar Method.', *The Journal of Parasitology*, 63(5), pp. 883–886.

Joët, T., Eckstein-Ludwig, U., Morin, C. and Krishna, S. (2003) 'Validation of the hexose transporter of *Plasmodium falciparum* as a novel drug target.', *Proceedings of the National Academy of Sciences of the United States of America*, 100(13), pp. 7476–9.

Joët, T. and Krishna, S. (2004) 'The hexose transporter of *Plasmodium falciparum* is a worthy drug target', *Acta Tropica*, 89(3), pp. 371–374.

Johnson, J. D., Denuff, R. A., Gerena, L., Lopez-Sanchez, M., Roncal, N. E. and Waters, N. C. (2007) 'Assessment and continued validation of the malaria SYBR Green I-based fluorescence assay for use in malaria drug screening', *Antimicrobial Agents and Chemotherapy*, 51(6), pp. 1926–1933.

Kato, N., Sakata, T., Breton, G., Le Roch, K. G., Nagle, A., Andersen, C., Bursulaya, B., Henson, K., Johnson, J., Kumar, K. A., Marr, F., Mason, D., McNamara, C., Plouffe, D., Ramachandran, V., Spooner, M., Tuntland, T., Zhou, Y., Peters, E. C., Chatterjee, A., Schultz, P. G., Ward, G. E., Gray, N., Harper, J. and Winzeler, E. A. (2008) 'Gene expression signatures and small-molecule compounds link a protein kinase to *Plasmodium falciparum* motility.', *Nature Chemical Biology*, 4(6), pp. 347–356.

Katsuno, K., Burrows, J. N., Duncan, K., Huijsduijnen, R. H. Van, Kaneko, T., Kita, K., Mowbray, C. E., Schmatz, D., Warner, P. and Slingsby, B. T. (2015) 'Hit and lead criteria in drug discovery for infectious diseases of the developing world.', *Nature Publishing Group*, 14(11), pp. 751–758.

Ke, H., Lewis, I. A., Morrissey, J. M., McLean, K. J., Ganesan, S. M., Painter, H. J., Mather, M. W., Jacobs-Lorena, M., Llinas, M. and Vaidya, A. B. (2015) 'Genetic investigation of tricarboxylic acid metabolism during the *Plasmodium falciparum* life cycle.', *Cell Reports*, 11(1), pp. 164–174.

Ketteler, R. (2015) 'A new age in functional genomics using CRISPR / Cas9 in arrayed library screening', *Frontiers in Genetics*, pp. 1–15.

Klotz, F. W., Orlandi, P. A., Reuter, G., Cohen, S. J., Haynes, J. D., Schauer, R., Howard, R. J., Palese, P. and Miller, L. H. (1992) 'Binding of *Plasmodium falciparum* 175-kilodalton erythrocyte binding antigen and invasion of murine erythrocytes requires N-acetylneuraminic acid but not its O-acetylated form.', *Molecular and Biochemical Parasitology*, 51(1), pp. 49–54.

Knockaert, M., Gray, N., Damiens, E., Chang, Y. T., Grellier, P., Grant, K., Fergusson, D., Mottram, J., Soete, M., Dubremetz, J. F., Le Roch, K., Doerig, C., Schultz, P. G. and Meijer, L. (2000) 'Intracellular targets of cyclin-dependent kinase inhibitors: Identification by affinity chromatography using immobilised inhibitors.', *Chemistry and Biology*, 7(6), pp. 411–422.

Kochar, D. K., Saxena, V., Singh, N., Kochar, S. K., Kumar, S. V. and Das, A. (2005) '*Plasmodium vivax* malaria.', *Emerging Infectious Diseases*, 11(1), pp. 132–134.

Kramer, R. and Cohen, D. (2004) 'Functional genomics to new drug targets.', *Nature Reviews Drug Discovery*. Nature Publishing Group, 3, pp. 965.

Lakshmanan, V., Rhee, K. and Daily, J. (2011) 'Metabolomics and malaria biology.', *Molecular and Biochemical Parasitology*, 4(164), pp. 104–111.

Lambros, C. and Vanderberg, J. P. . (1979) 'Synchronization of *Plasmodium falciparum* Erythrocytic Stages in Culture.', *American Society of Parasitologists*, 65(3), pp. 418–420.

Lang-Unnasch, N. and Murphy, A. D. (1998) 'Metabolic Changes of the Malaria Parasite During the Transition From the Human To the Mosquito Host.', *Annual Review of Microbiology*, 52(1), pp. 561–590.

Lee, H. J., Georgiadou, A., Otto, T. D., Levin, M., Coin, L. J., Conway, D. J. and Cunnington, A. J. (2018) 'Transcriptomic Studies of Malaria: a Paradigm for Investigation of Systemic Host-Pathogen Interactions.', *Microbiology and Molecular Biology Reviews : MMBR*, 82(2), pp. e00071-17.

Lei, X. H. and Bochner, B. R. (2013) 'Using Phenotype MicroArrays to Determine Culture Conditions That Induce or Repress Toxin Production by *Clostridium difficile* and Other Microorganisms.', *PLoS ONE*, 8(2), pp. e56545.

Lian, L.-Y., Al-Helal, M., Roslaini, A. M., Fisher, N., Bray, P. G., Ward, S. A. and Biagini, G. A. (2009) 'Glycerol: an unexpected major metabolite of energy metabolism by the human malaria parasite.', *Malaria Journal*, 8(1), pp. 38.

Lunev, S., Batista, F. A., Bosch, S. S., Wrenger, C. and Groves, M. R. (2016) 'Identification and Validation of Novel Drug Targets for the Treatment of *Plasmodium falciparum* Malaria: New Insights.', in Rodriguez-Morales, A. J. (ed.) *Current Topics in Malaria*. Rijeka: InTech.

Lyttleton, C. (2016) 'Deviance and resistance: Malaria elimination in the greater Mekong subregion', *Social Science & Medicine*. Elsevier Ltd, 150, pp. 144–152.

Makler, M. T. and Hinrichs, D. J. (1993) 'Measurement of the lactate dehydrogenase activity of *Plasmodium falciparum* as an assessment of parasitemia.', *American Journal of Tropical Medicine and Hygiene*, 48(2), pp. 205–210.

Makler, M. T. and Hinrichs, D. J. (1993) 'Measurement of the Lactate Dehydrogenase Activity of *Plasmodium falciparum* as an Assessment of

Parasitemia.', *The American Journal of Tropical Medicine and Hygiene*, 48(2), pp. 205-210.

Manev, H. and Manev, R. (2010) 'Benefits of neuropsychiatric phenomics: Example of the 5-lipoxygenase- leptin-alzheimer connection.', *Cardiovascular Psychiatry and Neurology*, 2010, pp. 4–6.

Manolescu, A. R., Witkowska, K., Kinnaird, A., Cessford, T. and Cheeseman, C. (2007) 'Facilitated Hexose Transporters: New Perspectives on Form and Function.', *Physiology*, 22(4), pp. 234–240.

Markwalter, C. F., Davis, K. M. and Wright, D. W. (2016) 'Immunomagnetic capture and colorimetric detection of malarial biomarker *Plasmodium falciparum* lactate dehydrogenase.', *Analytical Biochemistry*, 493, pp. 30–34.

McNamara, C. and Winzeler, E. A. (2011) 'Target identification and validation of novel antimalarials.', *Future Microbiology*, 6(6), pp. 693–704.

Meshnick, S. R. (2002) 'Artemisinin: Mechanisms of action, resistance and toxicity', *International Journal for Parasitology*, 32(13), pp. 1655–1660.

Miller, L. H., Baruch, D. I., Marsh, K. and Doumbo, O. K. (2002) 'The pathogenic basis of malaria.', *Nature*, 415, pp. 673–679.

Miller, L. H., Baruch, D. I., Marsh, K. and Doumbo, O. K. (2002) 'The pathogenic basis of malaria.', *Nature*, pp. 673–679.

Mok, S., Ashley, E. A., Ferreira, P. E., Zhu, L., Lin, Z., Yeo, T., Chotivanich, K., Imwong, M., Pukrittayakamee, S., Dhorda, M., Nguon, C., Lim, P., Amaratunga, C., Suon, S., Hien, T. T., Ye Htut, M. A. F., Onyamboko, M. A., Mayxay, M., Newton, P. N., Tripura, R., J.Woodrow, C., Miotto, O., Kwiatkowski, D. P., Nosten, F., Day, N. P. J., Preiser, P. R., White, N. J., Dondorp, A. M., Fairhurst, R. M. and Bozdech, Z. (2015) 'Drug resistance. Population transcriptomics of human malaria parasites reveals the mechanism of artemisinin resistance.', *Science*, 347, pp. 431–435.

Moore, L. R., Fujioka, H., Williams, P. S., Chalmers, J. J., Grimberg, B., Zimmerman, P. and Zborowski, M. (2006) 'Hemoglobin degradation in malaria-infected erythrocytes determined from live cell magnetophoresis.', *The FASEB*

Journal., 20(6), pp. 747–749.

Muller, S., Cerdan, R. and Radulescu, I. (2016). 'Carbon Metabolism of *Plasmodium falciparum*' *Comprehensive analysis of Parasite Biology.*, pp. 371.

Ndiaye, D., Daily, J. P., Sarr, O., Ndir, O., Gaye, O., Mboup, S. and Wirth, D. F. (2005) 'Mutations in *Plasmodium falciparum* dihydrofolate reductase and dihydropteroate synthase genes in Senegal.', *Tropical Medicine and International Health*, 10(11), pp. 1176–1179.

Okombo, J. and Chibale, K. (2017) 'Insights into Integrated Lead Generation and Target Identification in Malaria and Tuberculosis Drug Discovery.', *Accounts of Chemical Research*, 50(7), pp. 1606–1616.

Olszewski, K. L. and Llinás, M. (2011) 'Central carbon metabolism of *Plasmodium* parasites.', *Molecular and Biochemical Parasitology*. Elsevier B.V., 175(2), pp. 95–103.

Penna-Coutinho, J., Cortopassi, W. A., Oliveira, A. A., Franca, T. C and Krettli, A. U. (2011) 'Antimalarial activity of potential inhibitors of *Plasmodium falciparum* lactate dehydrogenase enzyme selected by docking studies.', *PLoS ONE*, 6(7), pp. e21237.

R Core Team (2016) 'R: A Language and Environment for Statistical Computing'.

Ribeiro, S. M., Giménez-Cassina, A. and Danial, N. N. (2015) 'Measurement of Mitochondrial Oxygen Consumption Rates in Mouse Primary Neurons and Astrocytes BT - Mitochondrial Regulation: Methods and Protocols.', in Palmeira, C. M. and Rolo, A. P. (eds). New York, NY: Springer New York, pp. 59–69.

Robinson, J., Halliwell, J. A., McWilliam, H., Lopez, R. and Marsh, S. G. E. (2013) 'IPD - The Immuno Polymorphism Database', *Nucleic Acids Research*, 41(D1), pp. 1234–1240.

Le Roch, K. G., Zhou, Y., Blair, P. L., Grainger, M., Moch, J. K., Haynes, J. D., Vega, P. De, Holder, A. a, Batalov, S., Carucci, D. J. and Winzeler, E. a (2003) 'Discovery of Gene Function by Expression Profiling of the Malaria Parasite Life

Cycle', *Science*, 301, pp. 1503–1509.

Romanha, Á. J. (1986) 'Carbohydrate metabolism of malarial parasites', *Memórias do Instituto Oswaldo Cruz*, 81(2–3), pp. 149–152.

Rosenthal, P. J., Olson, J. E., Lee, G. K., Palmer, J. T., Klaus, J. L. and Rasnick, D. (1996) 'Antimalarial effects of vinyl sulfonyl cysteine proteinase inhibitors.', *Antimicrobial Agents and Chemotherapy*, 40(7), pp. 1600–1603.

RStudio Team (2016) 'RStudio: Integrated Development Environment for R'.

Salcedo-Sora, J. E., Caamano-Gutierrez, E., Ward, S. A. and Biagini, G. A. (2014a) 'The proliferating cell hypothesis: A metabolic framework for *Plasmodium* growth and development.', *Trends in Parasitology*. Elsevier Ltd, 30(4), pp. 170–175.

Saliba, K. J. and Kirk, K. (1999) 'pH Regulation in the Intracellular Malaria Parasite, *Plasmodium falciparum*.', *The Journal of Biological Chemistry*, 274(47), pp. 33213–33219.

Samuels, M. E. (2010) 'Saturation of the human phenome.', *Current Genomics*, 11(7), pp. 482–499.

Santos, G. and Torres, N. V. (2013) 'New Targets for Drug Discovery against Malaria.', *PLoS ONE*, 8(3), pp. e59968.

Scaria, J., Suzuki, H., Ptak, C. P., Chen, J.-W., Zhu, Y., Guo, X.-K. and Chang, Y.-F. (2015) 'Comparative genomic and phenomic analysis of *Clostridium difficile* and *Clostridium sordellii*, two related pathogens with differing host tissue preference.', *BMC genomics*, 16(1), pp. 448.

Sherman, I. (1979) 'Biochemistry of *Plasmodium* (malaria parasites).', *Microbiological Reviews*, 43(4), pp. 453–495.

Singh, B. and Cliff Simon Divis, P. (2008) 'Orangutans Not infected with *Plasmodium vivax* or *P. cynomolgi*, Indonesia.', *Clinical Infectious Diseases*, 46(2), pp. 165–171.

Sipes, I. G., McQueen, C. A. and Gandolfi, A. J. (1997) *Comprehensive toxicology*. New York: Pergamon.

Siwo, G. H., Smith, R. S., Tan, A., Button-Simons, K. A., Checkley, L. A. and Ferdig, M. T. (2015) 'An integrative analysis of small molecule transcriptional responses in the human malaria parasite *Plasmodium falciparum*.', *BMC Genomics*, 16(1), pp. 1030.

Slater, A. F. G. (1993) 'Chloroquine: Mechanism of Drug Action and Resistance in *Plasmodium falciparum*.', *Pharmacology and Therapeutics*, 57, pp. 203–235.

Slavic, K., Krishna, S., Derbyshire, E. T. and Staines, H. M. (2011) 'Plasmodial sugar transporters as anti-malarial drug targets and comparisons with other protozoa.', *Malaria Journal*, (165), pp. 1–10.

Smilkstein, M., Sriwilaijaroen, N., Kelly, J. X., Wilairat, P. and Riscoe, M. (2004) 'Simple and Inexpensive Fluorescence-Based Technique for High-Throughput Antimalarial Drug Screening.', *Antimicrobial agents and chemotherapy*, 48(5), pp. 1803–1806.

Spadafora, C., Gerena, L. and Kopydlowski, K. M. (2011) 'Comparison of the *in vitro* invasive capabilities of *Plasmodium falciparum* schizonts isolated by Percoll gradient or using magnetic based separation.', *Malaria Journal*. BioMed Central Ltd, 10(1), pp. 96.

Storey, B. T., Noiles, E. E. and Thompson, K. A. (1998) 'Comparison of Glycerol, Other Polyols, Trehalose, and Raffinose to Provide a Defined Cryoprotectant Medium for Mouse Sperm Cryopreservation', *Cryobiology*, 58, pp. 46–58.

Sutherland, C. J., Lansdell, P., Sanders, M., Muwanguzi, J., van Schalkwyk, D. A., Kaur, H., Nolder, D., Tucker, J., Bennett, H. M., Otto, T. D., Berriman, M., Patel, T. A., Lynn, R., Gkrania-Klotsas, E. and Chiodini, P. L. (2017) '*Pfk13* - independent treatment failure in four imported cases of *Plasmodium falciparum* malaria given artemether-lumefantrine in the UK', *Antimicrobial Agents and Chemotherapy*, 44, pp. AAC.02382-16.

Swinney, D. C. (2015) 'Drug Discoveries and Molecular Mechanism of Action.', *Successful Drug Discovery*, Wiley-VCH Verlag GmbH & Co. KGaA, pp. 19–34.

Sykes, M. L. and Avery, V. M. (2013) 'Approaches to protozoan drug discovery: Phenotypic screening', *Journal of Medicinal Chemistry*, 56(20), pp. 7727–7740.

Sylke, M., Cerdan, R., Radulescu, O., Guca, E. and Selzer, P. M. (2016) *Comprehensive Analysis of Parasite Biology: From Metabolism to Drug Discovery*. Edited by S. Müller, R. Cerdan, O. Radulescu, and P. M. Selzer. Wiley-Blackwell.

Teslaa, T. and Teitell, M. A. (2014) 'Techniques to monitor glycolysis.', *Methods in Enzymology*, 542, pp. 91–114.

Trager, W. and Jensen, J. B. (1976) 'Human malaria parasites in continuous culture', *Science*, 193(4254), pp. 673–5.

Travassos, M. A. and Laufer, M. K. (2009) 'Resistance to antimalarial drugs: molecular, pharmacological and clinical considerations', *Pediatric Research*, 65(5 Pt 2), pp. 64-70R.

Tuteja, R. (2007) 'Malaria - An overview', *FEBS Journal*, 274(18), pp. 4670–4679.

Vaas, L. A. I., Sikorski, J., Michael, V., Göker, M. and Klenk, H.-P. (2012) 'Visualization and Curve-Parameter Estimation Strategies for Efficient Exploration of Phenotype Microarray Kinetics.', *PLoS ONE*, 7(4), pp. e34846.

Vaas, L., Hofner, B. and Göker, M. (2013) 'opm: an R package for analysing OmniLog(R) phenotype microarray data.', *Bioinformatics*, 29(14), pp. 1823–1824.

Vehkala, M., Shubin, M., Connor, T. R., Thomson, N. R. and Corander, J. (2015) 'Novel R pipeline for analyzing biologic phenotypic microarray data.', *PLoS ONE*, 10(3), pp. 1–14.

Verlinde, C. L. M. J., Hannaert, V., Blonski, C., Willson, M., Périé, J. J., Fothergill-Gilmore, L. A., Opperdoes, F. R., Gelb, M. H., Hol, W. G. J. and Michels, P. A. M. (2001) 'Glycolysis as a target for the design of new anti-trypansomite drugs.', *Drug Resistance Updates*, 4(1), pp. 50–65.

Verlinden, B. K., De Beer, M., Pachaiyappan, B., Besaans, E., Andayi, W. A., Reader, J., Niemand, J., Van Biljon, R., Guy, K., Egan, T., Woster, P. M. and Birkholtz, L. M. (2015) 'Interrogating alkyl and arylalkylpolyamino (bis)urea and (bis)thiourea isosteres as potent antimalarial chemotypes against multiple lifecycle forms of *Plasmodium falciparum* parasites.', *Bioorganic and Medicinal Chemistry*, 23(16), pp. 5131–5143.

Viti, C., Tatti, E. and Giovannetti, L. (2016) 'Phenotype MicroArray analysis of cells: fulfilling the promise', *Research in Microbiology*, 167(9–10), pp. 707–709.

Wang, H., Wang, J., Li, L., Hsiang, T., Wang, M., Shang, S. and Yu, Z. (2016) 'Metabolic activities of five botryticides against *Botrytis cinerea* examined using the Biolog FF MicroPlate.', *Scientific Reports*, 6, pp. 31025.

Warhurst, D. C. (2001) 'A Molecular Marker for Chloroquine-Resistant *falciparum* Malaria.', *New England Journal of Medicine.*, 344(4), pp. 299–302.

Weiss, G. E., Crabb, B. S. and Gilson, P. R. (2016) 'Overlaying Molecular and Temporal Aspects of Malaria Parasite Invasion.', *Trends in Parasitology.*, 32(4), pp. 284–95.

Wells, T. N. C., van Huijsduijnen, R. H. and Van Voorhis, W. C. (2015) 'Malaria medicines: a glass half full?', *Nature Reviews Drug Discovery*, 14(6), pp. 424–442.

Wendel, W. B. (1943) 'Respiratory and carbohydrate metabolism of malaria parasites (*Plasmodium Knowlesi*).', *Journal of Biological Chemistry.*, 148, pp. 21–34.

White, N. (2009) 'Malaria.', in Cook, G. and Zumla, A. (eds) *Manson's Tropical Diseases*. 22 ed. Edinburgh: Saunders Ltd.

WHO World Malaria Report (2015) 'World Malaria Report 2015', *World Health*, pp. 243.

WHO World Malaria Report (2016) *World Malaria Report 2015*.

WHO World Malaria Report (2017) *World Malaria Report 2016*.

Witkowski, B., Lelièvre, J., Barragán, M. J. L., Laurent, V., Su, X. Z., Berry, A. and Benoit-Vical, F. (2010) 'Increased tolerance to artemisinin in *Plasmodium falciparum* is mediated by a quiescence mechanism.', *Antimicrobial Agents and Chemotherapy*, 54(5), pp. 1872–1877.

Wiwanitkit, V. (2007) '*Plasmodium* and host lactate dehydrogenase molecular function and biological pathways: Implication for antimalarial drug discovery.', *Chemical Biology and Drug Design*, 69(4), pp. 280–283.

Woodrow, C. J., Burchmore, R. J. and Krishna, S. (2000) 'Hexose permeation pathways in *Plasmodium falciparum*-infected erythrocytes.', *Proceedings of the National Academy of Sciences of the United States of America*, 97(18), pp. 9931–6.

Wu, M., Neilson, A., Swift, A. L., Moran, R., Tamagnine, J., Parslow, D., Armistead, S., Lemire, K., Orrell, J., Teich, J., Chomicz, S. and Ferrick, D. A. (2006) 'Multiparameter metabolic analysis reveals a close link between attenuated mitochondrial bioenergetic function and enhanced glycolysis dependency in human tumor cells.', *AJP: Cell Physiology*, 292(1), pp. C125–C136.

Appendix:

Table 1: Plate map of the mammalian phenotype microarray plate PM-M1. PM-M1 contains a variety of mono-, di- and polysaccharides targeted at assessing carbohydrate metabolism (Bochner, 2003).

A1 Negative Control	A2 Negative Control	A3 Negative Control	A4 α - Cyclodextrin	A5 Dextrin	A6 Glycogen	A7 Maltitol	A8 Maltotriose	A9 D-Maltose	A10 D-Trehalose	A11 D-Cellobiose	A12 β -Gentiobiose
B1 D-Glucose-6- Phosphate	B2 α -D-Glucose- 1-Phosphate	B3 L-Glucose	B4 α -D-Glucose	B5 α -D-Glucose	B6 α -D-Glucose	B7 3-O-Methyl- D-Glucose	B8 α -Methyl-D- Glucoside	B9 β -Methyl-D- Glucoside	B10 D-Salicin	B11 D-Sorbitol	B12 N-Acetyl-D- Glucosamine
C1 D- Glucosaminic Acid	C2 D-Glucuronic Acid	C3 Chondroitin- 6-Sulfate	C4 Mannan	C5 D-Mannose	C6 α -Methyl-D- Mannoside	C7 D-Mannitol	C8 N-Acetyl- β -D- Mannosamin e	C9 D-Melezitose	C10 Sucrose	C11 Palatinose	C12 D-Turanose
D1 D-Tagatose	D2 L-Sorbose	D3 L-Rhamnose	D4 L-Fucose	D5 D-Fucose	D6 D-Fructose-6- Phosphate	D7 D-Fructose	D8 Stachyose	D9 D-Raffinose	D10 D-Lactitol	D11 Lactulose	D12 α -D-Lactose

E1 Melibionnic Acid	E2 D-Melibiose	E3 D-Galactose	E4 α -Methyl-D- Galactoside	E5 β -Methyl-D- Galactoside	E6 N-Acetyl- Neuraminic Acid	E7 Pectin	E8 Sedoheptulos an	E9 Thymidine	E10 Uridine	E11 Adenosine	E12 Inosine
F1 Adonitol	F2 L- Arabinose	F3 D-Arabinose	F4 β -Methyl-D- Xylopyranosid e	F5 Xylitol	F6 Myo-Inositol	F7 Meso- Erythritol	F8 Propylene glycol	F9 Ethanolamine	F10 D,L- Glycerol- Phosphate	F11 α - Glycerol	F12 Citric Acid
G1 Tricarballic Acid	G2 D,L-Lactic Acid	G3 Methyl lactate	G4 D- Methyl pyruvate	G5 Pyruvic Acid	G6 α -Keto- Glutaric Acid	G7 Succinamic Acid	G8 Succinic Acid	G9 Mono-Methyl Succinate	G10 L-Malic Acid	G11 D-Malic Acid	G12 Meso-Tartaric Acid
H1 Acetoacetic Acid (a)	H2 γ -Amino-N- Butyric Acid	H3 α -Keto- Butyric Acid	H4 α -Hydroxy- Butyric Acid	H5 D,L- β - Hydroxy- Butyric Acid	H6 γ -Hydroxy- Butyric Acid	H7 Butyric Acid	H8 2,3- Butanediol	H9 3-Hydroxy-2- Butanone	H10 Propionic Acid	H11 Acetic Acid	H12 Hexanoic Acid

Table 2: Carbohydrate substrates that displayed a statistically significant decrease in metabolism in comparison to untreated trophozoites are displayed below for each treatment condition.

Treatment	Well	Substrate	Average Omnilog units	Student t-Test ($P < 0.05$)
CQ	D02	L-Sorbose	89.9	0.02
	D06	D-Fructose-6-Phosphate	83.03	0.001
	E07	Pectin	53.7	0.001
	F03	D-Arabinose	58.3	0.003
DHA	A11	D-Cellobiose	55.5	0.009
	C02	D-Glucuronic acid	66.0	0.012
	C07	D-Mannitol	44	0.012
	D01	D-Tagatose	138	0.008
	D07	D-Fructose	94.2	0.01
	D09	D-Raffinose	40.2	0.041
	D12	α -D-Lactose	53.1	0.002
	E06	N-Acetylneuraminic acid	43.2	0.001
	E10	Uridine	39	0.02
	E12	Inosine	40.3	0.001
	F04	β -Methyl-D-Xylopyranoside	31.8	0.006
	F05	Xylitol	31.9	0.02
	F06	myo-Inositol	33.6	0.005
	F08	Propylene Glycol	40.4	0.02
	F11	Glycerol	43.8	0.007
	G01	Tricarballic acid	43.8	0.01
	G02	D,L-Lactic acid	36.4	0.04
G04	Methyl pyruvate	41.8	0.02	
G08	Succinic acid	44.1	0.02	
G11	D-Malic acid	46	0.02	

	H04	α -Hydroxybutyric acid	46.2	0.02
	D01	D-Tagatose	153	0.008
	D02	L-Sorbose	76.6	0.02
	D06	D-Fructose-6-Phosphate	79.6	0.001
	D12	α -D-Lactose	55.8	0.001
PYR	E01	Melibionic acid	48.3	0.02
	E07	Pectin	52.2	0.0001
	E11	Adenosine	47.7	0.008
	H04	α -Hydroxybutyric acid	54.3	0.02
	H08	2,3-Butanediol	52.8	0.03

Table 3: Kinetic parameters of trophozoite-stage *P. falciparum* parasites either untreated or treated with, CQ disulphate, DHA or PYR on different carbohydrate sources.

Substrate	Mean rate of colour production (Mean $\lambda \pm$ SD)				Mean lag phase (Mean $\mu \pm$ SD)				Mean total formazan production (Mean AUC \pm SD)			
	UT	CQ	DHA	PYR	UT	CQ	DHA	PYR	UT	CQ	DHA	PYR
L-Sorbose	140± 9.46	58.0± 52.3	106± 11.9	102± 21.4	3.17± 0.144	2±3.46	2.25± 1.59	1.92± 0.12	1406± 126	999± 68.3	1001± 143	1033± 113
D-Fructose-6-Phosphate	151± 18.3	0±0	58.7± 41.5	81.7±60.1	1.75± 1.56	0±0	0±0	0±0	1426± 82.4	1033± 36.3	786± 17.8	1020± 83.5
D-Arabinose	35.7± 31.3	0±0	14.7± 20.8	15.7± 22.2	0.83± 1.44	0±0	0±0	0±0	634± 68.6	626± 65.7	508± 14.2	597± 10.2
D-Cellobiose	19.4± 33.6	58.4± 7.05	13.0± 18.3	48.4± 34.3	0.67± 1.15	1.25± 1.39	0±0	0±0	854± 86.8	916± 56.0	631± 56.5	848± 54.4
D-Glucuronic acid	109± 16.2	98.9± 10.2	40.4± 32.9	89.4± 12.6	0.92± 1.59	0.92± 1.59	3.5± 2.76	1.83± 1.74	974± 50.7	959± 12.7	745± 100	940± 30.5
D-Mannitol	21.0± 36.4	0±0	34.3± 5.45	37.2± 27.5	0.25± 0.43	0±0	0±0	0±0	659± 41.6	623± 72.6	468± 42.8	597± 57.8
D-Tagatose	31.3± 0.20	27.3± 0.96	27.2± 2.01	27.5± 1.41	0±0	0±0	0.68± 0.36	0.45± 0.35	1994± 65.1	1899± 71.6	1721± 70.2	1777± 51.8
D-Fructose	154± 20.74	136± 15.36	135± 24.49	128± 17.12	1.92± 1.77	1.58± 1.28	2.17± 1.55	1.92± 1.45	1393± 21.20	1287± 68.94	1197± 56.89	1245± 37.30
D-Raffinose	15.9± 27.5	12.4± 21.4	0±0	28.8± 20.6	0.67± 1.15	0.25± 0.43	0±0	0±0	602± 81.4	640± 68.1	481± 27.1	586± 35.2
α -D-Lactose	19.0± 32.9	55.8± 6.02	13.8± 19.6	48.9± 6.97	0.67± 1.15	0.25± 0.43	0±0	0±0	844± 70.6	780± 44.1	612± 49.4	707± 49.3
N-Acetylneuraminic acid	2.01± 3.47	18.0± 31.2	15.0± 21.3	42.7± 30.2	0±0	0.25± 0.43	0±0	0±0	646± 32.7	621± 70.3	465± 37.7	651± 32.7
Uridine	0±0	0±0	0±0	10.2± 14.4	0±0	0±0	0±0	0.25± 0.35	588± 24.9	608± 26.3	479± 47.0	568± 21.3
Inosine	17.4± 30.1	10.7± 18.5	0±0	37.9± 2.18	0±0	0±0	0±0	0±0	671± 69.5	649± 44.7	498± 17.6	642± 38.4
β -Methyl-D-Xylopyranoside	10.2± 17.7	0±0	19.2± 13.6	13.5± 19.2	0.25± 0.43	0±0	0±0	0±0	551± 38.2	576± 10.2	411± 39.8	554± 15.8
Xylitol	0±0	0±0	9.77± 13.8	13.0± 18.4	0±0	0±0	0±0	0.08± 0.12	604± 28.6	641± 100	412± 54.7	556± 34.6
myo-Inositol	34.3± 31.2	28.5± 24.8	0±0	13.0± 18.4	1± 1.15	0.17 0.29	0±0	0.08± 0.12	670± 88.4	603± 38.4	440± 59.8	571± 33.5

Propylene Glycol	10.7±	28.5±	0±0	13.0±	0.75±	0.17	0±0	0.08±	563±	603±	440±	571±
	18.6	24.8		18.4	1.30	0.29		0.12	42.4	38.4	59.8	33.5
Glycerol	30.5±	13.8±	0±0	12.1±	0±0	0±0	0±0	0±0	711±	656±	533±	633±
	31.0	23.9		17.1					82.8	35.0	13.4	16.5
Tricarballic acid	54.7±	18.0±	35.8±	18.1±	0.25±	0±0	0.08±	0±0	688±	706±	513±	647±
	3.66	31.2	3.30	25.6	0.43		0.12		16.5	79.5	18.2	52.6
D,L-Lactic acid	0±0	22.7±	1.87±	0±0	0±0	0.25±	0.61±	0±0	560±36.7	587±85.5	446±30.7	559±32.3
		20.1	1.34			0.43	0.86					
Methyl pyruvate	36.2±	27.0±	23.4±	14.2±	0.75±1.30	0.33±	0±0	0±0	667±	637±	469±	584±
	31.5	23.9	17.2	20.0		0.58			122	53.1	63.1	29.8
Succinic acid	37.2±	22.0±	0±0	47.3±	0.75±1.30	0.17±	0±0	0±0	698±	684±	501±	643±
	32.7	30.2		4.93		0.29			72.5	86.7	36.1	58.9
D-Malic acid	17.9±	31.4±	0±0	24.3±	0±0	0.25±	0±0	0±0	760±	745±	534±	662±
	27.1	28.8		17.2		0.43			151	85.7	42.7	11.8
Pectin	45.8±	16.2±	12.4±	31.1±	1±1.15	0±0	0±0	0±0	796±	634±	569±	630±
	39.9	28.0	17.5	22.0					40.1	23.5	69.1	7.43
α-Hydroxybutyric acid	22.6±	20.4±	13.8±	28.0±	0±0	0±0	1.31±1.56	0.67±0.	782±	742±	593±	564±
	33.9	30.5	12.0	20.6				94	63.3	60.2	77.9	91.0
α-D-glucose	47.0	0±0	13.0	13.9	1.75	0±0	0.08	0±0	653	621	507	571
	12.1		18.4	19.7	1.64		0.12		145	46.7	55.3	47.9

Table 4: A Comparison of the carbohydrate sources which produced a positive signal in untreated trophozoite-stage *P. falciparum* parasites in the PM system as compared to literature. Carbohydrate substrates displaying either a weak signal (AIV of ≤ 4), a positive signal (AIV between 5 and 6) or a strongly positive signal (AIV ≥ 7) are shown below. No NADH production/signal is indicated by, -.

Metabolite	Literature	Experiment	AIV value	Nutrient category	Literature reference
D-Glucose-6-Phosphate	Positive signal	Positive signal	5	Monosaccharide	(Berg, Tymoczko and Stryer, 2002; Ginsburg and Abdel-Haleem, 2017)
α -D-Glucose-1-Phosphate	Positive signal	Weak signal	2	Monosaccharide	(Berg, Tymoczko and Stryer, 2002)
α -D-Glucose	Positive signal	Weak signal	4	Monosaccharide	(Romanha, 1986)
3-O-Methyl-D-Glucose	Positive signal	Positive signal	5	Monosaccharide	(Ginsburg and Abdel-Haleem, 2017)
D-Mannose	Positive signal	Positive signal	5	Monosaccharide	(Berg, Tymoczko and Stryer, 2002)
D-Tagatose	Positive signal	Strongly positive signal	9	Monosaccharide	(Berg, Tymoczko and Stryer, 2002)
L-Sorbose	Positive signal	Strongly positive signal	8	Monosaccharide	(Berg, Tymoczko and Stryer, 2002)

D-Fructose-6-Phosphate	Positive signal	Strongly positive signal	8	Monosaccharide	(Joët and Krishna, 2004; Storey, Noiles and Thompson, 1998; Divo <i>et al.</i> , 1985)
D-Fructose	Positive signal	Strongly positive signal	8	Monosaccharide	(Joët and Krishna, 2004)
Adenosine	Positive signal	Weak signal	4	Nucleoside triphosphate	(Joët <i>et al.</i> , 2003)
Glycerol	Positive signal	Weak signal	4	Simple polyol compound	(Berg, Tymoczko and Stryer, 2002; Lian <i>et al.</i> , 2009)
Sucrose	Positive signal	Weak signal	2	Disaccharide	(Berg, Tymoczko and Stryer, 2002)
α -Cyclodextrin	-	Positive signal	5	Cyclic oligosaccharide	(Crandall <i>et al.</i> , 2007)
Dextrin	-	Positive signal	6	Monosaccharide	(Crandall <i>et al.</i> , 2007)
Glycogen	-	Positive signal	5	Polysaccharide	(Berg, Tymoczko and Stryer, 2002)
Maltitol	-	Weak signal	4	Disaccharide-derived polyol	(Robinson <i>et al.</i> , 2013)
Maltotriose	-	Weak signal	4	Trisaccharide	(Berg, Tymoczko and Stryer, 2002)
D-Maltose	-	Weak signal	4	Disaccharide	(Ginsburg and Abdel-Haleem, 2017)
D-Cellobiose	-	Positive signal	5	Disaccharide	(Berg, Tymoczko and Stryer, 2002)

β -Gentiobiose	-	Positive signal	6	Disaccharide	(Robinson <i>et al.</i> , 2013)
D-Salicin	-	Weak signal	4	Disaccharide	(Ginsburg and Abdel-Haleem, 2017)
D-Glucosaminic Acid	-	Positive signal	5	Monosaccharide	(Robinson <i>et al.</i> , 2013)
D-Glucuronic Acid	-	Positive signal	6	Monosaccharide	(Berg, Tymoczko and Stryer, 2002)
Chondroitin-6-Sulfate	-	Positive signal	5	Heteropolysaccharide	(Robinson <i>et al.</i> , 2013)
α -Methyl-D-Mannoside	-	Positive signal	5	Monosaccharide	(Robinson <i>et al.</i> , 2013)
D-Mannitol	-	Weak signal	4	Monosaccharide	(Robinson <i>et al.</i> , 2013)
D-Melezitose	-	Weak signal	4	Trisaccharide	(Robinson <i>et al.</i> , 2013)
Palatinose	-	Strongly positive signal	8	Disaccharide	(Woodrow, Burchmore and Krishna, 2000)
Lactulose	-	Weak signal	4	Disaccharide	(Robinson <i>et al.</i> , 2013)
α -D-Lactose	-	Weak signal	4	Disaccharide	(Ginsburg <i>et al.</i> , 1983)
Melibionnic Acid	-	Weak signal	4	Monosaccharide	(Ginsburg <i>et al.</i> , 1983)
D-Galactose	-	Weak signal	4	Monosaccharide	(Robinson <i>et al.</i> , 2013)
Pectin	-	Weak signal	4	Heteropolysaccharide	(Robinson <i>et al.</i> , 2013)
Meso-Erythritol	-	Weak signal	4	Sugar alcohol	(Robinson <i>et al.</i> , 2013)
Citric Acid	-	Weak signal	4	Tricarboxylic acid	(Ginsburg <i>et al.</i> , 1983)
Tricarballic Acid	-	Positive signal	5	Tricarboxylic acid	(Robinson <i>et al.</i> , 2013)
Succinic Acid	-	Weak signal	4	Dicarboxylic acid	(Robinson <i>et al.</i> , 2013)

L-Malic Acid	-	Weak signal	4	Dicarboxylic acid	(Robinson <i>et al.</i> , 2013; Ke <i>et al.</i> , 2015)
D-Malic Acid	-	Weak signal	4	Dicarboxylic acid	(Robinson <i>et al.</i> , 2013; Ke <i>et al.</i> , 2015)
γ -Amino-N-Butyric Acid	-	Positive signal	5	Carboxylic acid	(Robinson <i>et al.</i> , 2013)
α -Hydroxy-Butyric Acid	-	Positive signal	5	Carboxylic acid	(Robinson <i>et al.</i> , 2013)
Butyric Acid	-	Weak signal	4	Carboxylic acid	(Robinson <i>et al.</i> , 2013)
2,3-Butanediol	-	Positive signal	5	Hydroxyl Compound	(Robinson <i>et al.</i> , 2013)
Acetic Acid	-	Positive signal	5	Organic Acid	(Robinson <i>et al.</i> , 2013)
Hexanoic Acid	-	Positive signal	5	carboxylic acid derived from hexane	(Robinson <i>et al.</i> , 2013)

Table 5: MetaPrint map carbohydrate substrate hexagon index values

Substrate	MetaPrint Hexagon Index Number
Negative Control 1	50
Negative Control 2	50
Negative Control 3	50
α -Cyclodextrin	19
Dextrin	39
Glycogen	60
Maltitol	9
Maltotriose	21
D-Maltose	41
Trehalose	41
D-Cellobiose	41
Gentiobiose	61
D-Glucose-6-Phosphate	59
α -D-Glucose-1-Phosphate	47
L-Glucose	14
α -D-Glucose 1	28
α -D-Glucose 2	10
α -D-Glucose 3	57
3-O-Methylglucose	22
α -Methyl-D-Glucoside	48
β -Methyl-D-Glucoside	53
Salicin	2
D-Sorbitol	48
N-Acetyl-D-Glucosamine	45
D-Glucosaminic acid	58
D-Glucuronic acid	20
Chondroitin Sulfate C	57
Mannan	28

D-Mannose	35
α -Methyl-D-Mannoside	36
D-Mannitol	33
N-Acetyl-D-Mannosamine	1
D-Melezitose	58
Sucrose	28
Palatinose	38
D-Turanose	26
D-Tagatose	38
L-Sorbose	38
L-Rhamnose	52
L-Fucose	52
D-Fucose	31
D-Fructose-6-Phosphate	39
D-Fructose	38
Stachyose	44
D-Raffinose	14
D-Lactitol	1
Lactulose	56
α -D-Lactose	42
Melibionic acid	11
D-Melibiose	48
D-Galactose	54
α -Methyl-D-Galactoside	51
Methyl- β -D-Galactoside	51
N-Acetylneuraminic acid	1
Pectin	56
Sedoheptulosan	14
Melibionic acid	46
Thymidine	29
Uridine	54
Adenosine	15

Inosine	15
Adonitol	54
L-Arabinose	46
D-Arabinose	51
B-Methyl D Xylopyranoside	48
Xylitol	54
Myo-inositol	59
i-Erythritol	30
Propylene Glycol	42
Ethanolamine	12
D-L- α -Glycerol Phosphate	16
Glycerol	6
Citric acid	18
Tricarballic acid	49
D-L-Lactic acid	53
D-Lactic acid Methyl Ester	54
Methyl pyruvate	49
Pyruvic acid	15
α -Ketoglutaric acid	28
Succinamic acid	17
Succinic acid	5
Mono Methylsuccinate	55
L-Malic acid	1
D-Malic acid	6
m-Tartaric acid	11
Lithium acetoacetate	43
γ -Amino N Butyric acid	44
α -KetoButyric acid	18
α -Hydroxybutyric acid	43
B-Hydroxybutyric acid	44
γ -Hydroxybutyric acid	10
Butyric acid	22

2-3-Butanediol	25
3-Hydroxy-2-butanone	24
Propionic acid	19
Acetic acid	40
Hexanoic acid	28